This is to certify that the
dissertation entitled

VASCULAR REACTIVE OXYGEN SPECIES METABOLISM AND ITS INFLUENCE ON VENOMOTOR TONE AND HYPERTENSION

presented by

IRINA THEODORA SZASZ

has been accepted towards fulfillment
of the requirements for the

Ph.D. degree in Microbiology and Molecular Genetics

Stephanie W Watts
Major Professor's Signature

8/19/2009
Date

MSU is an Affirmative Action/Equal Opportunity Employer

VASCULAR REACTIVE OXYGEN SPECIES METABOLISM AND ITS INFLUENCE ON VENOMOTOR TONE AND HYPERTENSION

By

Irina Theodora Szasz

A DISSERTATION

Submitted to
Michigan State University
in partial fulfillment of the requirements
for the degree of

DOCTOR OF PHILOSOPHY

Microbiology and Molecular Genetics

2009

ABSTRACT

VASCULAR REACTIVE OXYGEN SPECIES METABOLISM AND ITS INFLUENCE ON VENOMOTOR TONE AND HYPERTENSION

By

Irina Theodora Szasz

Reactive oxygen species (ROS) are signaling mediators with multiple effects on vascular function. ROS and oxidative stress have been implicated in the pathogenesis of cardiovascular diseases such as hypertension. Veins and arteries both contribute to the regulation of blood pressure (BP). As compared to arteries, far less is currently known about venous ROS metabolism and its functional impact. We tested the hypothesis that the metabolism and handling of ROS would be different in veins compared to arteries and that venomotor function, as influenced by ROS, would play a role in experimental hypertension.

We observed higher superoxide and hydrogen peroxide (H_2O_2) levels, as well as higher antioxidant capacity for H_2O_2, in rat venous compared to corresponding arterial tissues. There were multiple differences in ROS metabolizing enzymes between arteries and veins, such as a higher expression of DUOX1, CuZn SOD and catalase in venous compared to arterial tissue. Xanthine oxidase (XO) had a higher protein and mRNA expression, as well as higher activity in veins compares to arteries. During deoxycorticosterone acetate (DOCA)-salt hypertension, the higher expression of XO was maintained by veins, and there were indications of an increase in venous, but not arterial XO activity. The

contractile impact of ROS was also higher in veins compared to arteries. XO appeared to play little role in normal arterial contractile function, however it seemed to contribute to normal venous ET-1-mediated contraction. In normotensive rats, the endothelial function of arteries and veins was similar. During DOCA-salt hypertension, arteries, but not veins, were affected by endothelial dysfunction. XO did not appear to contribute to the arterial hypertensive dysfunction by either ROS or urate production. We inhibited XO activity *in vivo* using the XO inhibitor allopurinol, expecting as consequences a lowering of venomotor tone and therefore an effect on BP depending on the administration timing: either a lowering of BP if allopurinol was administered when DOCA-salt hypertension was established or an attenuation of hypertension development if it was administered before the DOCA-salt treatment. We monitored XO metabolites in the urine, serum and tissues of allopurinol-treated animals, overall observing increases in XO substrates and decreases in XO products. Despite what we considered effective XO inhibition, we did not observe any effect on BP in DOCA-salt hypertensive rats, regardless of the timing of this intervention.

These results suggest there are differences in ROS metabolism and functional impact inherent to the blood vessel type. Although we believe we excluded the involvement of XO in DOCA-salt hypertension pathogenesis, further studies are needed to uncover the role of ROS in venous contractile function and hypertension pathogenesis.

ACKNOWLEDGEMENT

Over the course of time I spent as a PhD student, I have had the privilege and pleasure of working with and learning from a number of remarkable people.

I thank, first and foremost, my mentor, Dr. Stephanie Watts. I am a scientist today because of her. She supported me in countless ways professionally and personally. Her energy, generosity and honesty are an inspiration for the future mentor I hope to become. There truly are not enough words to express my gratitude for her. Thank you, Stephanie!

I thank Dr. Wei Ni and Dr. Keshari Thakali, who have both helped me in the beginning of my PhD and have remained not only my models but also my friends.

I have the utmost respect for the rigorous scientific methods applied by our technicians. I learned a lot of technical subtleties from Janice Thompson, who also helped me immensely in the everyday life of the lab; and Robert Burnett provided crucial help for a big part of the experiments contained within my thesis. I am extremely grateful for their support.

I thank the other graduate and undergraduate students who are or have been in the Watts lab, especially Patrick Davis, whose practical and moral support were and are invaluable, and Becca Sattler-Leja, my first student, who probably taught me at least as much as I taught her and who has also helped with a lot of experiments contained within this thesis.

I owe the Department of Microbiology and Molecular Genetics my being here and I consider myself privileged to have been admitted into its graduate program. I am also grateful to Drs Gregory Fink, Andrea Amalfitano, Susan Conrad and Richard Schwartz, who, as members of my guidance committee, have been instrumental in providing me with a lot of valuable feed-back that helped refine and strengthen my work.

I have benefitted scientifically from being a part of the PPG group at MSU and collaborating in various ways with Dr. Galligan, Dr. Fink and the people in their laboratories. I am also grateful to the Department of Pharmacology and Toxicology in its entirety, which has been my happy research home throughout these years.

I am honored to have received a predoctoral fellowship from the American Heart Association, which has financially supported a large part of my PhD.

My special thanks go to Dr. Elizabeth Linder, my colleague, mentor and most important, the best friend one could ever dream of. I am lucky to have met Elizabeth and I hope to always have her in my life.

I would not exist without the infinite support of my friends and family: Miha Marina, all my friends from around the world, and the entire Szasz family (Ivan, Lili, Dan, Gina and Cristi).

TABLE OF CONTENTS

LIST OF TABLES

LIST OF FIGURES

Images in this dissertation are presented in color.

LIST OF ABBREVIATIONS

4-HNE	4-hydroxy-nonenal
ACh	acetylcholine
Ang II	angiotensin II
BCA	bicinchoninic acid
BH_4	tetrahydrobiopterin
BP	blood pressure
BSA	bovine serum albumin
CA	carotid artery
CO	cardiac output
COX	cyclooxygenase
CVD	cardiovascular disease
DBP	diastolic blood pressure
DDC	diethyldithiocarbamate
DOCA	deoxycorticosterone acetate
DPI	diphenyleniodonium
DUOX	dual oxidase
ET-1	endothelin 1
H_2O_2	hydrogen peroxide
HPLC	high performance liquid chromatography
HSV	human saphenous vein
HUVEC	human umbilical vein endothelial cell
IMA	internal mammary artery
JV	jugular vein
LNNA	Nω-Nitro-L-arginine
LOX	lipoxygenase
MAP	mean arterial pressure

MCFP	mean circulatory filling pressure
NADPH	nicotinamide dinucleotide phosphate (reduced)
NE	norepinephrine
NOS	nitric oxide synthase
$PGF_{2\alpha}$	prostaglandin F 2 alpha
PE	phenylephrine
PSS	physiological salt solution
ROS	reactive oxygen species
RT-PCR	real time polymerase chain reaction
SBP	systolic blood pressure
SEM	standard error of the means
SHR	spontaneous hypertensive rat
SMA	superior mesenteric artery
SMV	superior mesenteric vein
SOD	superoxide dismutase
TPR	total peripheral resistance
UA	uric acid
VC	vena cava
VSMC	vascular smooth muscle cell
XDH	xanthine dehydrogenase
XO	xanthine oxidase

INTRODUCTION

I. General characteristics of arteries and veins

A. Structure

Arteries and veins, two separate components of the vascular system, are different structurally and functionally. While arteries carry oxygenated blood from the heart to the peripheral tissues at a high pressure, therefore requiring a more elastic and muscular structure, veins carry blood from the tissues back to the heart at a low pressure, providing capacitance, therefore requiring more distensible, less muscular walls (fig 1).

Both artery and vein are composed of similar layers: the innermost layer or the tunica intima, containing endothelial cells; the tunica media, which is largely composed of smooth muscle, elastin and collagen; and the outermost tunica adventitia, containing mainly fibroblasts, collagen and elastin. Small blood vessels called *vasa vasorum* integrate into the adventitia of larger vessels, providing nutrients to the vascular wall itself.

Several characteristics, in addition to a different distribution and relative abundance of these layers, distinguish arteries from veins. The delineation of the three layers is more obvious in an artery compared to a vein. This is particularly illustrated when viewing the thoracic vena cava *vs* the thoracic aorta from the same rat (fig 2). The media of an artery, flanked by two elastic laminas, is typically thicker than that of a vein, while the elastic component of a vein is

smaller compared to that of an artery, in favor of a much larger adventitial component in the vein. The greater relative contribution of the smooth muscle layer to the thickness of the vascular wall in arteries compared to veins can be appreciated in figure 2A. These differences are confirmed by immunohistochemical staining for α-actin, a smooth muscle marker (fig 2B). Larger veins possess venous valves on the luminal side of the wall, which help prevent backflow of blood. The cardiovascular system is not abruptly split into the two components (arteries and veins). Rather, a gradual transition of tissue characteristics ensues: from the heart to the large elastic arteries, then smaller muscular arteries/arterioles to, finally, the capillary section, having just one endothelial layer, and then back from the peripheral tissues, through less muscular venules, to large capacitance veins possessing all the components of the vessel wall and back to the heart (43).

B. Function

Due to these structural differences, there are also inherent differences in the contractility and synthetic properties of arteries and veins that can impact overall cardiovascular function. These differences in contractility, however, may vary according to vascular beds, similarly to the structural differences. The magnitude of the contractile force developed by a vein in response to receptor-dependent and independent agonists is smaller compared to that developed by an artery. The time needed to reach half maximal contraction, a measure of response

speed, is shorter for a vein than for an artery (61) The capacity to relax in response to certain agonists that induce the production of endothelium-derived relaxant factors is decreased in veins compared to arteries, in some vascular beds (70, 125, 131). Similarly, specific differences exist in the contractile response of arteries and veins to a series of receptor-dependent agonists, the best studied of them being endothelin-1 (ET-1), a potent, though not selective, venoconstrictor. There seem to be fundamental arterial-venous differences in the endothelin system, such as receptor expression and interaction (153), processing of endothelin-related peptides (169) or functional responses to endothelin peptides and ET receptor agonists (152, 167).

Different properties of arterial and venous grafts used in bypass surgery, leading to different outcomes, have stimulated research on comparing these vessel types and the factors that influence their long term patency. Venous smooth muscle cells appear to have a higher growth rate compared to their arterial counterparts, both in basal conditions (177) as well as in response to various mitogenic stimuli. Endothelium function is also different in veins compared to arteries. Venous endothelium produces less prostacyclin (101) and NO (130) than arterial endothelium, and its overall response to atherogenic stimuli is different. Endothelial intercellular junctions are generally tighter in arteries than in veins. In venules, at the post-capillary level, the organization of these junctions is especially loose, thus making this sector of vasculature the primary site of inflammatory permeability (23).

These intrinsic properties ultimately reflect the difference in the gene expression pattern of arteries and veins. The most prominent differences in basal gene expression between arteries and veins can be seen in the signaling molecules that regulate selective expression of Eph-B_4 (receptor) in veins and ephrin-B_2 (ligand) in arteries, creating a cell-cell interaction system that establishes arterial and venous endothelial identity during vasculogenesis (179). Other differences with significant potential for influencing specific vascular function have been identified through the use of gene arrays (1, 24, 25, 112). Although most of these studies focus on the endothelium and the vascular smooth muscle layers of these blood vessels, fibroblasts and other components of the adventitia could also play important roles in vascular function and pathogenesis. Our studies on whole genome expression profiling of rat aorta and vena cava whole tissues have indicated a potential anti-inflammatory/anti-apoptotic profile of venous compared arterial tissue (145).

Several arterio-venous differences in properties may also be explained by the differences in the characteristic environment each of these blood vessel types is exposed to. The most obvious of these factors is the higher pressure regime experienced by arteries compared to veins. The blood flow and the resulting shear stress are also considerably higher in arteries compared to veins. Venous blood, carrying metabolites and lymph products, is also less oxygenated than the arterial blood, and characterized by a lower pH (43).

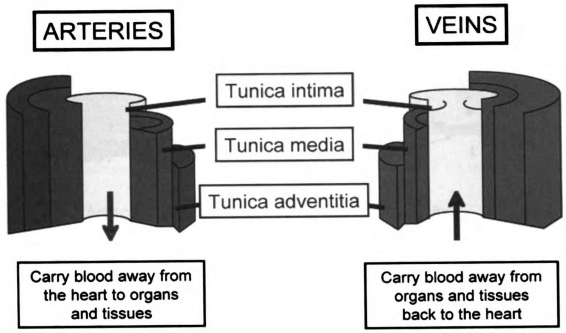

Figure 1. Diagram of generic artery and vein.

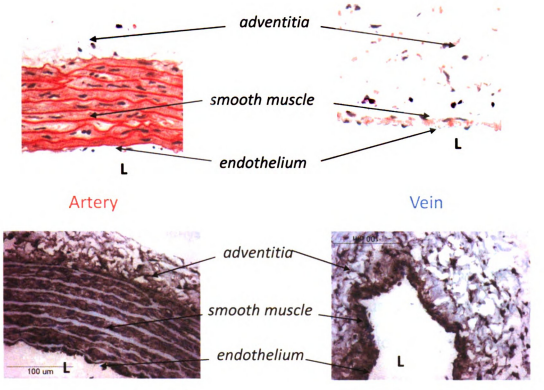

Figure 2. A. Modified trichrome Masson staining of rat aorta (left) and vena cava (right). **B.** Immunohistochemical staining for alpha-actin in rat aorta (left) and vena cava (right). Blood vessel layers are indicated by arrows. The luminal side is indicated by L.

C. Pathology

There are overall differences in the venous response to pathophysiological conditions that commonly affect arteries, such as atherosclerosis or hypertension, when veins do not undergo the same atheromatous, remodeling or endothelial dysfunction changes observed in arteries (43, 168).

Almost all vascular research currently performed is focused on arteries, while veins are generally overlooked when considering the contribution of the vascular system to systemic pathophysiology. Yet, besides being a passive clearance conduit of every organ and tissue, veins hold most of the circulating blood (~70%). This volume can be actively moved by venous contraction or external compression (121), making veins a potential contributor to the pathophysiology of hypertension (detailed below). Venous grafts are used in coronary artery bypass graft (CABG) surgery with different properties and outcomes compared to arteries (101, 132). Additionally, veins also develop specific pathologies, such as deep vein thrombosis and chronic venous insufficiency. Although they do not constitute the particular focus of this work, all these facts point out the need for a better understanding of the basic physiology of the venous system.

II. The role of veins in blood pressure regulation and hypertension

A. Hypertension epidemiology

Cardiovascular disease (CVD) is the leading cause of death in USA and globally for both women and men, with an estimated 17 million deaths/year worldwide (93). In USA, each year, CVD causes more deaths than the next four leading causes of death combined (cancer, accidents, chronic lower respiratory diseases and diabetes melittus). Examples of CVD include coronary heart disease, cerebrovascular disease, hypertension and congestive heart failure (89).

Hypertension (high blood pressure) is defined as a systolic blood pressure (SBP) higher than 140 mmHg and/or a diastolic blood pressure (DBP) higher than 90 mmHg. Currently, hypertension afflicts approximately a quarter of the adult population (93). Due to the health risks associated with high blood pressure, a condition called "pre-hypertension" was recently defined as a SBP between 120-139 mmHg and/or a DBP of 80-89 mmHg. In the US, approximately 37% adult population is prehypertensive (89).

Hypertension contributes to CVD not only by itself but also as a major risk factor for other CVDs, such as coronary artery disease, heart failure, peripheral artery disease and stroke. Thus, half of the patients with a first heart attack and two thirds of those with a first stroke are hypertensive. Although largely asympthomatic, hypertension – "the silent killer" – can lead to serious complications of target organs (heart, brain, kidney, eye, peripheral arteries). In USA alone, the total estimated costs for high blood pressure in 2009 are $ 73.4 billion (89). These statistics have remained almost unchanged in spite of research efforts that have resulted in significant progress in hypertension therapy in the last decades. The cause of hypertension is unknown in around 90% of

cases (essential hypertension), most likely a multitude of hereditary as well as environmental factors contributing to its occurrence.

B. Mechanisms of blood pressure regulation

Blood pressure (BP) is a highly regulated physiological parameter, its control being ensured by many complex systems and organs, such as the autonomic nervous system, the kidney or the vascular system (fig 3). BP is a direct product of two major cardiovascular parameters: cardiac output (CO) and total peripheral resistance (TPR), an increase in either one or both leading to an increase in BP. The vascular system plays a major role in this equation by changing its tone (contraction) or structure (remodeling). Thus, the arterial side is responsible for increases in TPR, while the venous side influences the CO. CO is also critically influenced by the contractility of the heart and by the volume of blood, in its turn controlled by the kidney.

C. Role of veins in hypertension

In most cases of established human hypertension there is an increase in TPR without changes in the CO. Therefore the prevailing opinion in the field is that hypertension is caused by changes in the tone and/or structure of small arteries and arterioles, and the majority of hypertension research is being conducted on renal, autonomic nervous system and arterial mechanisms of increases in TPR

(144). However, more recent reports point to the potentially critical role of veins during the developmental stages of hypertension (39, 96, 111, 120, 174). The vascular system can be viewed as a fluid holding system, the pressure of which will be determined by both the total volume of fluid contained and by the distensibility, or the fluid holding capacity of the system. With no changes in blood volume or myocardium contractility, a key factor that determines CO and BP is the vascular capacitance, or the blood holding capacity of the vascular system. Due to the structural differences discussed above, veins have a much higher compliance compared to arteries (30 times higher), resulting also in a much higher capacitance compared to arteries. Thus, ~70% of the total circulating blood volume resides in veins, particularly veins in the splanchnic region. The smallest changes in venomotor tone may therefore have a large impact on this volume of blood (106), which thus shifted, is redistributed to the central, less distensible, compartment of circulation (composed of larger veins such as the vena cava), which then directly affects the "effective blood volume" or the volume of blood contained in the arterial circulation, with immediate effects on blood pressure (38, 91, 126).

There are several lines of evidence supporting the role of veins in hypertension. Borderline, as well as early human hypertension (initial stages), are correlated with increases in central blood volume and/or CO, as well as decreased venous compliance (90, 91, 126). Venous capacitance is also decreased in the established stage of human hypertension (90). Additionally, increases in mean circulatory filling pressure (MCFP), which is a gross measure of venomotor tone

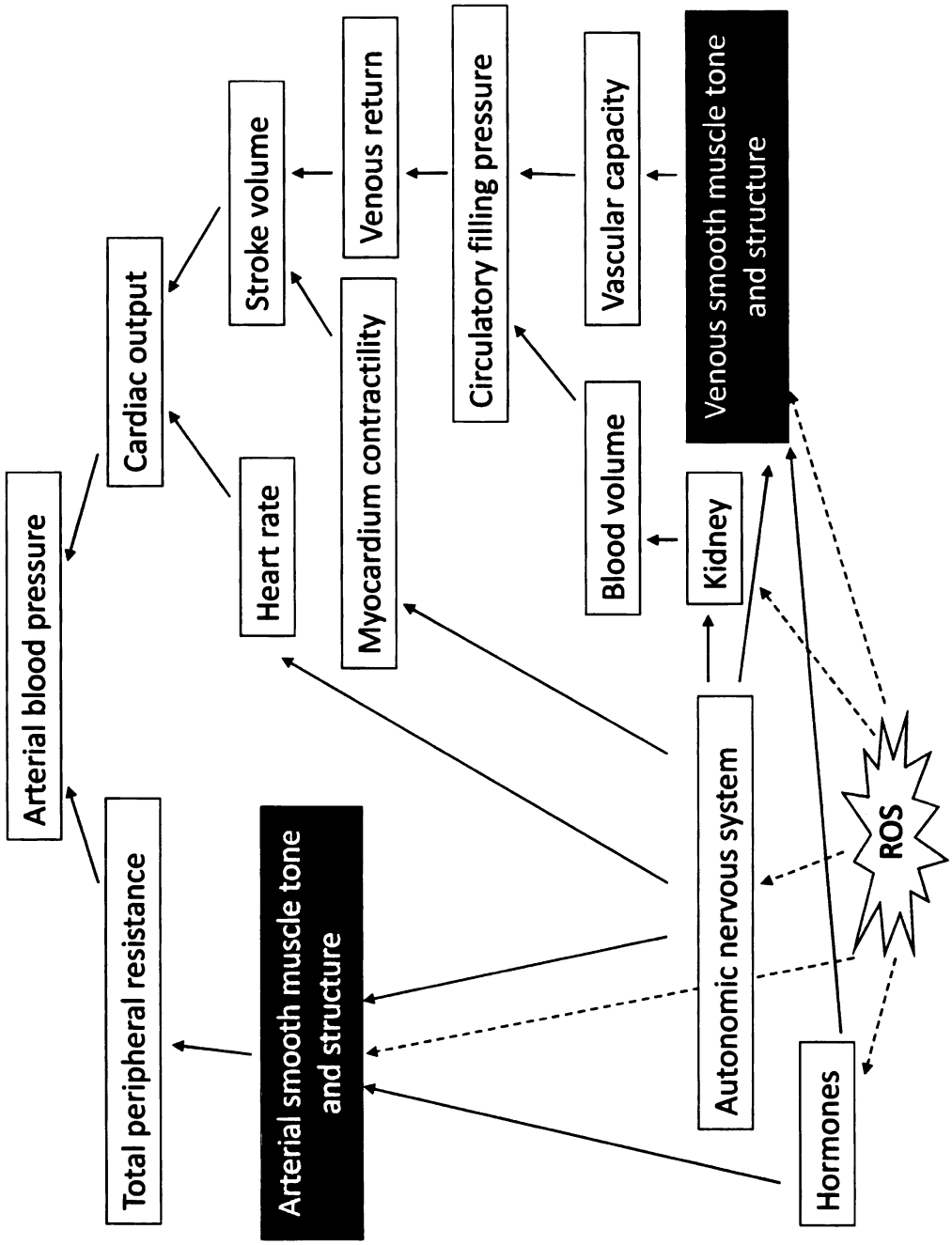

Figure 3. Diagram of blood pressure regulation systems and organs. The potential places of modulation by reactive oxygen species are indicated with dashed arrows.

and a direct determinant of CO at a constant blood volume, were observed during established mineralocorticoid hypertension in rats (39), in the developmental stages of hypertension in the spontaneous hypertensive rat (96), as well as in Goldblatt renal hypertensive rats (174). These changes appear causative, rather than adaptive, since the increase in MCFP preceded that in BP.

These data further support that the hemodynamic impact of venoconstriction on blood pressure may be important. Thus, changes in venomotor tone in the initial phases of hypertension may lead to a dynamic redistribution of blood that triggers an increase in BP. Subsequently, arteries adapt to the new pressure regime by remodeling towards a less elastic, more muscular and fibrous structure, with increased TPR, that then drives the sustained increase in blood pressure.

III. Vascular reactive oxygen species (ROS) metabolism

A. ROS chemistry

ROS are important vascular signaling molecules or mediators of oxidative stress. They are, by definition, highly reactive intermediates of oxygen metabolism, constantly being generated and destroyed by both environmental and endogenous systems. Produced by a gradual reduction of molecular oxygen, ROS include both unstable free radicals (chemical species having unpaired electrons in their outermost shell) like the superoxide or the hydroxyl radical, and longer-lived non-free radical oxidants like hydrogen peroxide (H_2O_2) (fig 4). A

Figure 4. Basic diagram of reactive oxygen species metabolism.

related family of reactive intermediates bearing importance in vascular biology is the reactive nitrogen species (RNS), including nitric oxide (NO) and the series of radicals produced after the interaction of the latter with the superoxide anion.

The delicate balance in the continuous cycle of ROS generation and inactivation is maintained by enzymatic and non-enzymatic endogenous systems. We have previously reviewed the subject of ROS metabolism in arteries and veins (146). The various producers and destroyers of ROS are listed (table 1), but only the most comprehensively studied ones will be detailed in the following section. Their order does not bear any reflection of their relative importance, overall or specifically in vascular tissues.

B. Cellular mechanisms of ROS production

1. Mitochondria

The mitochondrial respiratory chain is the main energy source for the cell. Situated in the inner mitochondrial membrane, it catalyzes electron transfer using over 80 peptides organized in four complexes. The transfer of electrons, shuttled by coenzyme Q and cytochrome C, usually leads to the formation of ATP by a fifth complex. However, a certain amount (1-2% *in vitro*) of electrons leak (40), principally from complex III but also from complex I, generating superoxide (134, 138). The rate of mitochondrial ROS production, the levels of mitochondrial DNA oxidative damage and the degree of membrane fatty acid unsaturation (potentially a target of lipid peroxidation by ROS) are all inversely linked to

ROS producers	ROS destroyers
Mitochondrial respiratory chain	Superoxide dismutase family
Nox and Duox families	Catalase
Xanthine oxidase	Glutathione system
Superoxide dismutase family	Selenoproteins (glutathione peroxidase,
Uncoupled nitric oxide synthase	thioredoxin reductase, etc)
Monoamine oxidase	Peroxiredoxins
Lipoxygenase	Antioxidant ROS scavengers (A,C, E
Cyclooxygenase	vitamins, ceruloplasmin, ubiquinone, uric acid,
Cytochrome P450	bilirubin, etc)
Haber-Weiss and Fenton reactions	NO
Environment (ionizing radiation, etc)	Uncoupling proteins (?)
NO (reactive nitrogen species)	

Table 1. Reactive oxygen species sources and degradation systems.

maximum longevity in animals (5). These facts are among the evidence that supports the free radical theory of aging. Since superoxide production is directly dependent on the proton motive force, a feedback mechanism has been proposed for the uncoupling proteins (UCP 1, 2 and 3). Activated by superoxide and lipid peroxidation, these proteins seem to act by slightly reducing the proton motive force and hence energy production as a trade-off for a decreased ROS production from the mitochondrial complexes I and III (12, 30).

Several lines of evidence indicate mitochondria may be critically involved in cardiovascular disease pathogenesis, by altered mechanisms related to mitochondrial mediated ATP generation, apoptosis and, more recently, calcium signaling (34). However the link between mitochondrial-mediated ROS production and cardiovascular disease is still a subject of investigation. Angiotensin II, famously stimulating superoxide generation through NADPH oxidase with many related important cardiovascular implications, may also activate superoxide release from mitochondria (73, 181). Potentially important vascular roles of mitochondrial ROS are highlighted by reports such as those suggesting that the protective effect of estradiol on cerebral vasculature endothelial function is mediated by a decrease in mitochondrial ROS production (26).

2. NADPH oxidases

The Nox family of NADPH oxidases is another major source of ROS. The classic example is the phagocytic NADPH oxidase, a multisubunit enzyme involved in

host defense. The phagocytic NADPH oxidase is composed of two membrane-bound catalytic subunits, Nox2 (formerly known as $gp91^{phox}$) and $p22^{phox}$, forming the central flavocytochrome b_{558}, and four cytosolic regulatory subunits, $p47^{phox}$, $p40^{phox}$, $p67^{phox}$ and Rac (29). NADPH oxidase requires for its activation a series of phosphorylation and translocation events, triggered by pathogen recognition (22). Deliberate generation of ROS by the professional phagocyte during the "oxidative burst" is a rapid and powerful weapon of defense against pathogens. A genetic lack of NADPH oxidase activity in patients suffering from chronic granulomatous disease (CGD), a condition characterized by recurrent, life-threatening infections, illustrates the importance of the beneficial side of ROS chemistry (29). Based on the homology with Nox2, several other members of the human Nox family have been identified, each of them seemingly having different activation requirements and expression patterns. Nox1, Nox3 and Nox4 are more similar in structure to Nox2 and they all require at least $p22^{phox}$ for activation. Duox1 and Duox2 are Ca^{2+}-activated dual oxidases with a C terminal NADPH oxidase domain and an N terminal peroxidase domain. Nox5 is closer to the Duox1/2 in structure and is also Ca^{2+}-activated, but lacks the peroxidase domain (140).

Several features of Nox enzymes expressed in blood vessels, that distinguish them from the generic phagocyte NADPH oxidase (129), have made researchers in the field collectively term them "the vascular oxidase". Compared to superoxide production from the phagocyte NADPH oxidase, vascular oxidase basal superoxide production is significantly lower (less than 1% (59)). While

phagocyte NADPH oxidase activity is primarily inducible, vascular oxidase has a constitutive activity that can be further increased by agonists like angiotensin II (124). Although not fully clarified, it appears that Nox4 is the subunit responsible for the constitutive vascular oxidase activity. The cellular site of superoxide production by vascular oxidase appears to also be different: vascular oxidase produced-superoxide has been repeatedly detected intracellularly (84). Finally, the physiological role of superoxide production by the blood vessel cells is distinct: instead of cytotoxic superoxide production as a defense mechanism against pathogens, ROS released by the vascular oxidase participate in cell signaling, consistent with their comparative low tissue levels (84).

Various endogenous and external stimuli modulate the NADPH oxidase subunits expression and/or activity. Expression of one or more of these subunits is upregulated in human umbilical vein endothelial cell (HUVEC) culture in response to angiotensin II, ET-1, oxidized LDL, pulsatile shear stress and phorbol myristate acetate (PMA) (27, 84, 95). They are conversely downregulated by treatment with statins, PPAR agonists or estradiol (84, 123). Angiotensin II, TGFβ, TNFα, serum, PDGF, $PGF_{2\alpha}$, PMA and LDL upregulated various NADPH oxidase subunits expression in the case of cultured arterial smooth muscle cell (84, 85). Long term treatment with AT_1 receptor blockers downregulated Nox2 mRNA expression in human artery biopsies (124).

In hypertension, the already increased vascular superoxide generation is further increased with NADH or NADPH and lowered through treatment with the NADPH oxidase inhibitor apocynin (6, 87). Aortic mRNA expression of $p22^{phox}$ is

increased in the DOCA-salt (10) and SHR (180) models of hypertension. The angiotensin II infusion hypertension model has increased expression of all NADPH oxidase subunits (100). In the same model, inhibition of NADPH oxidase activity by treatment with gp91 ds-*tat*, a chimeric peptide that blocks the association of $p47^{phox}$ with Nox2, lead to a decrease in superoxide production and attenuated the AngII-induced BP elevation (119).

3. Xanthine oxidase

Xanthine oxidoreductase (*XOR*) is an evolutionarily conserved housekeeping gene, encoding for an enzyme that catalyzes the last steps of purine metabolism (fig 5): the transformation of hypoxanthine and xanthine to uric acid, with superoxide generated as by-product. XOR is a flavoprotein that possesses one molybdopterin, two iron-sulfur groups and one FAD, functions as a 145 KDa homodimer, and has ~90% homology from mouse to rat to human (11). There are two isoforms of XOR, each of them utilizing different electron acceptors: xanthine dehydrogenase (XDH), which requires NAD^+; and xanthine oxidase (XO), which requires molecular oxygen. XDH is convertible to XO by reversible sulfhydryl oxidation or by irreversible proteolytic modifications (105). Although both isoforms have ROS generating potential, *in vivo* XO is by far the more important superoxide/H_2O_2 source, making XDH to XO conversion in situations such as ischemia/reperfusion or inflammation of pathophysiological significance (53). XO and its potential pathophysiological role in cardiovascular disease are discussed in greater detail below.

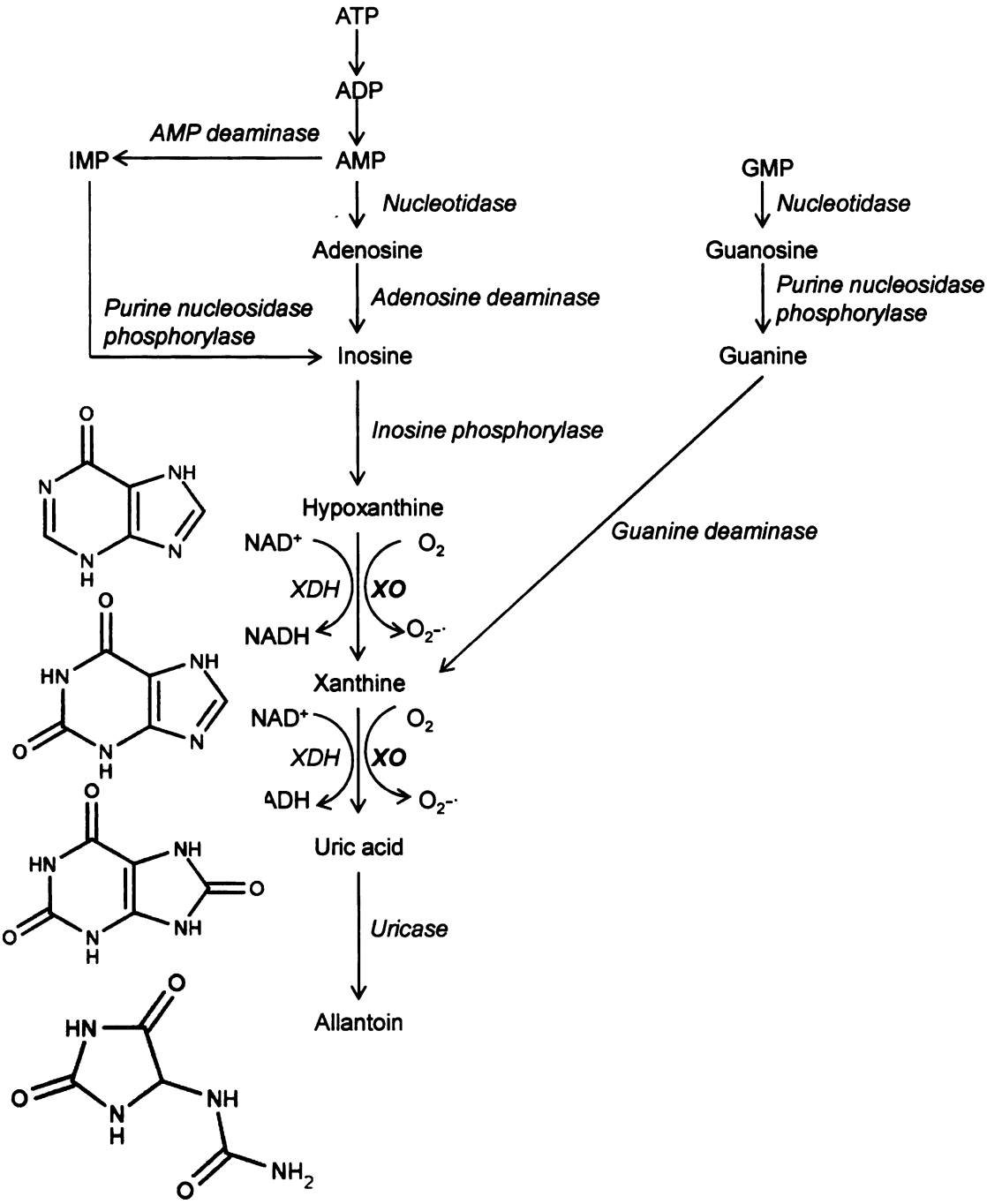

Figure 5. Purine catabolism. Structures of hypoxanthine, xanthine, uric acid and allantoin are displayed on the left.

4. Nitric oxide synthase (NOS)

NOS, the enzyme responsible for NO generation, has three isoforms: NOS1 (the neuronal NOS), NOS2 (the inducible NOS) and NOS3 (the endothelial NOS). In physiological conditions, NOS catalyzes the transformation of L-arginine into L-citrulline and NO, using several cofactors: NADPH, FAD, FMN and 5,6,7,8 tetrahydrobiopterin (BH_4). However, if the enzyme is depleted of BH_4 or of L-arginine, it becomes uncoupled, and transfers electrons to molecular oxygen rather than the substrate L-arginine, producing superoxide (41). Furthermore, interaction of superoxide with nitric oxide generates peroxynitrite, the second in the family of reactive nitrogen species, capable of producing a cascade of deleterious effects through oxidation, nitration and nitrosation of molecules (8).

The classical view on nitric oxide synthase isoforms is summarized in their alternative names: the neuronal NOS (NOS1), and the endothelial NOS (NOS3) have constitutive expression in neurons and endothelial cells, respectively, while the inducible NOS (NOS2) is the only calcium independent, transcriptionally-regulated isoform, typically found in macrophages (128). This paradigm has changed considerably in recent years: all three isoforms have been identified in arteries and veins, as well as in HUVEC culture. Furthermore, red blood cells appear to express a membrane associated NOS3, capable of modulating vascular tone (75). Recent studies have even suggested a mitochondrial-specific NOS (80), although its existence has not been proven yet. To our knowledge, no study has yet compared arteries and veins in terms of NOS isoforms expression.

Normal endothelial function, crucial in maintaining cardiovascular homeostasis, depends, among others, on normal NOS functioning. A reduction in the arterial endothelium-dependent vascular relaxation, defined as endothelial dysfunction, has been documented in atherosclerosis and hypertension. Besides decreased NO bioavailability, a malfunctioning NOS can also influence vascular function by becoming uncoupled, in the absence of L-arginine or BH_4, with consecutive production of superoxide and potentially peroxynitrite. Further uncoupling can occur by oxidation of the existent BH_4 (127). The role of BH_4 depletion in NOS uncoupling and hypertension development is illustrated by the fact that treatment of DOCA-salt hypertensive mice with BH_4 leads, by recoupling of NOS, to lowering of BP (82). Uncoupling of NOS does not occur in $p47^{phox-/-}$ mice, supporting the idea that NADPH oxidases are required for BH_4 oxidation. There is no clear evidence indicating that NOS uncoupling follows the same rules in veins as it does in arteries.

C. Cellular mechanisms of ROS destruction

1. Superoxide dismutases (SODs)

A central role in the regulation of ROS levels is attributed to superoxide dismutases, a family of enzymes responsible for superoxide breakdown, with the resultant production of H_2O_2. This otherwise spontaneous dismutation reaction (at rates dependent on superoxide concentrations) is significantly accelerated by SOD, the enzyme with the highest turnover number from all characterized

enzymes. There are three known SODs: the cytosolic CuZn SOD (SOD1), an unusually stable homodimer, the mitochondrial Mn SOD (SOD2), functioning as a tetramer, and the extracellular EC-SOD (SOD3), a tetramer with a C terminal heparin binding region. There is a great body of evidence supporting the beneficial role of SOD (31, 65, 94). Knock-out experiments showed neonatal lethality of mice lacking Mn SOD and reduced lifespan and multiple abnormalities in mice lacking CuZn SOD. Furthermore, overexpression studies of SODs strongly suggest a protective role of these enzymes in many diseases as well as in aging. Additionally, mutations in the SOD1 gene leading to the production of a toxic variant of CuZn SOD are linked to 20-25% cases of familial amyotrophic lateral sclerosis (FALS or Lou Gehrig's disease), a fatal neurologic condition (114).

The blood vessel wall of both arteries and veins expresses all three SODs. The cytosolic CuZn SOD has ubiquitous and high expression throughout the vascular layers. Mitochondrial Mn SOD is relatively less expressed compared to CuZn SOD and EC-SOD, but is also ubiquitous (31). Extracellular SOD, produced largely by VSMC, is localized between arterial intima and media (139) and is thought to contribute substantially to the total SOD activity in the vasculature. In addition to its primary and important role in scavenging extracellular superoxide, EC-SOD may also be expressed intracellularly and translocated to the nucleus *via* its heparin-binding domain, which could function as a nuclear localization signal (NLS) (109). Rats have lower vascular EC-SOD levels compared to other species, due to a change in the amino acid sequence of the protein that leads to

lower heparin binding, potentially influencing the results of SOD expression studies performed in this species (31).

Arterial expression and/or activity of CuZn SOD and Mn SOD increased in animal models of hypertension (160, 161). EC-SOD deficient mice had higher blood pressures in two hypertension models compared to the wild type animals (67). Conversely, overexpression of EC-SOD improved vascular function in hypertensive animals (17).

2. Catalase

Catalase is a homotetrameric heme-containing enzyme that catalyzes the conversion of H_2O_2 into water and oxygen with one of the highest turnover rates known in enzymology (~10^7 l/mol/sec). Catalase is usually found in peroxisomes, cellular organelles involved in multiple metabolism pathways, where it functions in detoxification of H_2O_2 resulted from SOD action on superoxide (155). If not otherwise inactivated, H_2O_2 may continue the ROS cascade with the formation of the hydroxyl radical. The latter, generated through a reaction with transition metals such as Fe^{2+} *via* the Fenton/Haber-Weiss chemistry (fig 3), is a highly reactive radical that to our knowledge cannot be destroyed enzymatically. The only protection from its dangerous oxidative potential is therefore left to antioxidant scavengers and metal chelators.

Catalase, as well as other ROS enzymes, has been correlated with aging. There is not a clear association between catalase function and cardiovascular disease. Catalase mutations have been linked with hypertension (182). Mice

overexpressing catalase have shown evidence of cardioprotection from adriamycin-induced ischemia-reperfusion (58), as well attenuation of BP increases in response to norepinephrine and angiotensin II (176). However, catalase null mice do not have an obvious cardiovascular phenotype (58).

3. Other ROS degrading systems

Another ROS consuming system is the glutathione redox cycle. Glutathione peroxidase transfers electrons from the reduced form of glutathione to H_2O_2 with the formation of water and oxygen; subsequently, the oxidized glutathione disulfide is reduced by glutathione reductase. There are other selenoproteins with similar activity to glutathione peroxidase, such as thioredoxin reductase or selenoprotein P, all of which work as antioxidant enzymes.

Because of their widespread therapeutic use as antioxidants, endogenous ROS scavengers such as vitamin C and E should also be noted. However, when considering the antioxidant properties of such compounds, it should be appreciated that they are not enzymes, therefore a new molecule is needed for each superoxide anion that is scavenged. These vitamins are therefore poor ROS scavengers. Clinical trials testing antioxidants on cardiovascular disease patients have found no evidence of beneficial effects on BP or other common cardiovascular end-points – the so-called "oxidative paradox" (76). However, these trials were conducted with orally-administered, weak ROS scavengers only active on superoxide, but not on H_2O_2. Numerous other factors (such as the insufficient doses or their unknown intracellular concentration and activity) have

been overlooked. Most importantly, these trials included patients with chronic cardiovascular disease, where increased ROS could already be a disease effect rather than a pathogenetic factor.

IV. ROS involvement in vascular function

ROS mediate effects in all three blood vessel layers. At the endothelial level, superoxide directly interacts with NO and decreases its bioavailability, while the resultant peroxynitrite may oxidize BH_4 leading to eNOS uncoupling, further decrease in NO levels and increase in superoxide production (8, 127). At the smooth muscle level, both superoxide and H_2O_2 may interfere with K^+ and Ca^{2+} channel function, as well as with signaling pathways that modulate vascular contraction: MAPK, PI3 kinase, and Rho kinase (2, 13). Additionally, ROS may stimulate signaling pathways that mediate the expression of pro-inflammatory molecules (such as NF-κB), as well increase the proliferation and migration of vascular smooth muscle cells (VSMCs), properties that become relevant in the case of cardiovascular disease such as atherosclerosis and hypertension (18, 157). In the adventitia, ROS induce collagen production, as well as metalloprotease activation, both these effects contributing to the arterial remodeling observed in hypertension (54, 157). A summary diagram of vascular effects of ROS is presented in figure 6.

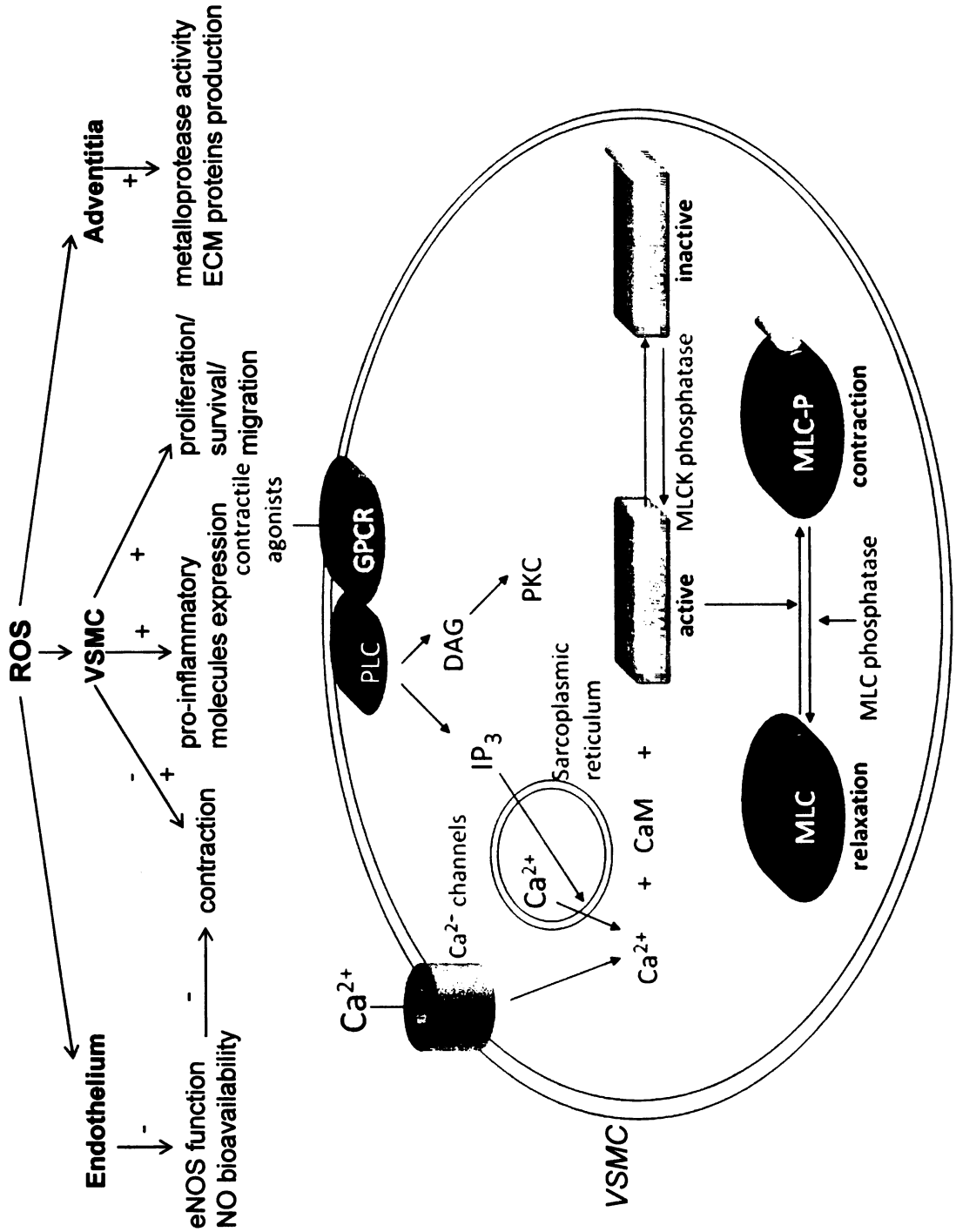

Figure 6. Diagram summarizing the effects of ROS on vascular function. +, - represent stimulation and inhibition, respectively. The mechanisms responsible for the vascular contraction in response to agonists relevant to this work (such as norepinephine, angiotensin II or endothelin-1) are represented below.

V. Comparisons of arterial and venous ROS metabolism

Few studies have compared basal ROS production in arteries and veins, and their conclusions were contradictory. Basal superoxide production, measured through nitroblue tetrazolium reduction to formazan, was increased in porcine venous grafts compared to arterial grafts (132). In contrast, using lucigenin-enhanced chemiluminescence, no difference in basal superoxide production was found in rings from human internal mammary artery (IMA) compared to saphenous vein (HSV) (51). These were however blood vessels from patients with cardiovascular disease, and from two different vascular beds. The increase in superoxide release, following the addition of the NOS inhibitor, L-NMMA, was greater in human arteries (IMA) compared to veins (HSV) (52). This suggests a greater basal NO production in arteries that contributes to the quenching of superoxide in comparison to veins. Accordingly, basal peroxynitrite formation was higher in IMA compared to HSV (52).

Besides this quantitative difference in ROS production between arteries and veins, there is probably also different utilization of ROS by arteries and veins, both in physiological cell signaling and in oxidative stress during vascular pathogenesis. For instance, H_2O_2 modulates vascular tone, acting as a contraction-inducing agent in some vascular beds and as a relaxant in others (44, 150). There is a greater contraction to H_2O_2 in veins compared to arteries, possibly reflecting a difference in K^+ channel activity and Ca^{2+} influx (150).

Only one research group has systematically compared ROS sources in human arteries and veins (Guzik *et al* (50-52)). These studies have shown that subunits of NADPH oxidase ($p22^{phox}$, $p47^{phox}$ and $p67^{phox}$ proteins as well as $p22^{phox}$ and Nox2) mRNA are present and increased in abundance in the human saphenous vein (HSV) compared to the internal mammary artery (IMA). Nox4 mRNA expression was higher in the IMA and Nox1 mRNA had similarly low expression in both types of vessels. In a study employing the use of specific chemical inhibitors, NADPH oxidase contribution to the total basal vascular superoxide production was found to be more important in the case of HSV compared to the IMA, while xanthine oxidase seemed to have a more significant contribution in the case of IMA. No significant difference was found between these vessels in terms of their CuZn SOD (cytosolic SOD isoform) and Mn SOD (mitochondrial SOD isoform) protein expression and activity.

VI. Oxidative stress and role of ROS in hypertension

In certain amounts, ROS are normal constituents of cells, participating in physiological signaling processes, the extent of which is yet to be determined. However, increased ROS levels in the cell, resulting either from their overwhelming generation or impaired destruction, have a substantial impact on normal cellular function. This imbalance between prooxidant and antioxidant factors, defined as oxidative stress, can affect cellular homeostasis either through direct oxidative damage of basic cellular components (proteins, lipids

and nucleic acids) or through the activation of various redox sensitive signaling pathways leading to defective cellular function, aging, disease or apoptosis. ROS involvement in cellular signaling has been reviewed extensively. In summary, a series of major signaling pathways, such as MAPK, PI3K/Akt, NF-κB, p53 and the heat shock response can potentially be activated in response to ROS or oxidative stress. In the vascular system, oxidative stress can impair function through direct oxidative damage, endothelial dysfunction, decreased NO bioavailability, impaired contractility, platelet aggregation and ROS mediated inflammation, proliferation and remodeling (18, 54, 127, 157).

The presence of increased markers of oxidative stress (peroxidized lipids, oxidized proteins, increased GSSG, 8-oxo-guanine, DNA breaks, etc) has been identified in many pathophysiological situations. However, in most cases, establishing whether oxidative stress plays a causal role or is a mere reflection of the effects of the disease process itself on cellular function has proven to be a difficult task.

As far as hypertension is concerned, a great body of evidence supports the idea that ROS are involved in its pathogenesis. Increased markers of oxidative stress are found in human hypertensive subjects as well as in various animal models of hypertension (118, 149, 157). Treatment of these models with ROS scavengers or SOD mimetics (57, 108, 173), inhibitors of NADPH oxidase (10, 119, 170), inhibitors of xanthine oxidase (103, 163), BH_4 (157), targeted gene delivery of SOD (35) or NADPH oxidase inhibitors (68, 170) normalizes BP or prevents the development of hypertension and/or attenuates target organ damage.

Furthermore, genetic deficiency in ROS-generating enzymes protects some animals from experimental hypertension (81), while lack of antioxidant capacity causes increased hypertension in others (31, 149).

VII. Xanthine oxidase: role in cardiovascular disease

A. XO expression

XO expression in blood vessels has been difficult to detect. Human small vessel arterial endothelium showed XO immunoreactivity (88), and XO mRNA was identified in cultured rat pulmonary arterial endothelial cells (28). Moreover, measurable XO activity has been detected in arteries and cultured endothelial cells. However, XO from the circulation can also bind to endothelial cells *via* heparin binding sites (62). Therefore, there is still some controversy on whether XO is functional in the blood vessel or is only acquired through association with blood.

B. XO activity

XO has previously been demonstrated as capable of generating ROS in normal vascular tissues (9, 16). Increased XO activity was observed in human atherosclerotic arteries, as well as in several animal models of hypertension, lending support to the idea of the contributing role of XO in cardiovascular disease. The spontaneously hypertensive rat (SHR) displayed increased renal

XO activity during the development of hypertension (79). The same model exhibited higher mesenteric artery XO activity (141). Similarly, mesenteric artery XO activity was increased in the DOCA-salt model of hypertension (16). Both the expression and the activity of XO were increased in aorta of aging rats (104). The increase in ROS production in cultured arterial endothelial cells in response to shear stress has been attributed to XO activity (98). Increased superoxide production by XO was observed in coronary arteries from patients with coronary artery disease (136).

XO effects in pathophysiology may be mediated by at least one other mechanism that is not related to XO-mediated ROS production: the production of uric acid, a molecule with controversial cardiovascular effects that can act both as an antioxidant and as a deleterious by-product (see below).

C. Uric acid in vascular biology

Uric acid or urate (UA) is a small organic molecule formed as a result of XO metabolism of xanthine. In most species, uric acid is further catabolized by uricase (or urate oxidase) to allantoin, which is then readily excreted through urine. Higher primates and humans, as a result of a mutation, do not express uricase (178). In these species, uric acid is the final product of purine catabolism. Uric acid has a very low solubility in water and can form crystals of monosodium urate in certain conditions (high concentrations, acidic pH, presence of other molecules) (135).

Therefore, uric acid was traditionally viewed as metabolically inert, yet capable of exerting harmful effects as a result of crystallization, the most common pathophysiological consequence of which is the development of arthritic gout (135). Even in the absence of gout, studies have shown hyperuricemia to be a risk factor for several cardiovascular diseases, associated with metabolic syndrome and an independent predictor for kidney disease and all-cause mortality (32, 66, 72).

Hyperuricemia can be experimentally induced in rodents by treatment with the uricase inhibitor oxonic acid. This has lead to development of hypertension and endothelial dysfunction, accompanied by renal fibrosis, increase in juxtaglomerular renin and decrease in renal nitric oxide synthase (NOS) expression, in the absence of crystal formation in the kidney (71, 97). Additionally, in cultured bovine aortic endothelial cells, uric acid inhibited both the basal and the vascular endothelial growth factor (VEGF)-stimulated NO production (71). Taken together, these results suggest uric acid to be an overall deleterious molecule.

However, there are several other lines of evidence pointing to the more complicated and potentially beneficial roles of uric acid. *In vitro*, uric acid acts as an antioxidant for superoxide, hydroxyl radical, H_2O_2 and other ROS (7). Importantly, these reactions occur at uric acid concentrations that are in the range of low to normal human uricemia. The antioxidant effects of uric acid were confirmed in various biological systems by studies demonstrating attenuation or protection from oxidative stress in the presence of uric acid (7). These effects

might become especially relevant when considering the known correlation between increased ROS and endothelial dysfunction (15). Uric acid may not only react with superoxide, but also with peroxynitrite (resulted from the reaction between superoxide and NO), decreasing the amount of peroxynitrite and giving rise to a reaction product that has endothelium-independent vasorelaxant properties (133). On the other hand, uric acid has been shown *in vitro* to be able to react irreversibly with NO itself, quenching NO in a manner similar to superoxide (46).

In stark contrast with Khosla *et al.* (71), and giving support to the idea of a beneficial role for uric acid, are studies performed in humans by Waring *et al (165, 166)*. Administering uric acid to patients with diabetes type I or smokers with endothelial dysfunction lead to an increase in forearm blood flow in response to acetylcholine (ACh), a measure of endothelial function, and a gross measure of NO bioavailability (166). Conversely, lowering uricemia in patients with diabetes type II and associated endothelial dysfunction did not improve their endothelial function (165).

To further complicate the image of uric acid roles in vascular biology, a urate transporter (SLC22A12) was recently identified on the membrane of human vascular smooth muscle cells (115). In this type of cells, uric acid was shown to increase proliferation by increasing the expression of platelet-derived growth factor (PDGF) (117) and activating the renin-angiotensin-system (20).

Thus it is unclear whether uric acid effects are overall beneficial or deleterious at the level of the vascular system generally, and on endothelial function specifically.

D. *In vivo* effects of XO inhibition

The beneficial effects of in *vivo* treatments with XO inhibitors constitute one of the strongest pieces of evidence pointing to the role of XO in cardiovascular disease, and in particular, in hypertension. Various human and animal studies have demonstrated beneficial effects of XO inhibition in hypertension, coronary artery disease or cardiomyopathies by lowering blood pressure, decreasing end organ damage, improving endothelial function and heart function (110).

Pharmacological inhibition of XO classically involves use of purine analogues, such as allopurinol or oxypurinol. Allopurinol serves both as an inhibitor and as a substrate (suicide inhibitor) for XO, which catalyzes its transformation to oxypurinol. Allopurinol is also metabolized by the phosphoribosyltransferases hypoxanthine-guanine phopshoribosyltransferase (HGPRT) and by orotate phosphoribosyltransferase. Oxypurinol, the product of allopurinol metabolism, has a longer half-life compared to allopurinol (22 h compared to approx 1-3 h for allopurinol) as well as a lower K_i (11). Another means of inhibiting XO is by tungsten diet. This approach however, leads to inhibition of all other molybdenum-containing enzymes, such as aldehyde oxidase and sulfite oxidase (74). More recently, febuxostat, a new inhibitor of XO was approved for human

use for the management of gout. As it inhibits XO through a different mechanism, febuxostat is devoid of non-specific effects that allopurinol or other purine analogues may have, such as inhibition of purine nucleoside phosphorylase and orotidine-5'-monophosphate decarboxylase, both also involved in nucleotide catabolism (148). Unfortunately, no genetic models may be employed as a tool to study of XO functions, as XO null mice die at week 6 (164).

Allopurinol treatment improved vascular function in diabetic rats (64), while oxypurinol improved coronary and peripheral endothelial function in coronary artery disease patients (3). Treatment with oxypurinol acutely decreased the blood pressure in the SHR model, while it had no effect on the BP of normal counterparts (103). Treatment with allopurinol (100 mg/kg/day) also decreased systolic blood pressure (SBP) in the DOCA-salt hypertensive rat (163). A unique clinical study seeking an association between allopurinol administration and BP decrease has recently been published (33). Its authors observed a decrease in SBP with allopurinol in newly diagnosed hypertensive adolescents that have concomitant hyperuricemia.

Several other studies, however, have reported a lack of effects of XO inhibition on BP. Chronic treatment of SHR with allopurinol did not prevent the development of hypertension in this model (78, 175). Allopurinol also could not prevent development of glucocorticoid-induced hypertension (107) and L-NAME-induced hypertension (69).

Thus the effects of XO inhibition through allopurinol treatment on blood pressure are overall mixed, appearing to be species and model-dependent.

ROS and oxidative stress are involved in cardiovascular diseases such as hypertension. ROS effects on vascular function are varied and complex. Arterial ROS production and the contribution of arterial oxidative stress to hypertension have been extensively studied in experimental models of hypertension. However, similar to other physiological characteristics of veins, little is known about the venous generation and destruction of ROS, as well as about their consequences on venous function and how they might be different from the ones in arteries. Although venomotor function may impact blood pressure regulation, it is unclear whether alterations of this function mediated by ROS could contribute to hypertension pathogenesis. We investigated this idea in the work described next.

Throughout this research, we used mostly the rat thoracic aorta and vena cava tissues. They were chosen as model vessels to reflect the states of the arterial and venous system respectively, as they are large enough to allow for experimental manipulation in most protocols. Additionally, a large body of data from literature already existed on these blood vessels, facilitating the progress of this research.

The deoxycorticosterone acetate (DOCA)-salt model of hypertension was chosen because it is a low renin, salt-sensitive (therefore vascular capacitance)-dependent model, where increases in MCFP (thus venomotor tone) have been observed. Moreover, both endothelin-1 (ET-1), a potent venoconstrictor and ROS are known to play a role in this model. Furthermore, in this model, the increase in BP occurs over a long period of time, allowing for mechanistic studies.

HYPOTHESIS

ROS metabolism and handling is different in veins compared to arteries. Venomotor function, as influenced by ROS, plays a role in experimental hypertension.

Specific aims

1. Determine if there is a difference in ROS metabolism between arteries and veins in basal conditions and in hypertension.

2. Determine if there is a difference in the impact of ROS on arterial versus venous contractile function in basal conditions and in hypertension.

3. Determine whether venous function and blood pressure can be influenced by changing ROS levels *in vivo.*

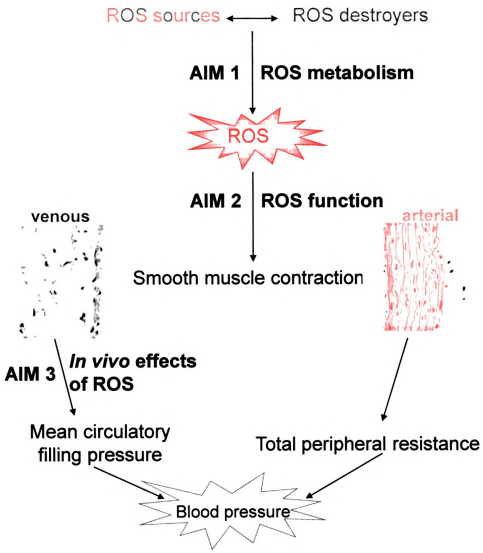

Figure 7. Diagram of working hypothesis.

METHODS

I. Animal use

All animal procedures were approved and performed in accordance with regulations of the Institutional Animal Care and Use Committee at Michigan State University. Male Sprague-Dawley rats (225-250 g) were purchased from Charles River Laboratories (Indianapolis, IN). Until euthanasia or surgical use, all rats were kept in clear plastic boxes, with access to standard rat chow (Teklad®) and tap/treatment water *ad libitum*.

A. Euthanasia

Rats were euthanized with pentobarbital (60-80 mg/kg i.p.).

B. DOCA-salt hypertension

Rats were uninephrectomized under isoflurane anesthesia (0.8 L/min, to effect). DOCA rats received a subcutaneous implant at the nape of the neck of a pellet of 200 mg/kg deoxycorticosterone acetate (DOCA) and were given drinking water supplemented with 1% NaCl and 0.2% KCl for a duration of 4 weeks. The sham rats were uninephrectomized (surgery control group) but were not implanted with DOCA and were given tap water. Animals received analgesic (carprofen 5 mg/kg s.c., at the time of surgery and 2 days postop.) and antibiotic (enrofloxacin 10 mg/kg i.m. at the time of surgery) treatment.

C. Blood pressure measurements

1. Tail-cuff measurement of systolic blood pressure

For *in vitro* tissue experiments performed as part of the first and second specific aim, systolic BP (SBP) was measured at the end of the 4 week DOCA-salt treatment to validate increase in SBP, using a standard tail-cuff method in the SC1000 Single Channel System (Hatteras Instruments, Cary, NC). DOCA rats SBPs were increased by at least 50 mmHg over sham SBPs (sham SBP ranging from 100 to 120 mmHg, DOCA SBP ranging from 175 to 225 mmHg).

2. Radiotelemetric measurement of mean arterial pressure (MAP)

For *in vivo* experiments performed as part of the third specific aim, MAP was measured through the use of radiotelemetry. Under isoflurane anesthesia (0.8 L/min, to effect), radiotelemeter devices (TA11PA-C40, Data Sciences International, St. Paul, MN) with attached catheters with pressure-sensing tips were implanted into a subcutaneous pouch in the abdominal wall through a 1-1.5 cm incision in the left inguinal area. Catheters were introduced into the left femoral artery 3 to 5 mm distal to the level of the peritoneal wall, and the tip was advanced to the abdominal aorta. Animals received analgesic (carprofen 5 mg/kg s.c., at the time of surgery and 2 days postop.) and antibiotic (enrofloxacin 10 mg/kg i.m. at the time of surgery) treatment. Rats were allowed 3 days to recover postoperatively, before the start of baseline recording. Parameters (systolic pressure, diastolic pressure, mean arterial pressure, pulse pressure, heart rate and activity) were recorded throughout the duration of the study, at a sampling

rate of 10 seconds each 10 minute interval (Dataquest ART 4.1, DSI). Data is presented as mean ± SEM of 24h-averaged parameters.

D. *In vivo* allopurinol administration

Allopurinol was administered orally at 50 mg/kg/day mixed in the DOCA-salt water, in the case of *in vivo* experiments for allopurinol effects on BP; and at 50 mg/kg/day or 100 mg/kg/day mixed in water, in the case of *in vivo* experiments for dose-dependent effects of allopurinol on XO metabolites. Water intake was monitored daily and allopurinol concentrations in the drinking water were varied according to this intake, in order to keep the same desired dosage.

E. Sample collection

1. Tissue

At the time of sacrifice, tissues of interest were removed and gently cleaned of outer adipose tissue and then used in one of the protocols described below. Tissues used were: thoracic aorta, caudal vena cava (VC), carotid arteries, jugular veins, superior mesenteric artery, superior mesenteric vein, heart, liver and right kidney.

2. Urine

Urine samples were collected by temporarily housing rats in metabolic cages that allow for separation of urine from feces and solid debris. Samples were collected after 24 hour periods. The total volume of urine for 24 h was measured and used for normalization.

3. Serum

Whole blood was collected into plastic tubes (non-heparin coated) by cardiac puncture from deeply anesthetized rats (pentobarbital 60-80 mg/kg i.p.). After 30 minutes at room temperature, clotted blood was spun (2500g, 10 minutes, twice, mechanically separating the clot from sides of tube if necessary between the two centrifugations), and the supernatant (serum) was collected.

II. Basal superoxide levels by lucigenin-enhanced chemiluminescence measurements

Rings of aorta, VC, superior mesenteric artery and superior mesenteric vein were cleaned of outer adipose tissue and incubated in a modified Krebs-HEPES buffer (containing in mM: 20 HEPES, 119 NaCl, 4.6 KCl, 1.0 $MgSO_4 \cdot 7H_2O$, 0.15 Na_2HPO_4, 0.4 KH_2PO_4, 5 $NaHCO_3$, 1.2 $CaCl_2$, and 5.5 dextrose, pH=7.4) at 37°C for 1h with diethyl-dithio-carbamate (DDC), a superoxide dismutase (SOD) inhibitor. A TD 20/20 Luminometer (Turner Designs, Sunnyvale, CA) was used. Lucigenin (5 μM, concentration previously shown to avoid redox cycling (102)) was added for 10 minutes, and 10 consecutive luminometer readings (each 30 seconds long) were taken. Tiron (4,5-dihydroxy-1,3-benzene disulfonic acid), a

superoxide scavenger, was then added for 15 minutes to assess background and 10 more consecutive readings were taken. Tissues were blotted dry and weighed. The average of readings with tiron was subtracted from the average of readings without tiron, and this difference was multiplied by 2 for a resulting measure of luminescence/minute. This value was used as input for the following equation, resulted from a standard curve of superoxide concentrations, previously constructed with a cytochrome c reduction assay:

$$\text{superoxide} = \frac{\left(5.95 * \frac{lum}{\text{min}}\right) + 0.1}{weight\ (mg)}$$

Results are presented as nmol superoxide/(min*mg tissue).

III. Hydrogen peroxide (H_2O_2) measurements

A. Basal H_2O_2 levels

H_2O_2 production was measured using an Amplex Red H_2O_2 assay kit (Molecular Probes, Invitrogen, Carlsbad, CA) according to manufacturer's protocol. Aorta, VC, carotid artery and jugular vein were cleaned of outer adipose tissue and equilibrated for 1h at 37°C in the same modified Krebs-HEPES buffer (pH=7.4), as detailed for superoxide measurements. They were then incubated with Ultra Red working solution (100 μM) at 37°C for 1h. The supernatant was then transferred to a 96 well plate and fluorescence emission was measured (excitation=530 nm, emission=590 nm) on an Ascent Fluoroskan plate reader

(Thermo Fisher Scientific, Waltham, MA). For each experiment, a H_2O_2 standard curve constructed on the same 96-well plate was incubated with Ultra Red working solution (100 μM) at 37°C at the same time with the tissues and was used to determine H_2O_2 concentrations from samples (fig 8A). After each experiment, tissue total protein was determined by the Lowry method and used for normalization.

In other experiments, H_2O_2 measurements were made in the presence of the superoxide dismutase inhibitor diethyl-dithio-carbamate (DDC), in which case the latter was added at both incubation times (1h in modified Krebs-HEPES buffer and 1h with Ultra Red), at a 10 mM concentration.

B. Antioxidant capacity for H_2O_2

Antioxidant capacity of aorta and VC was measured using the Amplex Red H_2O_2 assay as detailed above. Incubation of aorta and VC rings with Ultra Red working solution (100 μM) was performed in the presence of 20 μM H_2O_2. H_2O_2 that was quenched by tissue was determined by subtracting the fluorescence values of samples incubated with 20 μM H_2O_2 from the fluorescence value of 20 μM H_2O_2 alone, and using the value obtained as input in the H_2O_2 standard curve. After each experiment, tissue total protein was determined by the Lowry method and used for normalization.

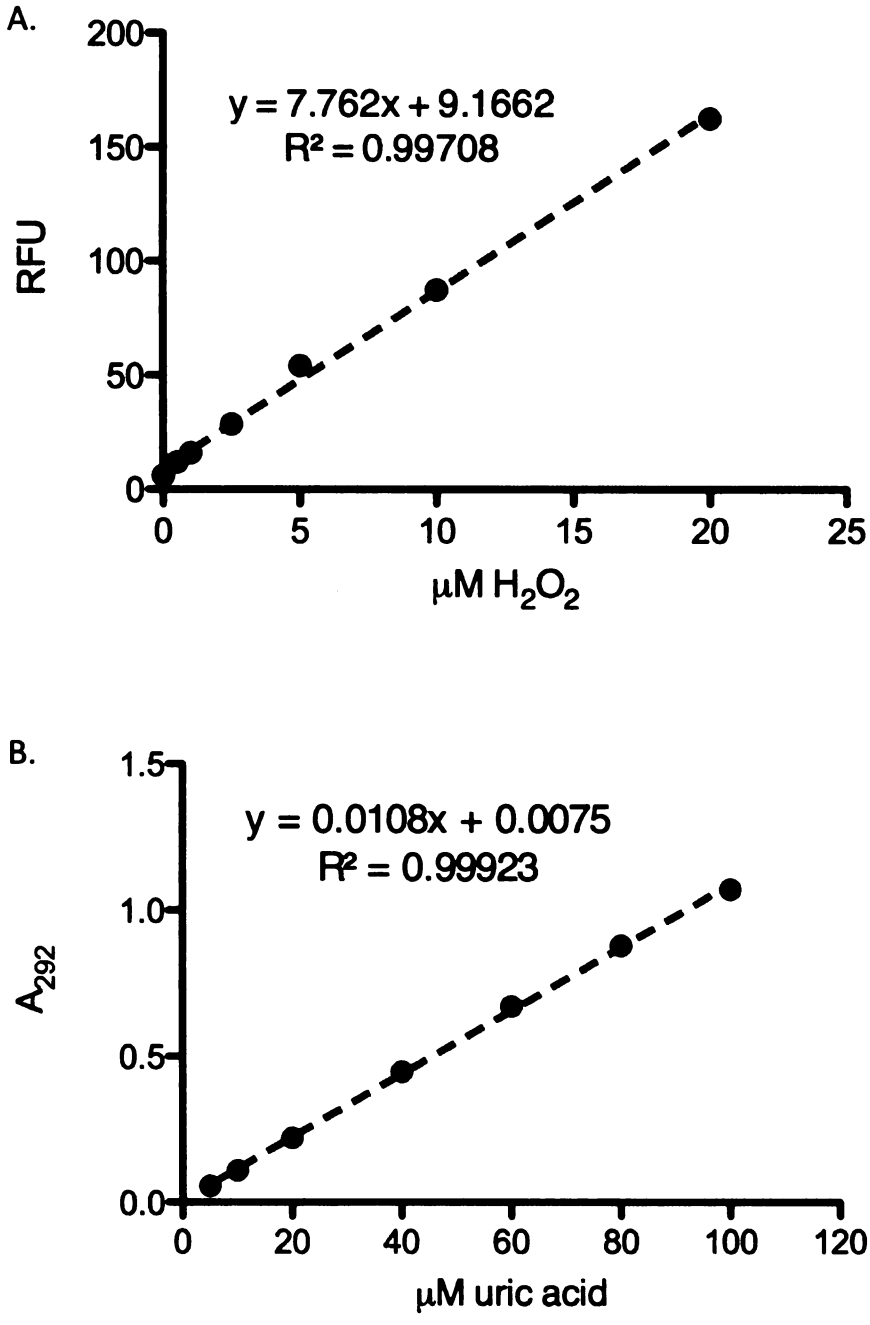

Figure 8. A. Representative standard curve of H_2O_2 for the Amplex Red H_2O_2 assay. Known concentrations of H_2O_2 are plotted against relative fluorescence units (RFU) obtained at 530 nm excitation with 590 nm emission. **B.** Representative standard curve of uric acid for the XO activity assay of urate production. Known concentrations of uric acid are plotted against absorbance at 292 nm.

C. Relative contribution of ROS metabolizing enzymes to basal H_2O_2 levels

The same protocol as for basal H_2O_2 production (IIIA, detailed above) was used. Inhibitors: apocynin (100 μM), allopurinol (100 μM), Nω-Nitro-L-arginine (LNNA, 100 μM), rotenone (10 μM), indomethacin (10 μM), ketorolac (10 mM), diphenylene iodonium (DPI, 10 μM) were incubated with tissues for 1h at 37°C in the modified Krebs-HEPES buffer, and again for 2h incubation at 37°C with Ultra Red reagent. The 2h Ultra Red reagent incubation time was chosen as yielding mid-range fluorescence signals from a time course study of H_2O_2 production measurements in aorta, vena cava, carotid artery and jugular vein (30 min, 1h, 2h and 3h) (data not shown). The remainder of the H_2O_2 measurement protocol was carried out as described above (IIIA).

IV. Protein concentration determination

A. Bicinchoninic acid (BCA) protein assay

Protein measurements in the tissue homogenates used for western blotting were made using the BCA assay (Sigma, St. Louis, MO) according to the manufacturer's protocol. Bovine serum albumin (BSA) protein standard was used to construct a standard curve with known protein concentrations (fig 9A). Samples and standards (5 μl q.s. to 100 μl with water) were incubated for 30 min at 37°C with 2 ml working reagent (BCA:copper (II) sulfate in a 50:1 ratio) and analyzed by end-point spectrophotometry at 562 nm.

B. Lowry protein assay

Protein measurements in the tissues used for H_2O_2 measurements were made using the Lowry method. Tissue samples were digested in 1M NaOH with sonication to solubilize. Bovine serum albumin (BSA) protein standard was used to construct a standard curve with known protein concentrations (fig 9B). Samples and standards (10 µl q.s. to 100 µl with 1M NaOH) were incubated for 10 min at RT with 1ml reagent A (sodium carbamate:KNa tartrate:$CuSO_4$ in a 100:1:1 ratio), followed by addition of 100 µl reagent B (Folin-Ciocalteu phenol reagent:water in a 1:1 ratio) for 1h at RT. Samples were then placed on a 96-well plate and analyzed by plate-reader end-point spectrophotometry at 750 nm.

C. Bradford protein assay

Protein measurements for tissue homogenates used for HPLC measurements and the XO activity assay for urate production were made using the Bradford protein assay (Bio-rad, Hercules, CA) according to the manufacturer's protocol. Bovine serum albumin (BSA) protein standard was used to construct a standard curve with known protein concentrations (fig 9C). Samples and standards (5 µl q.s. to 100 µl with water) were incubated for 5 min at RT with 900 µl Bradford working reagent and analyzed by end-point spectrophotometry at 595 nm.

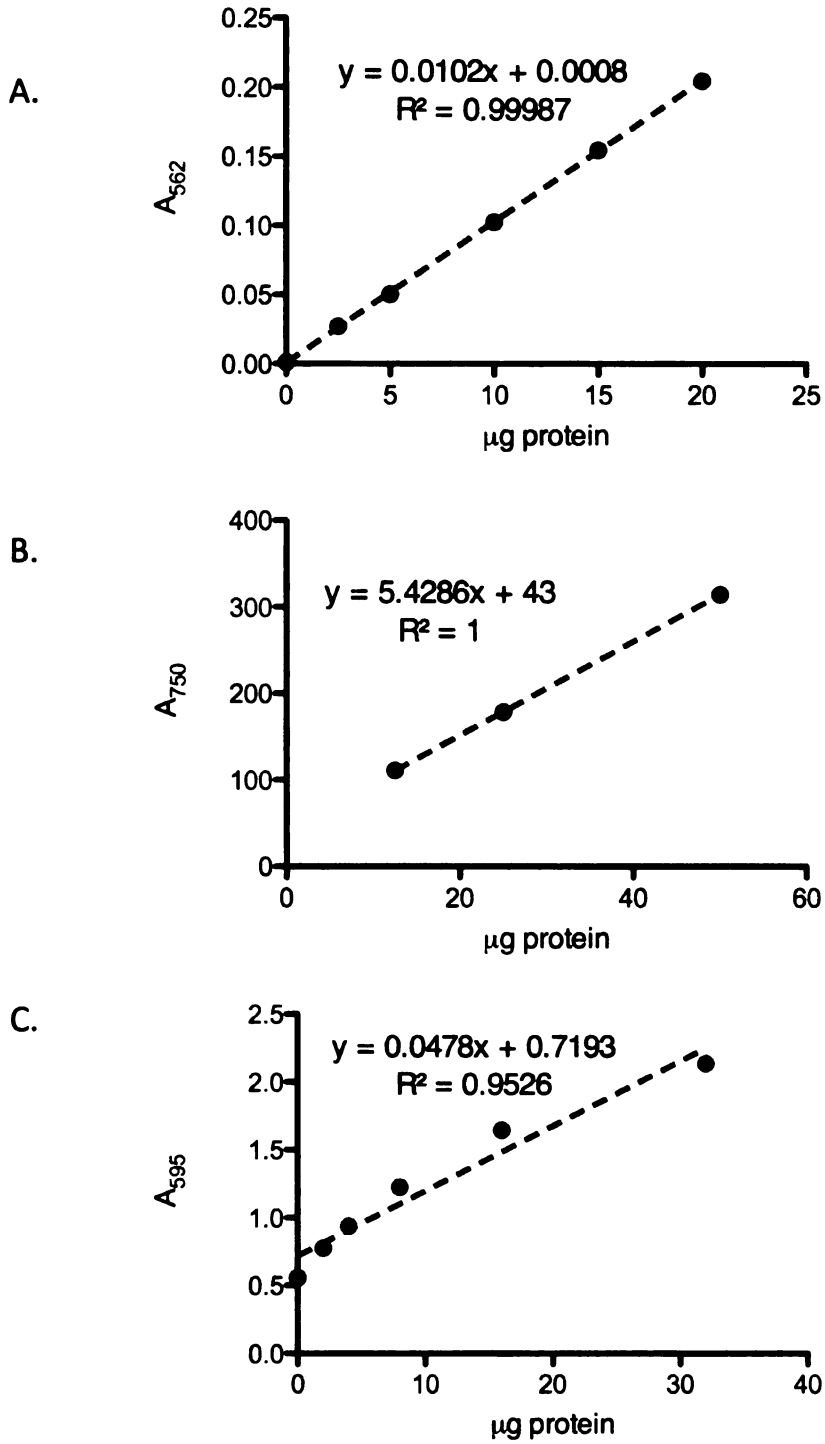

Figure 9. A. Representative standard curve of protein for the BCA protein assay. Known concentrations of BSA are plotted against absorbance at 562 nm. **B.** Representative standard curve of protein for the Lowry protein assay. Known concentrations of BSA are plotted against absorbance at 750 nm. **C.** Representative standard curve of protein for the Bradford protein assay. Known concentrations of BSA are plotted against absorbance at 595 nm.

V. Western blot analysis

A. Protein isolation

Thoracic aorta and vena cava were removed from the animal, placed in physiological salt solution (PSS) containing (mM): NaCl, 130; KCl, 4.7; KH_2PO_4, 1.18; $MgSO_47H2O$, 1.17; $NaHCO_3$, 14.8; dextrose, 5.5; $CaNa_2EDTA$, 0.03; $CaCl_2$, 1.6 (pH=7.2) and cleaned as described above. Tissues were quick frozen in liquid nitrogen, pulverized with a liquid nitrogen cooled mortar and pestle and solubilized in lysis buffer supplemented with protease inhibitors [0.5 M Tris HCl (pH=6.8), 10% SDS, 10% glycerol, 0.5 mM phenylmethylsulfonylfluoride (PMSF), 10 µg/ µl aprotinin, 10 µg/ µl leupeptin, 0.1 M orthovanadate). Homogenates were centrifuged (11,000g for 10 minutes, at 4°C) and supernatants were collected and stored at -80°C. Protein concentration was determined using the BCA assay (detailed above).

B. Western blotting

Thirty-five µg of protein from each sample and 10 µl positive control (rat kidney medulla for XO, CuZn SOD, Rac1; rat kidney cortex for MnSOD and OxPhosI; rat liver for 4-HNE and uricase; human endothelial cell lysate for eNOS; and human thyroid lysate for DUOX1) were separated on SDS-polyacrylamide gels (7, 10 or 12%) and transferred to nitrocellulose, PVDF or Immobilon-FL membranes. The membranes were blocked with 5% milk, 4% chick egg ovalbumin or LI-COR blocker for 3h at 4°C. They were then probed overnight at 4°C with specific

antibodies against XO (Rockland, Gilbertsville, PA and Abcam, Cambridge, MA), eNOS (BD Biosciences, San Jose, CA), Rac1 (Upstate, Millipore, Billerica, MA), $p47^{phox}$ (Santa Cruz, CA), DUOX1 (Santa Cruz, CA), CuZn SOD (Calbiochem, EMD Biosciences, San Diego, CA), Mn SOD (BD Biosciences, San Jose, CA), catalase (Abcam, Cambridge, MA), 39 KDa subunit of OxPhos complex I (Molecular Probes, Invitrogen, Carlsbad, CA), 4-HNE (Abcam) and uricase (Santa Cruz, CA). The appropriate horseradish peroxidase-linked or fluorescent secondary antibodies were added for 1h at 4°C, followed by visualization with ECL or the infrared imaging scanner Odyssey (LI-COR, Lincoln, NE). To ensure equal protein loading, gels were stained with Gel Code Blue (Pierce Chemical, Rockford, IL), and blots were reprobed with smooth muscle α-actin antibody (Oncogene, EMD Biosciences, San Diego, CA). Band density was quantified using NIH Image version 1.63. Smooth muscle α-actin expression per equal amount of total protein is significantly higher in aortic *vs* VC homogenates, therefore unless comparing the same type of tissue (e.g. sham with DOCA aorta samples), densitometry values were not normalized to α-actin, as this manipulation would have skewed results biasing expression of proteins of interest towards the VC.

VI. Immunohistochemistry of paraffin-embedded sections

Formalin-fixed, paraffin-embedded rat thoracic aorta and vena cava sections (8 μm) were washed twice in Histochoice Clearing Agent (Vector Laboratories,

Burlingame, CA) and 4 times in isopropanol for 3 min each to dewax. Rat liver sections were used as positive control for 4-HNE staining. Sections were unmasked by boiling them twice for 2 min each in Vector Antigen Unmasking solution. Endogenous peroxidase activity was blocked (0.3% H_2O_2 in phosphate-buffered saline, PBS) for 30 min. Sections were blocked for non-specific binding by incubating for 30 min with competing serum (1.5% in PBS). In a humidified chamber, sections were incubated overnight at 4 °C with competing serum (negative control) or with specific antibodies against XO (1:200, Rockland, Gilbertsville, PA and 5 µg/ml, Abcam, Cambridge, MA), DUOX1 (1 µg/ml, Santa Cruz, CA), CuZn SOD (5 µg/ml, Calbiochem, EMD Biosciences, San Diego, CA), catalase (5 µg/ml, Abcam, Cambridge, MA), 4-HNE (1 µg/ml, Abcam). The remaining steps were performed according to the manufacturer's protocol (Vector Laboratories, Burlingame, CA). Sections were washed 3 times in PBS and incubated for 30 min with the appropriate biotinylated secondary antibody. After washing 3 times in PBS and incubation for 30 min with Vectastain® ABC Elite reagent, sections were exposed to diaminobenzidine (DAB)/ H_2O_2 and staining was monitored and timed. Reactions were stopped by PBS. Sections were then counterstained with hematoxylin, dried and mounted. Photographs were taken using an inverted Nikon microscope with a Spot digital camera and the MetaMorph software (Molecular Devices, MDS Analytical Technologies, Toronto, Canada).

VII. mRNA expression

A. RNA isolation

Total RNA was isolated using the MELT™ Total Nucleic Acid Isolation System (Ambion/Applied Biosystems, Austin, TX) with the magnetic stand (Ambion) for 96-well plates. Aorta and vena cava were quickly cleaned in chilled DEPC-treated water. Sections of ~10 mg from each tissue were then cut into 4-6 smaller pieces and placed in the MELT Buffer with MELT Enzyme mix and vortexed for 20 minutes at RT. Samples were then centrifuged (11,000g for 3 min) and supernatants were taken through the remainder of the protocol according to manufacturer's instructions. The optional DNase digestion step was performed using Turbo DNase (Ambion). The final elution was carried out in 12.5 µl Elution Buffer. RNA samples were stored at -80°C.

B. RNA quality and quantity assessment

Total RNA was quantified at 260 nm using a Nanodrop ND-1000 spectrophotometer (Nanodrop, Wilmington, DE). The purity of RNA was verified by a 260/280 ratio of 2.0 ± 0.25 and a 260/230 ratio of 1.8 ± 0.15. The integrity of RNA isolated from aorta and vena cava by the MELT method was initially verified by electrophoresis of 1 µg RNA samples on agarose-MOPS-formaldehyde gels and UV visualization of ethidium bromide stained bands. Sharp 28S and 18S bands were observed in an approximate 2:1 ratio, with no signs of RNA degradation. Since the approximate yield from one whole VC is 1 µg RNA, we did not perform this analysis for RNA isolated for downstream procedures.

C. Reverse transcription

1. RT for real-time PCR

One µg total RNA was DNAse-treated (DNase I, Roche Applied Science, Mannheim, Germany) and then reverse-transcribed using oligo $(dT)_{12-18}$ primer, dNTP mix and Superscript II reverse transcriptase according to the manufacturer's protocol (Invitrogen, Carlsbad, CA). cDNA samples were stored at -20°C.

2. RT for PCR arrays

To perform SuperArray PCR arrays (see below), equal amounts of total RNA were reverse-transcribed using the RT² First Strand Kit (SA Biosciences, Frederick, MD) according to the manufacturer's protocol.

D. Primers

Primers for rat xanthine dehydrogenase (XDH) (GeneID 29289, mRNA sequence NM_017154) were designed using the Primer 3 software (122) (Whitehead Institute, Cambridge, MA), and synthesized at the Macromolecular Structure, Sequencing and Synthesis Facility at MSU; XO forward 5'-GCATGCCAGACCATACTGAA-3'; reverse 5'-AAATCCAGTTGCGGACAAAC-3'. Primers for DUOX1, DUOX2 and GAPDH were purchased from SuperArray (SA Biosciences, Frederick, MD).

E. Real-time PCR

Relative quantification of XO relative to GAPDH and of DUOX1 and DUOX2 relative to beta-2 microglobulin was performed using SYBR Green PCR Master Mix (Applied Biosystems, Foster City, CA) and the respective primers (0.1 μM), on a 7500 Real-Time PCR System (Applied Biosystems, Foster City, CA). Baseline values were established on the amplification curve with fluorescence on a linear scale during the initial cycles with no detectable amplification. The threshold was established on the amplification curve with fluorescence on a logarithmic scale, such that it crossed amplification curves in the lower 1/3 of the exponential amplification phase. A dissociation curve was performed at the end of each run to ensure a single product was amplified. Average cycle threshold (C_t) values for the housekeeping gene were subtracted from average C_t values for the gene of interest for a resulting ΔC_t value. Quantification was not performed using the typical $\Delta\Delta C_t$ quantification, as no tissue was considered control in comparing aorta and VC mRNA expression. Data are reported as mean ± SEM of $2^{-\Delta Ct}$ for each tissue.

F. PCR arrays

The Oxidative Stress and Antioxidant Defense PCR array (SA Biosciences, Frederick, MD) was used according to the manufacturer's protocol. Aorta and VC cDNA samples reverse-transcribed by the RT² First Strand Kit were mixed with RT² qPCR Master Mix, added on the 96-well plates with pre-aliquoted primers

against oxidative stress genes (84 genes) and amplified using the 7500 Real-Time PCR System (Applied Biosystems, Foster City, CA). Quantification of mRNA expression was performed using the manufacturer Excel-based analysis software, with beta-actin chosen for normalization from the six housekeeping genes included in the PCR array.

VIII. Xanthine oxidase (XO) activity assays

A. XO activity assay for urate production

Aorta and VC rings were cleaned in XO assay buffer (50 mM K phosphate, 0.1 mM EDTA, 1 mM oxonic acid; pH=7.4), pulverized in liquid nitrogen, solubilized in XO lysis buffer (XO assay buffer containing 10 mM DTT, 1 mM PMSF, 10 µg/ µl aprotinin, 10 µg/ µl leupeptin, 0.1M orthovanadate), sonicated and centrifuged (20,800g, 4°C, 30 min). Equal amounts of supernatant were then incubated with no additions, with 100 µM xanthine, or with 100 µM xanthine and 100 µM allopurinol at 37 °C for 30 min. Urate formation was measured spectrophotometrically at 292 nm in quartz cuvettes. The amount of uric acid produced was calculated using a uric acid standard curve (fig 8B). Protein concentration of homogenates was determined using the Bradford assay. XO activity was reported as the allopurinol-inhibitable uric acid production, normalized for protein.

B. XO activity assay for H_2O_2 production

XO H_2O_2-producing activity was measured using the Amplex Red H_2O_2 assay as detailed above for basal H_2O_2 production measurements (III A). Aorta and VC rings were incubated with Ultra Red working solution (100 μM) in the presence of 100 μM xanthine, or in the presence of 100 μM xanthine and 100 μM allopurinol. H_2O_2 concentrations from samples were calculated using a H_2O_2 standard curve (fig 8A) and were normalized to the total protein content of samples determined by the Lowry method. XO activity was determined by subtracting H_2O_2 production of samples incubated with 100 μM xanthine (substrate) and 100 μM allopurinol (inhibitor) from the H_2O_2 production of samples incubated with 100 μM xanthine alone.

IX. Isolated tissue bath contractility

Rings of aorta and VC were removed and cleaned of outer adipose tissue in physiological salt solution (PSS) containing (mM): NaCl, 130; KCl, 4.7; KH_2PO_4, 1.18; $MgSO_47H2O$, 1.17; $NaHCO_3$, 14.8; dextrose, 5.5; $CaNa_2EDTA$, 0.03; $CaCl_2$, 1.6 (pH=7.2). Rings were mounted in warmed (37°C), aerated (95% O_2, 5% CO_2) PSS in isolated tissue baths (30 or 50 ml) for measurements of changes in isometric force (PowerLab, ADInstruments, Colorado Springs, CO). Tissues were placed under optimal passive tension (previously determined as 4g for aorta and 1g for VC) and equilibrated for 1h with frequent buffer changes. The initial contraction to 10 μM α-adrenergic agonist (PE-phenylephrine for aorta, NE-

norepinephrine for VC) was used to verify viability of tissues and normalize any further isometric contractions. As previously described, the maximal contractions induced by PE (10 μM) and NE (10 μM) are similar in aorta (169). However, PE does not induce reproducible contractions of VC, and NE was used instead in this tissue. Endothelial integrity was tested in each experiment by measuring relaxation to ACh (10 μM) from the contraction to 20 μM $PGF_{2\alpha}$. In inhibition experiments, tissues were incubated in parallel with inhibitor (100 μM allopurinol, 100 μM LNNA, 10 μM DPI) or their vehicles for 1h prior to performing cumulative concentration response curves to agonists (NE, AngII, ET-1 or ACh). Concentration response curves to ACh (relaxation curves) were performed on tissues contracted with 20 μM $PGF_{2\alpha}$. Cumulative concentration response curves to uric acid (10^{-9}-10^{-4} M) were performed in the presence or absence of oxonic acid (uricase inhibitor, 10 μM). In other experiments, after 1h incubation with uric acid (100 μM) and oxonic acid (10 μM), allopurinol (XO inhibitor, 100 μM) or their vehicles (NaOH and DMSO, respectively), tissues were contracted with 20 μM $PGF_{2\alpha}$ and cumulative concentration response curves to ACh were constructed. The contraction induced by $PGF_{2\alpha}$ was not changed by the presence of uric acid, oxonic acid, allopurinol or their vehicles.

X. Blood uric acid measurement

Arterial blood was collected by cardiac puncture at the time of sacrifice and uric acid was determined using the UAsure meter and test strips (ApexBio, Taiwan) according to the manufacturer's protocol.

XI. High performance liquid chromatography (HPLC)

Tissue samples (aorta, vena cava, carotid artery, jugular vein, liver, kidney, heart) were collected at the time of sacrifice and cleaned in PSS as described above. They were then quick frozen in liquid nitrogen and pulverized in a liquid nitrogen cooled mortar and pestle. Homogenates were solubilized in 0.2 M acetic acid, sonicated and centrifuged (14,000g for 10 min at 4°C). Serum and urine samples were diluted 1:10 in 0.2 M acetic acid and centrifuged (14,000g for 10 min at 4°C). Analysis of XO metabolites from sample supernatants was performed using Waters HPLC (Waters, Milford, MA) coupled with Photo Diode Array detection. Separation of analytes was achieved on a Phenomenex Luna, 5 µm, C-18, 250 x 4.6 mm column. Mobile phase was 0.02 sodium acetate (pH=4.5 with acetic acid). A gradient with methanol was used to clear the column after elution of analytes. An example tracing demonstrating separation of standards under these conditions is represented in figure 10. The individual XO metabolites were analyzed at their respective maximum wavelength intensities (uric acid at 284 nm, xanthine at 266 nm, hypoxanthine at 249 nm, allantoin, oxypurinol and allopurinol at 210 nm). Peak height values for each metabolite obtained in the same retention time window as standards were used as input into standard curves constructed with known analyte concentrations. XO

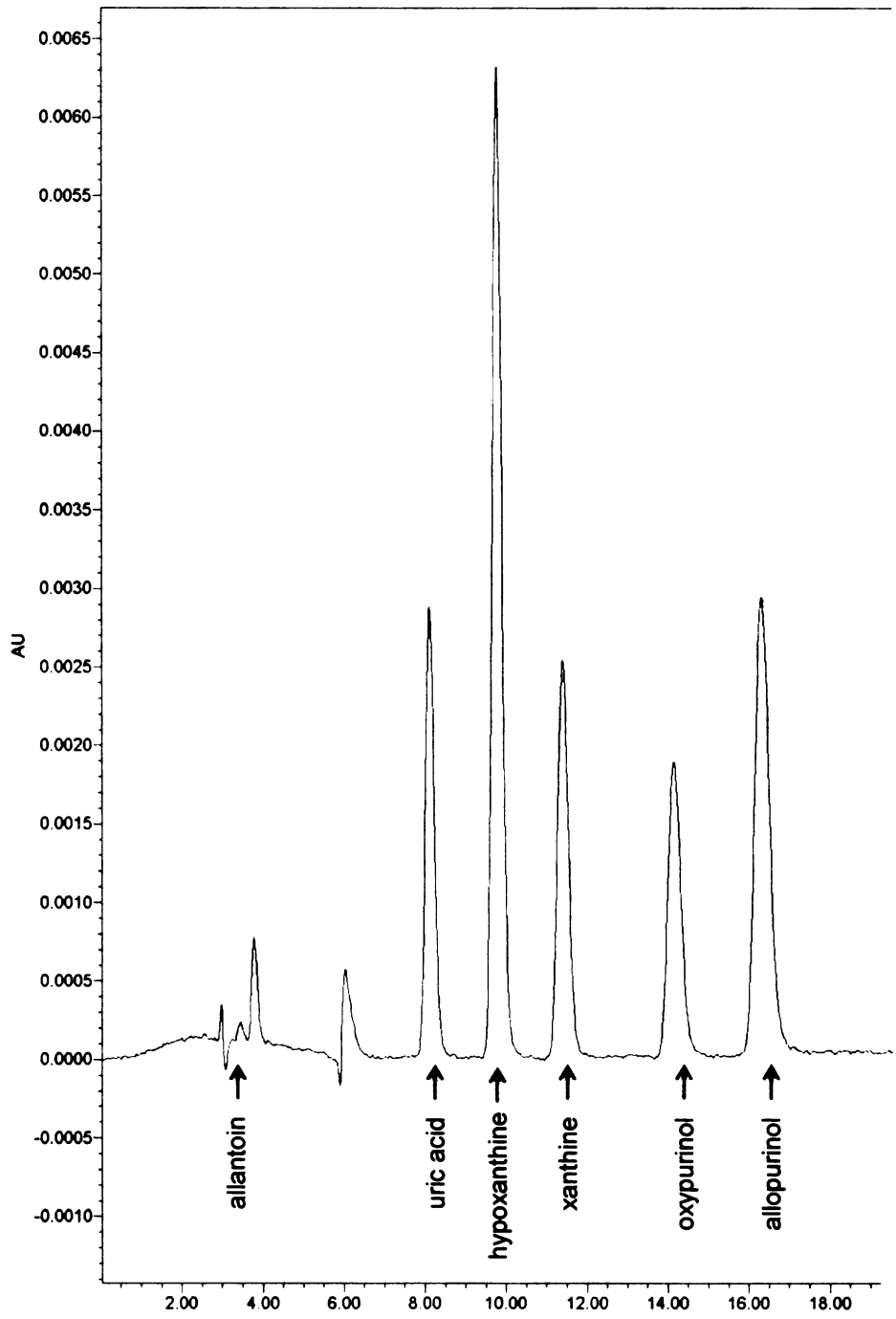

Figure 10. Representative high performance liquid chromatography (HPLC) tracing of standards for allantoin, uric acid, xanthine, hypoxanthine, xanthine, allopurinol and oxypurinol, as analyzed at 254 nm to display all analytes simultaneously.

metabolites were normalized to total protein content of HPLC samples determined by the Bradford method, with the exception of urine, for which XO metabolites were normalized to the total urine volume for 24h.

XII. Data analysis

Data are presented as mean ± SEM for the number of animals (N). Plotting and statistical analysis of data was accomplished using GraphPad Prism 5 (GraphPad, La Jolla, CA). When comparing groups, the appropriate Student's *t*-test or ANOVA analysis was performed. For *in vivo* experiments, a 2way repeated measures ANOVA with Bonferroni post-hoc analysis was performed. For association between uricemia and SBP, a non-parametric correlation (Spearman) analysis was performed. In all cases, a p value of ≤ 0.05 was considered statistically significant.

RESULTS

Overall hypothesis: ROS metabolism and handling is different in veins compared to arteries. Venomotor function, as influenced by ROS, plays a role in experimental hypertension.

Specific aim 1: Determine if there is a difference in ROS metabolism between arteries and veins in basal conditions and in hypertension

Rationale: Associations have been described between increased ROS production in arterial tissues and cardiovascular disease, although the precise enzymatic sources of this increase and its pathogenetic role are still a matter of debate. However, very little is known about ROS production and antioxidant defense in venous physiology, as well as about the potential dysregulation of venous ROS metabolism during diseases such as hypertension. We started this research by investigating the normal levels of ROS in arterial and venous tissue, their molecular sources, and corresponding changes during DOCA-salt hypertension.

I. ROS production

A. Superoxide production

Using lucigenin-enhanced chemiluminescence, we measured basal levels of superoxide anions in rings of aorta and vena cava (VC) from normal rats. We

observed a higher basal superoxide level in the VC compared to the aorta (fig 11A). Similarly, superoxide production was higher in venous than in the paired arterial tissue, when using a different artery-vein pair, the superior mesenteric artery (SMA) and vein (SMV) (fig 11B).

B. Hydrogen peroxide production

H_2O_2 production was measured using Amplex Red fluorescence in rat aorta and VC tissues (fig 12A). Normalized to protein content, basal H_2O_2 production was higher in VC compared to aorta. Similarly, H_2O_2 production was higher in venous than in the paired arterial tissue, when using a different artery-vein pair, the carotid artery and the jugular vein (fig 12B). The H_2O_2 production of all tissues was almost abolished by diethyl-dithio-carbamate (DDC), a superoxide dismutase inhibitor, suggesting that the vast majority of vascular H_2O_2 is superoxide-derived (fig 13).

Because the basal levels of ROS are the result of opposing activity of various systems of ROS generation and destruction, these results suggest that the normal rat veins have either a higher ROS production rate and/or a decreased ROS destruction rate, compared to normal rat arteries.

***II.* ROS destruction**

A. Antioxidant capacity for H_2O_2

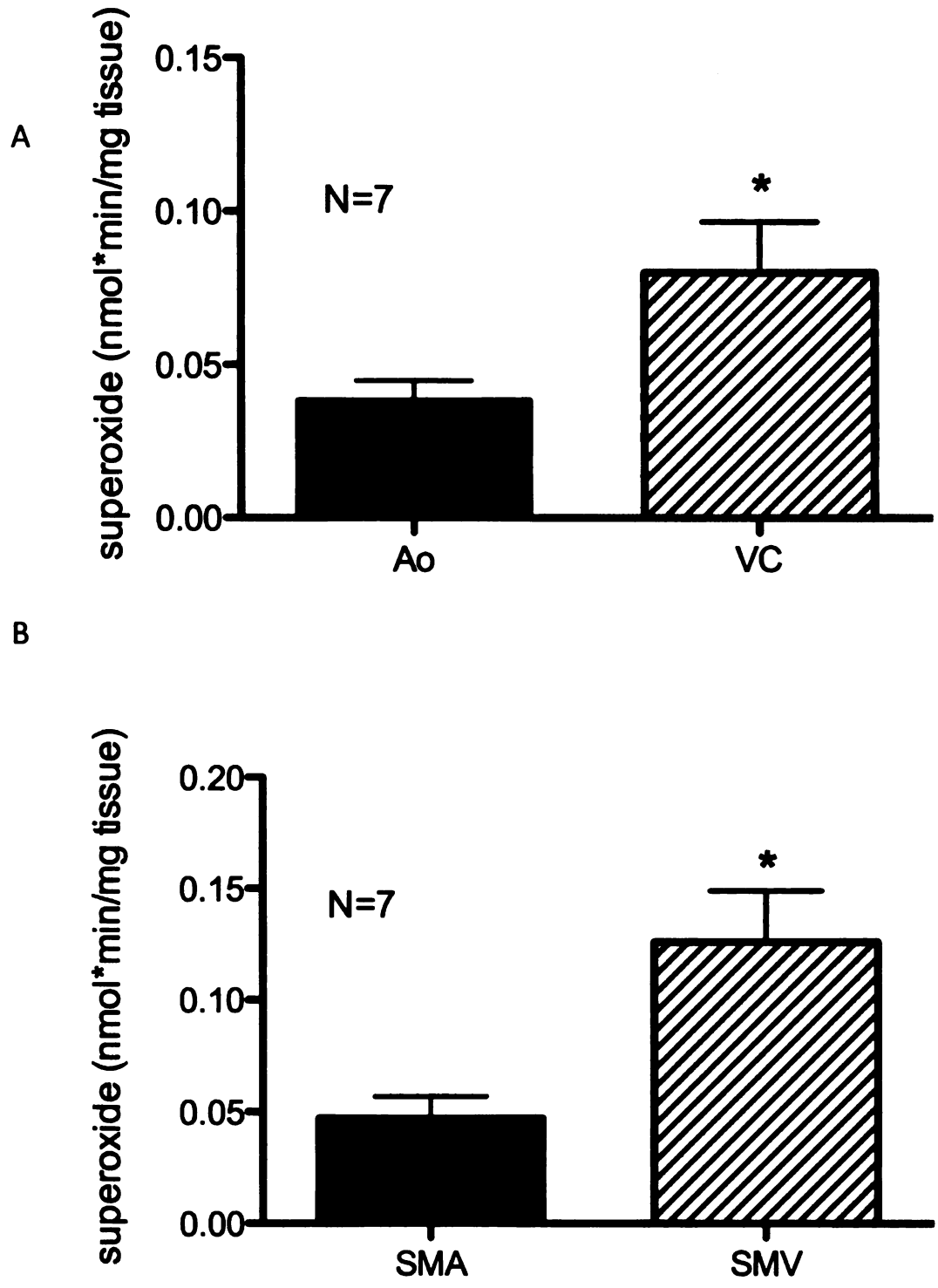

Figure 11. Basal superoxide production measured by lucigenin-enhanced chemiluminescence in normal rat tissues: aorta (Ao) and vena cava (VC) **(A)**; superior mesenteric artery (SMA) and vein (SMV) tissues **(B)**. Data are represented as mean ± SEM for the respective N. * represents a statistically significant ($p<0.05$) difference.

A

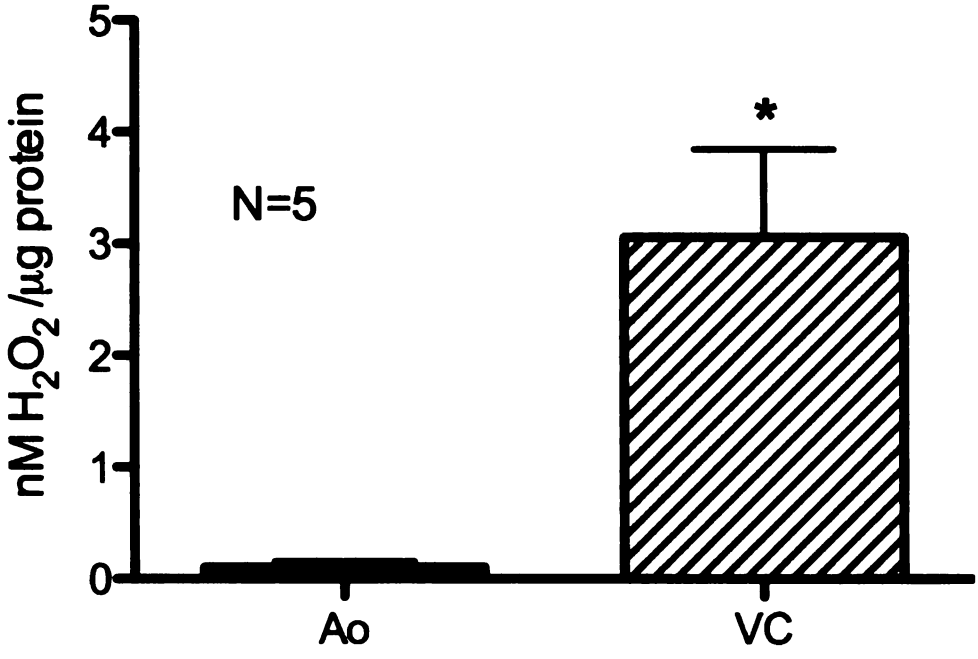

B

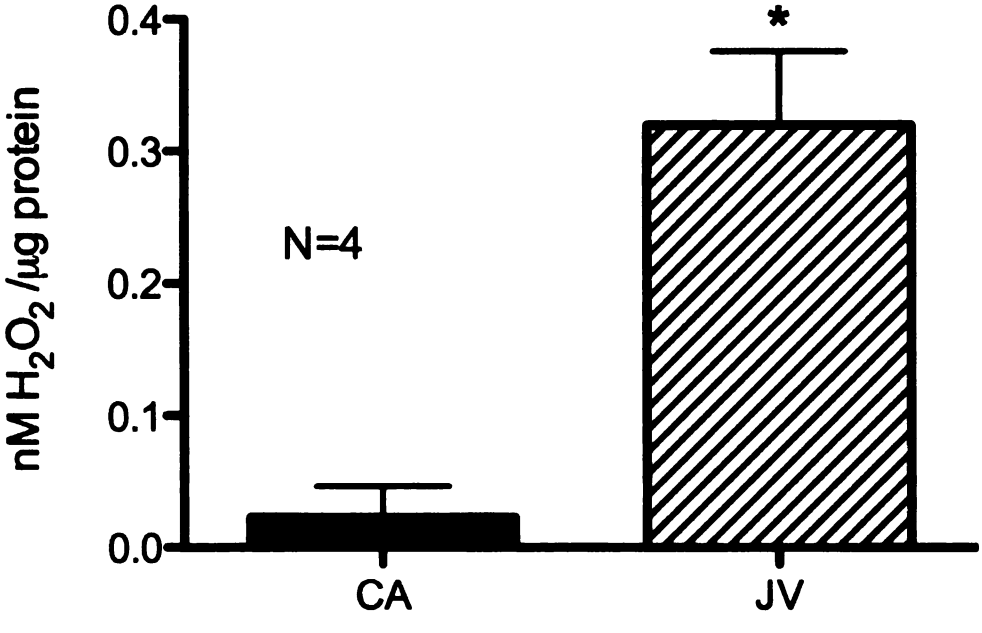

Figure 12. Basal hydrogen peroxide production measured by Amplex Red fluorescence in normal rat tissues: aorta (Ao) and vena cava (VC) **(A)**; carotid artery (CA) and jugular vein (JV) **(B)**. Data are represented as mean ± SEM for the respective N. * represents a statistically significant ($p<0.05$) difference.

A

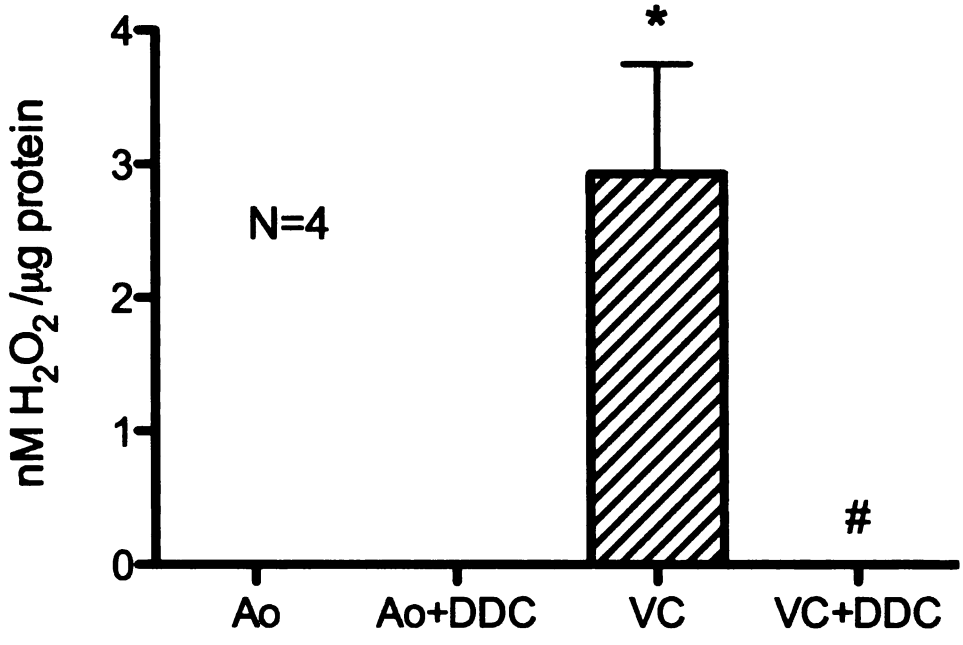

B

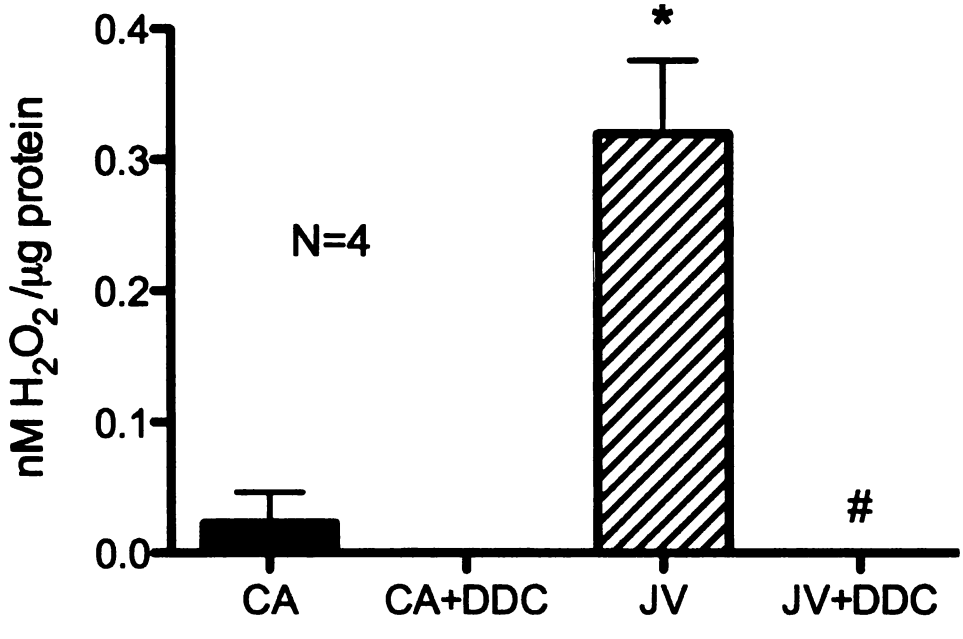

Figure 13. H_2O_2 production in basal conditions and in the presence of 10 mM diethyl dithiocarbamate (DDC, superoxide dismutase inhibitor) after 1h in normal rat aorta (Ao) and vena cava (VC) **(A)** and carotid artery (CA) and jugular vein (JV) **(B)**. Bars represent means ± SEM for the respective N. * represents statistically significant difference ($p<0.05$) between artery-vein, and # represents statistically significant difference ($p<0.05$) between control-DDC.

As a measure of antioxidant capacity, we tested the ability of normal aorta and VC to quench exogenous H_2O_2 by measuring the decrease in H_2O_2 concentration in the presence of tissue, using the Amplex Red H_2O_2 assay. The VC consumed significantly more exogenous H_2O_2 per amount of protein compared to the aorta in the presence of 20 μM H_2O_2 (fig 14).

B. 4-hydroxy-nonenal

After generation, regardless of source, ROS that are not degraded or that do not participate in cellular signaling may directly modify (oxidize) cellular components like proteins, lipids and DNA. We have investigated the expression level of 4-hydroxy-nonenal, a lipid peroxidation product typically used as a marker of oxidative stress, in normal aorta and VC. The immunohistochemical localization of 4-HNE was different in vascular cross-sections (fig 15A), and also appeared qualitatively higher in VC than in aorta, suggesting more lipid peroxidation may occur in the VC. The banding pattern of 4-HNE protein adducts in homogenates (fig 15B) also appeared to be different between aorta and VC, however in this case the staining intensity was observed to be higher in aorta samples, suggesting 4-HNE protein modifications may occur at a higher rate in the aorta.

III. ROS metabolizing enzymes

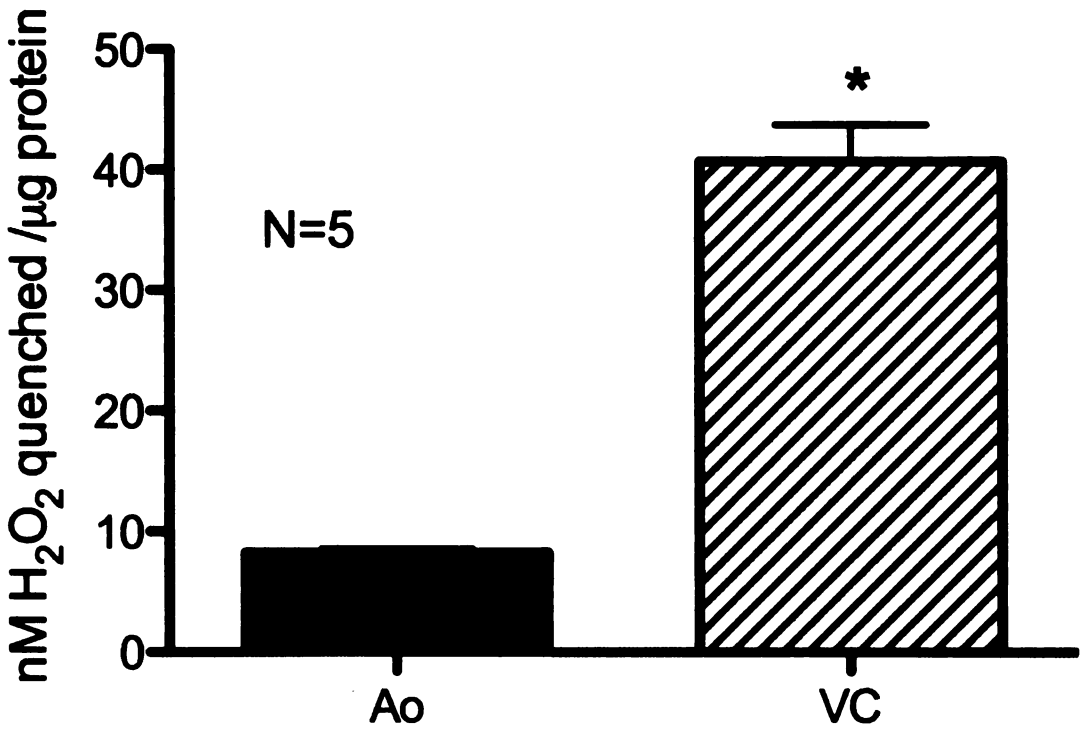

Figure 14. Antioxidant capacity for hydrogen peroxide (20 µM) of normal rat aorta (Ao) and vena cava (VC) tissues measured by Amplex Red fluorescence. Data are represented as mean ± SEM for the respective N. * represents a statistically significant ($p<0.05$) difference.

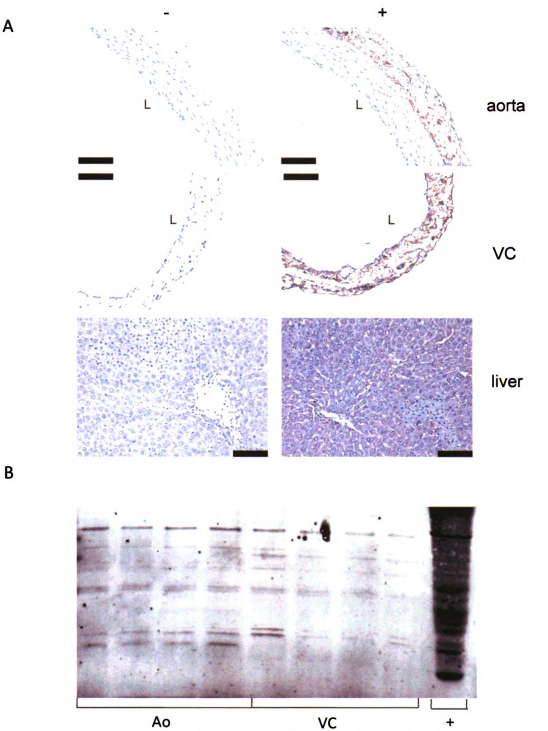

Figure 15. A. Immunohistochemical staining of 4-HNE (+, right) in normal rat aorta (top), vena cava (middle) and liver, used as positive control (bottom) as compared to no primary controls (-, left). The lumen is indicated by "L". Bar represents 100 µm. **B.** Western blot of 4-HNE protein adducts in aorta and vena cava homogenates, using the rat liver band pattern as positive control (+).

We have dissected the potential explanations for the differences in basal ROS levels between arteries and veins in three different ways: detecting differences in the protein expression (A) or in the mRNA expression of various ROS metabolizing enzymes (B), as well as pharmacologically inhibiting various enzymes that produce ROS and measuring the resulting decrease in basal ROS levels (C).

A. Protein expression of ROS metabolizing enzymes

We first analyzed protein expression of enzymes involved in the generation and/or destruction of ROS. Western blots displayed in figures 16-19 (A panels) were performed using protein isolates of aorta and vena cava from normal rats, and were followed by band densitometry analysis. The expression of XO, a cytosolic ROS generator (fig 16A), DUOX1, a membrane-bound ROS generator recently cloned as a Nox family member (fig 17A), CuZn SOD, the cytoplasmic isoform of superoxide dismutase (fig 18A) and catalase, a major H_2O_2-metabolizing enzyme (fig 19A) was significantly increased in VC compared to aorta.

No difference was observed between the aortic and VC protein expression of other important sources of vascular ROS: the endothelial isoform of nitric oxide synthase (eNOS); the mitochondrial isoform of superoxide dismutase (MnSOD); the small GTPase component of NADPH oxidase, Rac1; and the 39 KDa subunit of mitochondrial oxidative phosphorylation complex I, the most important mitochondrial ROS production site, as well as prohibitin, a mitochondrial marker

(data not shown). Use of a number of other commercially available antibodies for other ROS metabolizing enzymes was attempted without success or marked by technical difficulties: against other subunits of NADPH oxidase (Nox2/gp91^{phox}, p67^{phox}, p22^{phox}, p40^{phox}), other isoforms of NOS (iNOS, nNOS), cyclooxygenase (COX2) and lipoxygenase (5LOX).

Protein expression of XO, DUOX1, CuZn SOD and catalase in tissues was confirmed by immunohistochemical analysis of rat aorta and VC cross-sections (figures 16-19, respectively, B panels). Qualitatively, the XO and catalase staining appeared to be more intense and more diffuse in VC compared to aorta sections. CuZn SOD staining was intense in both aorta and VC sections, without appearing to be qualitatively different.

B. mRNA expression of ROS metabolizing enzymes

We have screened for differences in mRNA expression of ROS metabolizing enzymes with a PCR array approach, using the Oxidative Stress and Antioxidant Defense PCR array (SA Biosciences) for RNA samples from aorta and VC from normal rats. Table 2 lists the statistically significant observed differences in gene expression among the 84 oxidative stress-related genes included in the PCR array. mRNA expression of DUOX1, as well as DUOX2, was higher in normal VC than aorta. mRNA expression of NOX4, another Nox family member and important vascular ROS producer, was higher in aorta than in VC. By this method, no significant difference was observed in catalase or superoxide

dismutase isoforms mRNA expression, while XO was not included. RT-PCR experiments confirmed the higher mRNA expression of DUOX1 in VC compared to aorta, while that of DUOX2 displayed a similar trend (fig 20).

C. Relative contribution of ROS producing enzymes to basal vascular ROS levels

We also used a pharmacological approach to establish the relative contribution of various enzymatic ROS producers to the total levels of ROS in basal conditions. Using two rat artery-vein pairs: aorta - VC and carotid artery (CA) - jugular vein (JV), we examined H_2O_2 production in the presence of inhibitors for NADPH oxidase (100 μM apocynin), XO (100 μM allopurinol), eNOS (100 μM LNNA), mitochondrial complex I (10 μM rotenone), flavoenzymes (diphenyleniodonium, DPI, 10 μM) and cyclooxygenase (COX, 10 μM indomethacin/10 mM ketorolac). The results of these experiments were expressed as percentage of the basal H_2O_2 level from the same tissue and same animal and are displayed by inhibitor (fig 21 A-F) or by tissue (fig 22 A-D). No specific enzyme substrate was added at any point in these experiments. Apocynin reduced basal H_2O_2 production of all tissues, reaffirming the finding that NADPH oxidase is an important source of ROS in vascular tissues. Rotenone and DPI reduced basal H_2O_2 levels in veins, but not arteries, suggesting a relative higher dependence on mitochondria and flavoenzymes in veins compared to arteries. Inhibition of NOS with LNNA did not significantly alter basal H_2O_2 levels of any tissue, suggesting that NOS

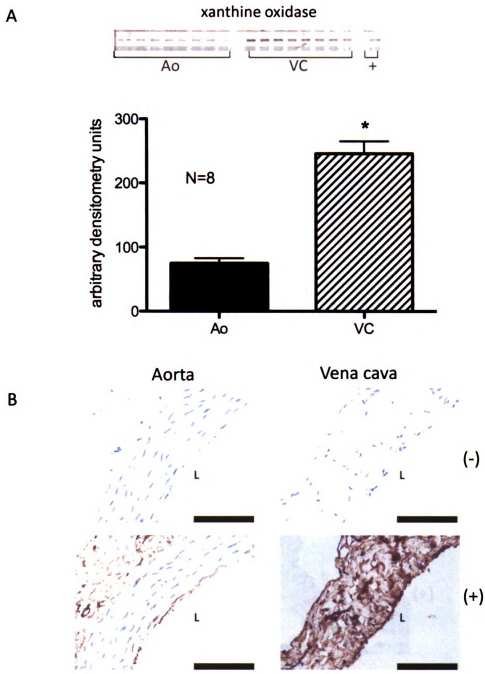

Figure 16. A. Western blot analysis of XO protein expression in normal rat aorta (Ao) and vena cava (VC) homogenates. + represents rat kidney medulla homogenate, used as a positive control. Band densitometry quantification of 130 KDa band depicted above, represented as mean ± SEM. * represents a statistically significant ($p<0.05$) difference. **B.** Immunohistochemical staining of normal rat aorta (left) and vena cava (right) sections, without primary antibody (top) and with anti-XO antibody (bottom). Scale bar represents 100 μm. "L" indicates the luminal side.

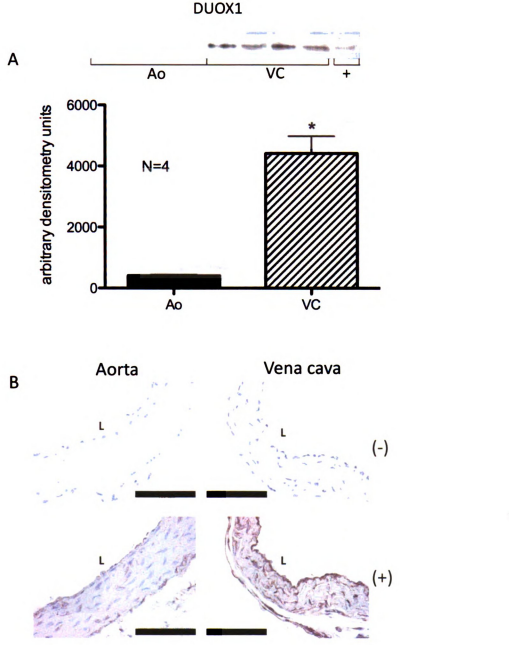

Figure 17. A. Western blot analysis of DUOX1 protein expression in normal rat aorta (Ao) and vena cava (VC) homogenates. + represents human thyroid homogenate, used as a positive control. Band densitometry quantification of DUOX1, represented as mean ± SEM. * represents a statistically significant ($p<0.05$) difference. **B.** Immunohistochemical staining of normal rat aorta (left) and vena cava (right) sections, without primary antibody (top) and with anti-DUOX1 antibody (bottom). Scale bar represents 100 μm. "L" indicates the luminal side.

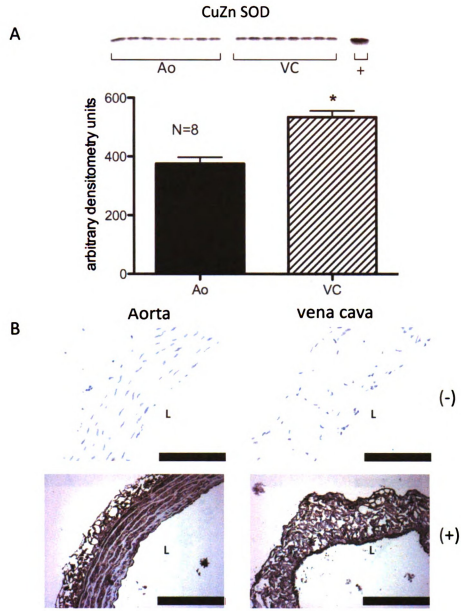

Figure 18. A. Western blot analysis of CuZn SOD protein expression in normal rat aorta (Ao) and vena cava (VC) homogenates. + represents rat kidney medulla homogenate, used as a positive control. Band densitometry quantification of 16 KDa band depicted above, represented as mean ± SEM. * represents a statistically significant ($p<0.05$) difference. **B.** Immunohistochemical staining of normal rat aorta (left) and vena cava (right) sections, without primary antibody (top) and with anti-CuZn SOD antibody (bottom). Scale bar represents 100 μm. "L" indicates the luminal side.

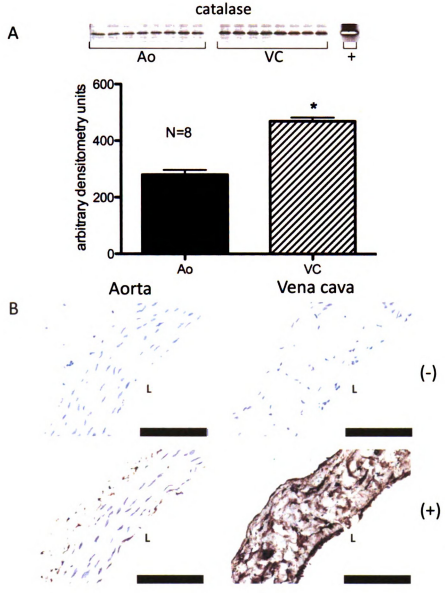

Figure 19. A. Western blot analysis of catalase protein expression in normal rat aorta (Ao) and vena cava (VC) homogenates. + represents rat kidney medulla homogenate, used as a positive control. Band densitometry quantification of 65 KDa band depicted above, represented as mean ± SEM. * represents a statistically significant ($p<0.05$) difference. **B.** Immunohistochemical staining of normal rat aorta (left) and vena cava (right) sections, without primary antibody (top) and with anti-catalase antibody (bottom). Scale bar represents 100 μm. "L" indicates the luminal side.

Higher in aorta	Fold change
Aminoadipate-semialdehyde synthase (predicted)	62.32
Cardiomyopathy associated 1 (predicted)	12.6
Nox4 (NADPH oxidase 4)	3.93
Flavin containing monooxygenase 2	3.61
Hemoglobin alpha, adult chain 1	3.55
Cytoglobin	3.49
Similar to Serine/threonine-protein kinase ATR (Ataxia telangiectasia and Rad3-related protein)	2.64
Glutathione peroxidase 5	2.61
Glutathione peroxidase 6	2.61
NADPH oxidase activator 1 (predicted)	2.61
Recombination activating gene 2 (predicted)	2.61
Thyroid peroxidase	2.61
Hemoglobin zeta	2.35

Higher in vena cava	Fold change
Myoglobin	39.17
Duox1 (Dual oxidase 1)	4.42
Solute carrier family 38, member 1	3.82
Solute carrier family 38, member 4	3.53
Neutrophil cytosolic factor 2 (predicted)	3.15
Duox2 (Dual oxidase 2)	2.76
Apolipoprotein E	2.47
Neuroglobin	2.3

Table 2. Results of oxidative stress and antioxidant defense genes PCR array, performed on normal rat aorta and vena cava whole tissue RNA samples.

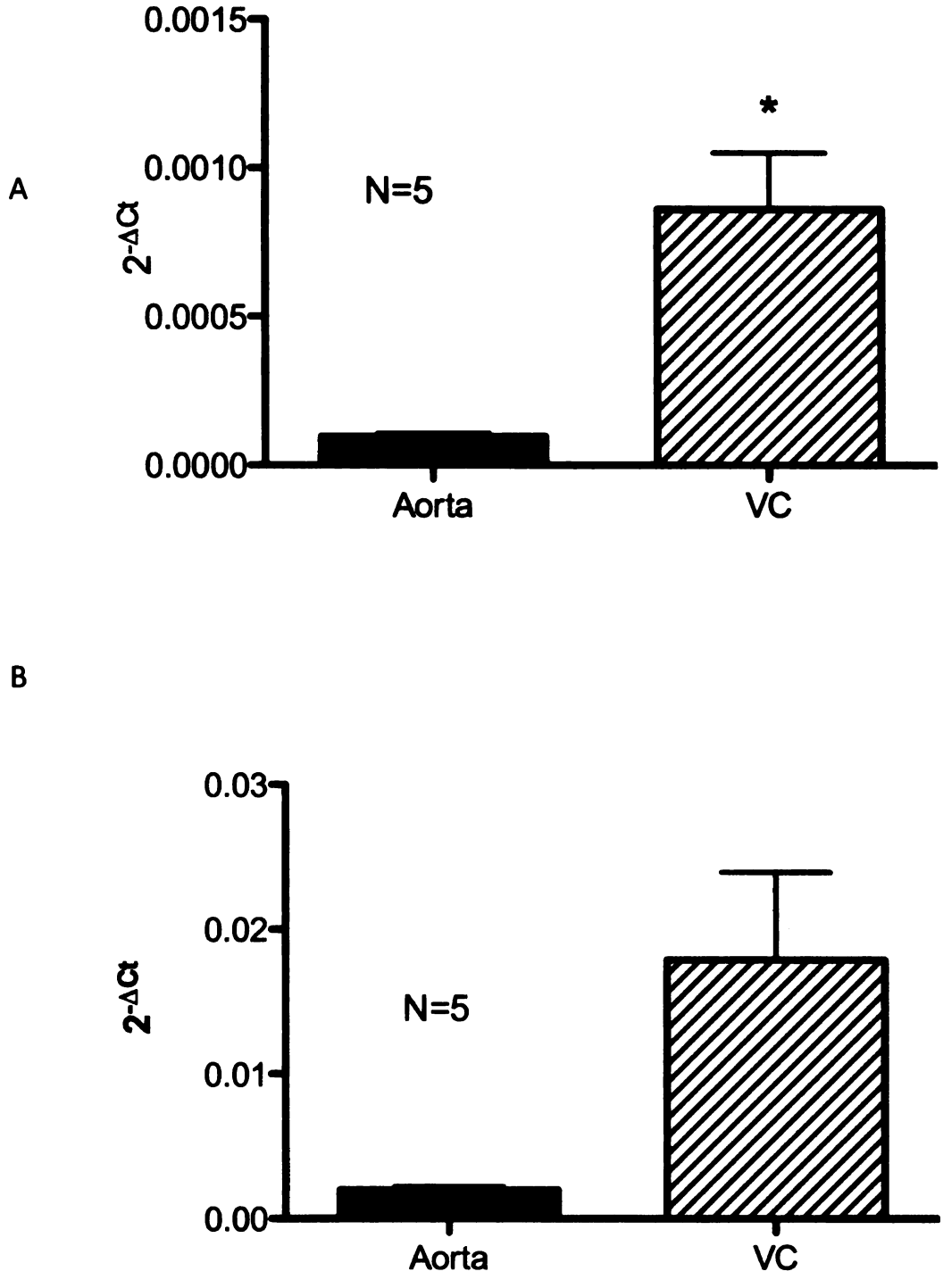

Figure 20. RT-PCR analysis of DUOX1 **(A)** and DUOX2 **(B)** mRNA expression in normal rat aorta (Ao) and vena cava (VC), expressed as change from beta-2-microglobulin ($2^{-\text{delta Ct}}$), and represented as mean ± SEM for the respective N. * represents a statistically significant ($p<0.05$) difference.

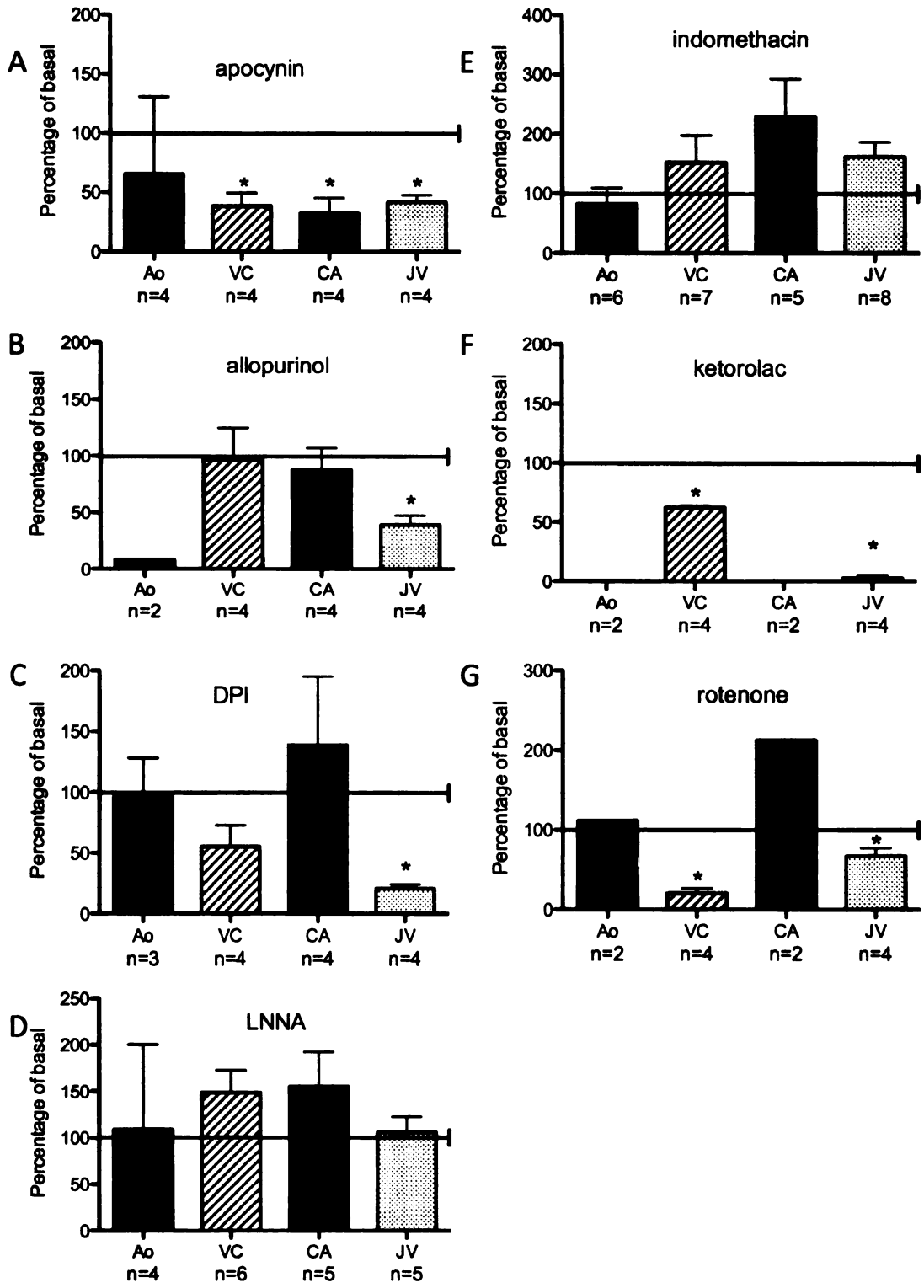

Figure 21. H_2O_2 production in normal rat aorta (Ao), vena cava (VC), carotid artery (CA) and jugular vein (JV) in the presence of ROS enzyme inhibitors, represented as percentage of the basal H_2O_2 production for the respective tissue, measured in the same animals. Bars represent means ± SEM for the respective N. * represents statistically significant decrease ($p<0.05$) compared to basal.

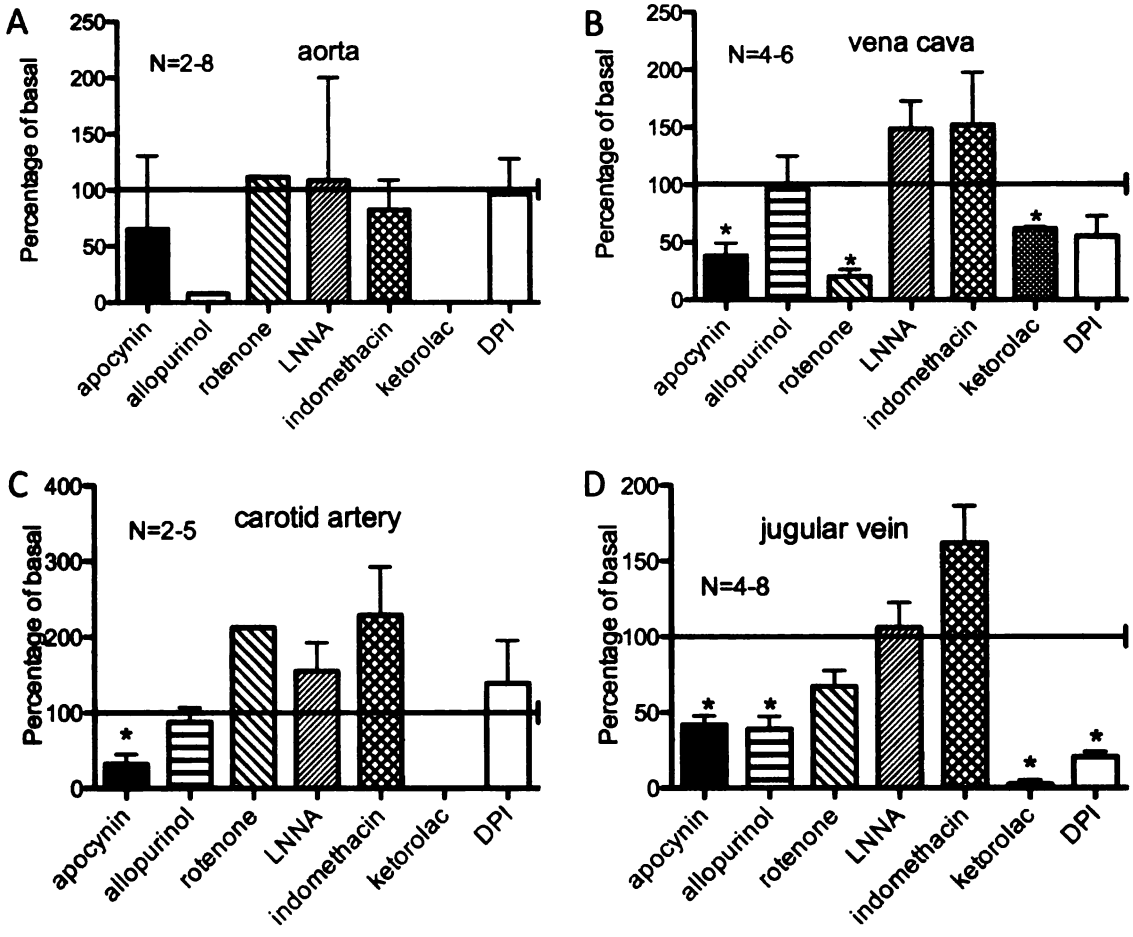

Figure 22. H_2O_2 production in normal rat aorta **(A)**, VC **(B)**, carotid artery **(C)** and jugular vein **(D)** in the presence of ROS enzyme inhibitors, represented as percentage of the basal H_2O_2 production for the respective tissue, measured in the same animals. Bars represent means ± SEM for the respective N. * represents statistically significant decrease ($p<0.05$) compared to control (basal).

uncoupling in the vasculature does not account for a major portion of superoxide production in normal conditions. Ketorolac reduced, but indomethacin had no effect on vascular H_2O_2 levels, rendering effects of COX inhibition inconclusive. Overall, the results of these experiments do not appear to overlap the results of the protein or mRNA analysis of ROS metabolizers (see discussion).

IV. ROS metabolism in DOCA-salt hypertension

A. Basal H_2O_2 levels

H_2O_2 production was measured using Amplex Red fluorescence in vascular tissues from DOCA-salt hypertensive rats (fig 23). Similarly to the normotensive conditions, basal H_2O_2 production (normalized to protein content) was higher in DOCA VC compared to DOCA aorta (fig 23A). The basal H_2O_2 production in the DOCA jugular vein was however not statistically different from the one in the DOCA carotid artery (fig 23B). The numerical results of these experiments cannot be directly compared to the ones in normotensive rats (fig 12), since the animals in the two sets were not age-matched.

B. Protein expression of ROS metabolizing enzymes

We investigated the protein expression of major ROS metabolizing enzymes in aorta and VC tissues from sham normotensive and DOCA-salt hypertensive rats. We used the same antibodies to detect protein expression as mentioned before

in the case of normal rats. The results obtained in sham normotensive rats were similar to those obtained previously in normal rats (fig 24, lanes 1-4 and 11-14). Protein expression of xanthine oxidase, catalase and CuZn SOD was higher in DOCA VC compared to DOCA Ao, while protein expression of $p47^{phox}$ was higher in DOCA Ao compared to DOCA VC (fig 24, lanes 6-9 and 16-19). Similarly to the situation in normal rats, no difference was observed in expression of MnSOD, Rac1 and eNOS between arterial and venous tissue from DOCA-salt hypertensive rats.

V. Xanthine oxidase in normal conditions and in DOCA-salt hypertension

A. XO protein expression

As previously shown, protein expression was higher in VC compared to aorta samples in both normotensive and DOCA-salt hypertensive rats (fig 16, 24). These results were obtained using a polyclonal XO antibody (Rockland). To further confirm the validity of these findings, we verified protein expression with a different XO antibody (Abcam), with similar results (not shown).

B. XO mRNA expression

Because circulating XO can bind to vascular endothelium (see discussion), we tested whether vascular XO is also locally produced by performing RT-PCR for XO mRNA. Importantly, XO mRNA was present in both aortic and VC samples.

In addition, relative quantification of XO to GAPDH mRNA (fig 25) showed that XO mRNA expression was higher in the VC compared to the aorta. During DOCA-salt hypertension, XO mRNA expression was maintained at a similar level in both types of tissues, with higher expression in DOCA VC compared to DOCA aorta.

C. XO activity

XO protein activity was measured through two independent assays. First, the formation of urate, the final product of XO-catalyzed reactions, was determined spectrophotometrically from tissue homogenates, in the presence of the XO substrate xanthine. The signal measured in the presence of the XO inhibitor allopurinol (100 μM) was considered as non-specific and was subtracted from the total. The resulting XO activity, expressed as the allopurinol-inhibitable uric acid production in the presence of xanthine, was normalized to the total protein content of samples. XO activity was higher in VC compared to aorta samples in normal rats (fig 26 A).

Second, the formation of H_2O_2 from whole tissues in the presence of xanthine was measured fluorometrically using the Amplex Red assay. Allopurinol was again used to subtract the non-XO derived H_2O_2 formation. XO activity expressed as allopurinol-inhibitable H_2O_2 production, was higher in VC compared to aorta (fig 26 B).

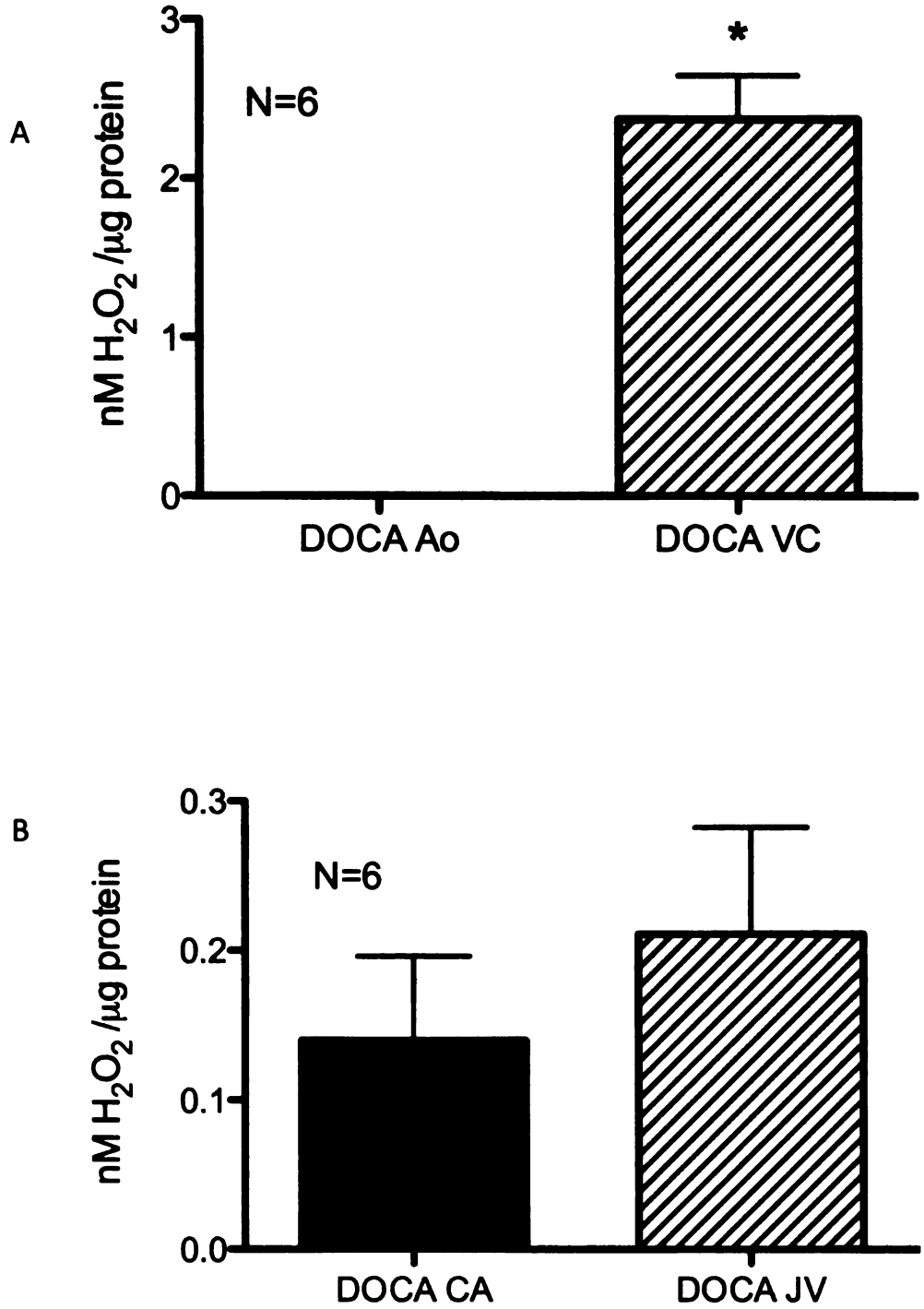

Figure 23. Basal hydrogen peroxide production measured by Amplex Red fluorescence in tissues from DOCA-salt hypertensive rats: aorta (Ao) and vena cava (VC) **(A)**; carotid artery (CA) and jugular vein (JV) **(B)**. Data are represented as mean ± SEM for the respective N. * represents a statistically significant ($p<0.05$) difference.

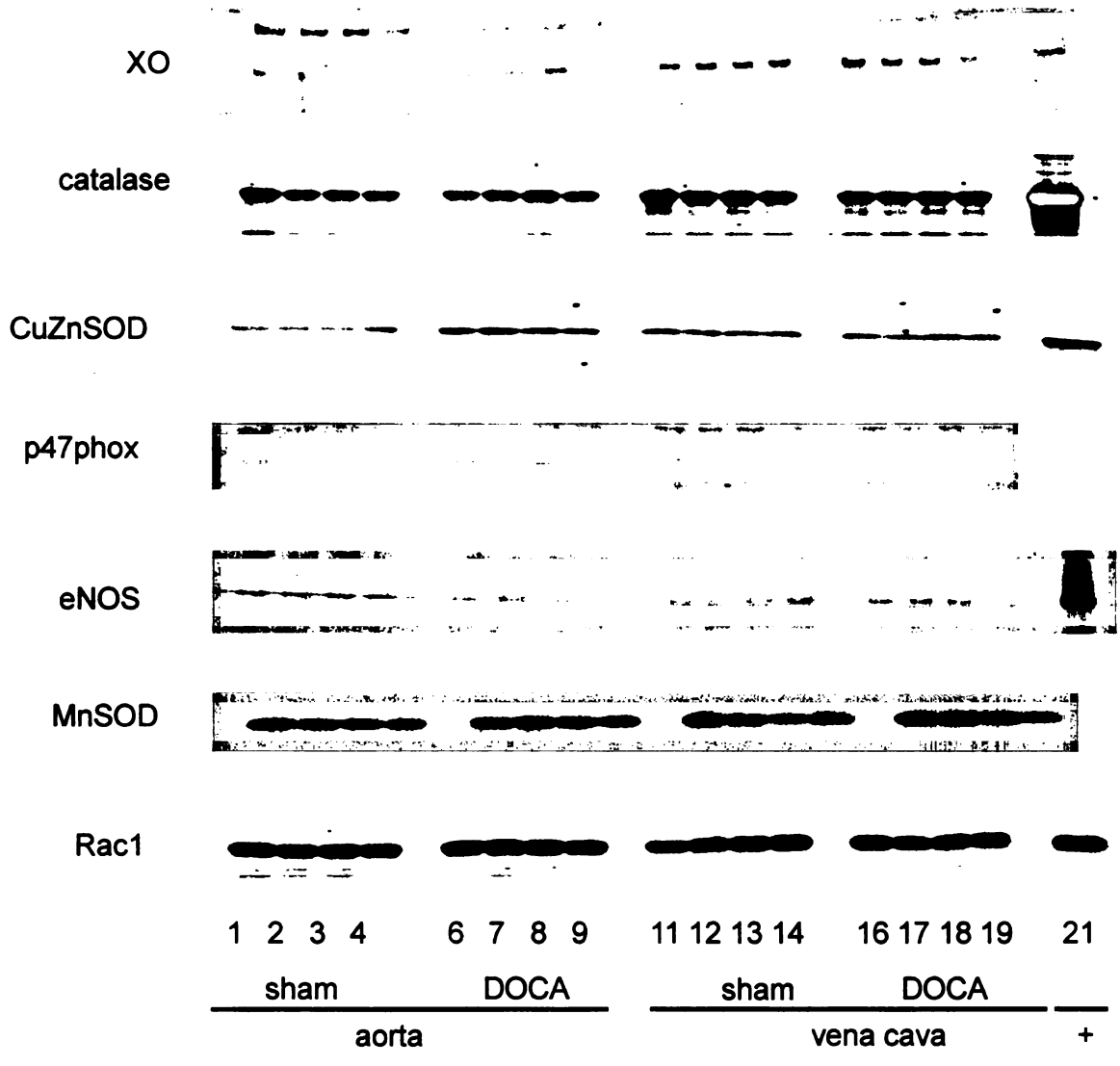

Figure 24. Western blot analysis of ROS metabolizing enzymes in sham aorta (lanes 1-4), DOCA aorta (lanes 6-9), sham vena cava (lanes 11-14) and DOCA vena cava (16-19). Positive controls (+) were loaded on lane 21.

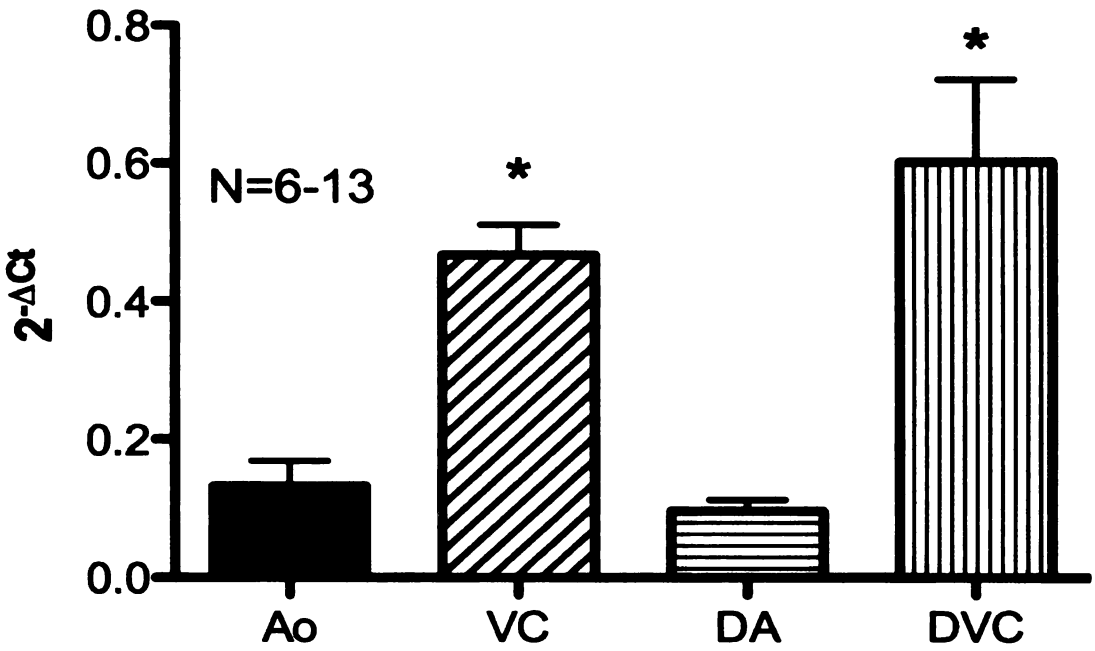

Figure 25. RT-PCR analysis of XO mRNA expression in normal rat aorta (Ao) and vena cava (VC), and DOCA-salt rat aorta (DA) and vena cava (DVC), expressed as change from GAPDH ($2^{-delta\ Ct}$), represented as mean ± SEM for the respective N. * represents a statistically significant ($p<0.05$) difference between artery-vein pair.

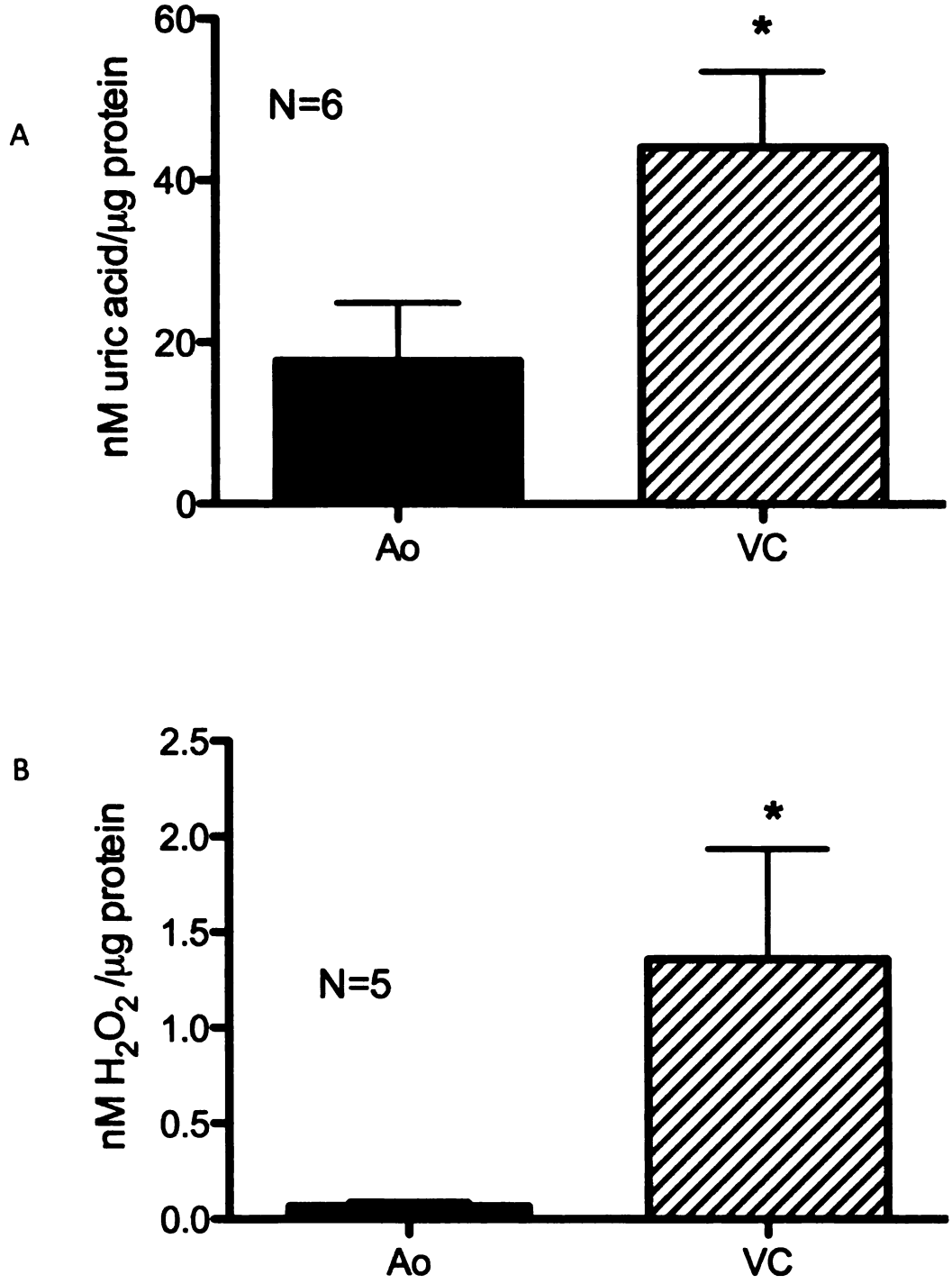

Figure 26. A. Xanthine oxidase activity in normal rat aorta (Ao) and vena cava (VC) homogenates as allopurinol-inhibitable urate production. **B.** Xanthine oxidase activity in rat aorta (Ao) and vena cava (VC) whole tissues as allopurinol-inhibitable hydrogen peroxide production. Data are represented as mean ± SEM for the respective N. * represents a statistically significant ($p<0.05$) difference.

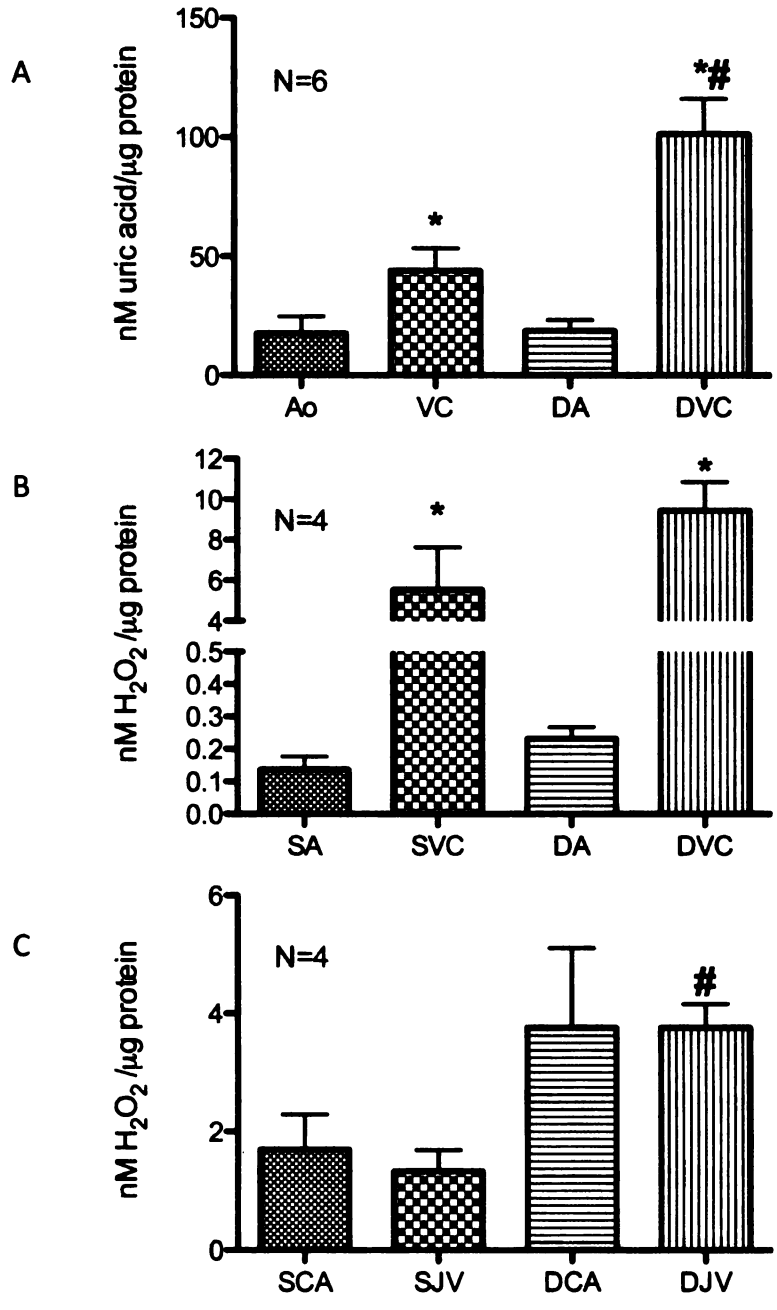

Figure 27. A. Xanthine oxidase activity in normal aorta (Ao), normal vena cava (VC), DOCA aorta (DA) and DOCA vena cava (DVC) homogenates as allopurinol-inhibitable urate production. **B.** Xanthine oxidase activity in sham aorta (SA), sham vena cava (SVC), DOCA aorta (DA) and DOCA vena cava (DVC) whole tissues as allopurinol-inhibitable hydrogen peroxide production. **C.** Xanthine oxidase activity in sham carotid artery (SCA), sham jugular vein (SJV), DOCA carotid artery (DCA) and DOCA jugular vein (DJV) whole tissues as allopurinol-inhibitable hydrogen peroxide production. Data are represented as mean ± SEM for the respective N. * represents a statistically significant ($p<0.05$) difference between artery-vein and # between sham-DOCA.

XO activity in aorta from DOCA-salt hypertensive rats was similar to that in normotensive rat aorta in both activity assays (fig 27A-B). However XO activity in DOCA VC was significantly increased compared to normal VC in the urate-based assay (fig 27A) and displayed a similar trend in the H_2O_2-based assay (fig 27B). The XO activity in jugular vein was not different from that in carotid artery in both sham and DOCA-salt hypertensive rats, however, the XO activity of both these tissues appeared increased in DOCA-salt hypertensive compared to sham normotensive rats, this increase being statistically significant in the case of the jugular vein (fig 27C).

Section summary: Comparisons of ROS levels by arterial and venous tissue have shown that the ROS production in veins was higher compared to corresponding arteries. The H_2O_2-degrading capacity of veins was similarly increased. There were multiple differences in ROS metabolizing enzymes between arteries and veins. There was a higher expression of DUOX1, CuZn SOD and catalase in venous compared to arterial tissue. The most consistent findings were related to xanthine oxidase. XO had a higher protein and mRNA expression, as well as higher activity in veins compares to arteries. During DOCA-salt hypertension, the higher expression of XO was maintained by veins, and there were strong indications of an increase in venous, but not arterial activity.

Specific aim 2: Determine if there is a difference in the impact of ROS on arterial versus venous contractile function in basal conditions and in hypertension

Rationale: ROS can influence vascular contraction, proliferation, remodeling and inflammation. Similarly to general characteristics of ROS metabolism, the functional impact of ROS is by far more extensively studied in arteries compared to veins. When testing the venous role in hypertension, vascular contraction is the most important function to be investigated. Since levels of ROS appeared overall to be higher in veins compared to arteries, we next examined whether the functional consequence of this difference impacts upon the vascular response to contractile stimuli in these blood vessels.

I. Direct impact of ROS on contractile function of arteries and veins.

To compare the functional impact of ROS on rat aorta and VC tissues, we exposed these vessels to extraneous superoxide in isolated tissue baths. Endothelium-intact aorta and VC rings both contracted in a concentration-dependent manner to exogenous superoxide, generated by the addition of increasing amounts of XO to xanthine (200 μM) in the tissue bath (figure 28). This contraction was larger in the VC compared to the aorta, when normalized to an α adrenergic-mediated response.

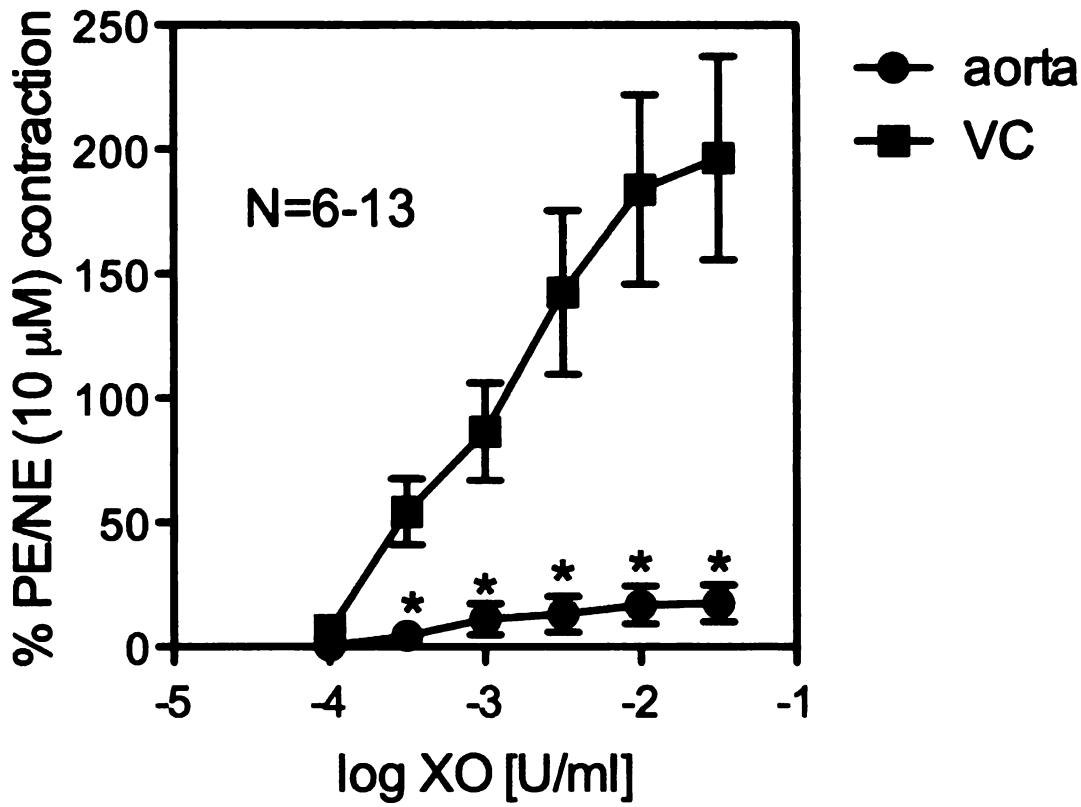

Figure 28. Cumulative xanthine oxidase concentration-response curves in the presence of 200 µM xanthine, of normal, endothelium-intact rat aorta (circles) and vena cava (squares) rings, represented as percentage of the initial contraction to 10 µM phenylephrine (PE) or norepinephrine (NE) for aorta and VC, respectively. Points represent mean ± SEM for the respective N. * represents a statistically significant ($p<0.05$) difference.

A similarly larger contraction in the VC compared to the aorta was observed in response to H_2O_2 in experiments previously published from our laboratory (see discussion).

II. Impact of XO on arterial and venous contractile function in normal rats

A. Impact of XO

To assess the potential involvement of XO-mediated ROS production on vascular reactivity, we tested the effects of the XO inhibitor allopurinol on vascular responses to several agonists in isolated tissue bath experiments (fig 29-30). We used agonists that are important endogenous effectors of vascular tone and that induce contractile responses in both aorta and VC: norepinephrine (NE) as a generic alpha adrenergic-agonist (panels A); and angiotensin II (AngII) (panels C) and endothelin-1 (ET-1) (panels D), peptides commonly associated with ROS production in vascular tissues. We also used acetylcholine (ACh) as a relaxing agent and a general measure of endothelial function (panels B). We used the same allopurinol concentration (100 μM) as in our previous *in vitro* XO activity experiments. This concentration effectively reduced increases in XO products (urate and H_2O_2) in the presence of substrate (xanthine). Allopurinol did not modify the contraction or relaxation of normal aorta rings to any of these agonists (fig 29). In the vena cava (fig 30), allopurinol (100 μM) did not have an effect on the NE-induced contraction or the ACh-induced relaxation (fig 30B), and the trend for a decreased AngII-induced contraction in its presence was not

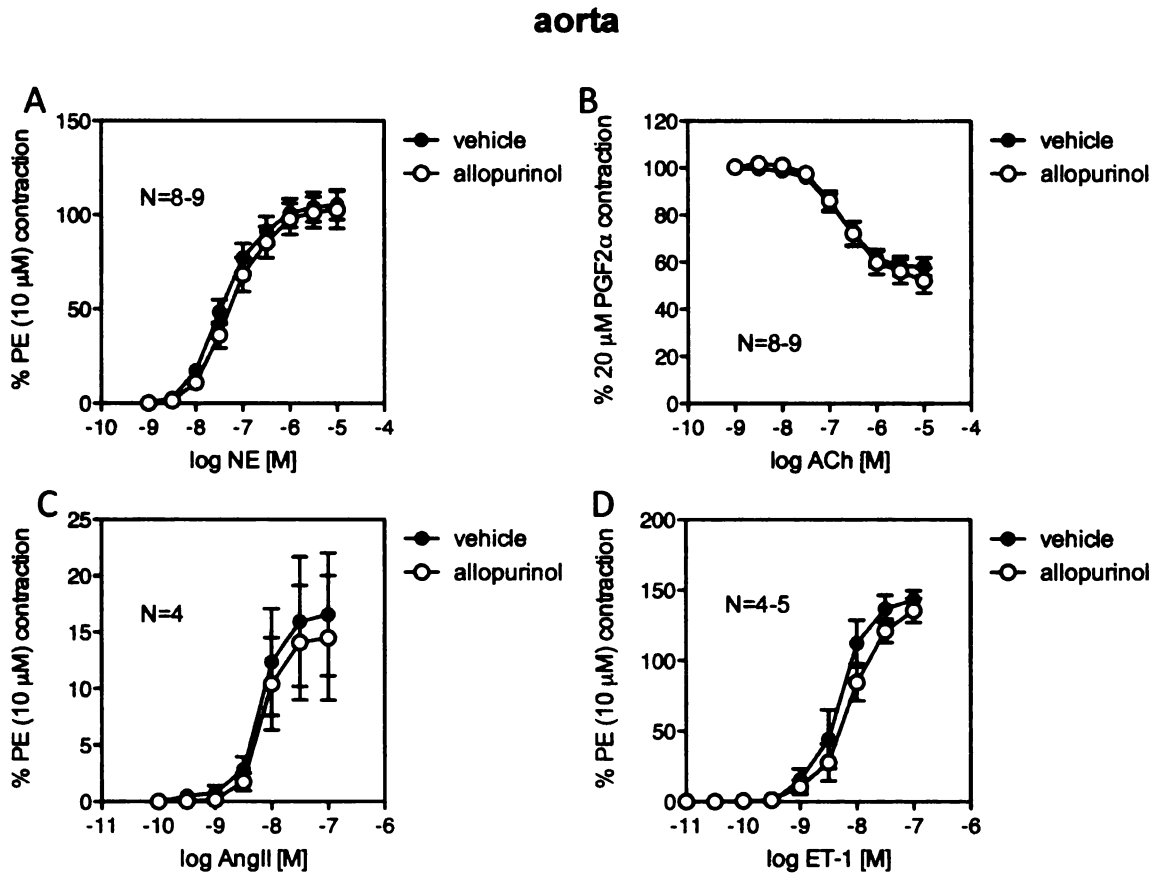

Figure 29. Cumulative concentration-response curves to norepinephrine **(A)**, acetylcholine **(B)**, angiotensin II **(C)** and endothelin-1 **(D)** of endothelium-intact rat aorta rings in the presence of allopurinol (100 µM) (open symbols) or vehicle (closed symbols), represented as percentage of contraction to 10 µM phenylephrine (PE) or 20 µM $PGF_{2\alpha}$. Points represent mean ± SEM for the respective N. * represents a statistically significant ($p<0.05$) difference.

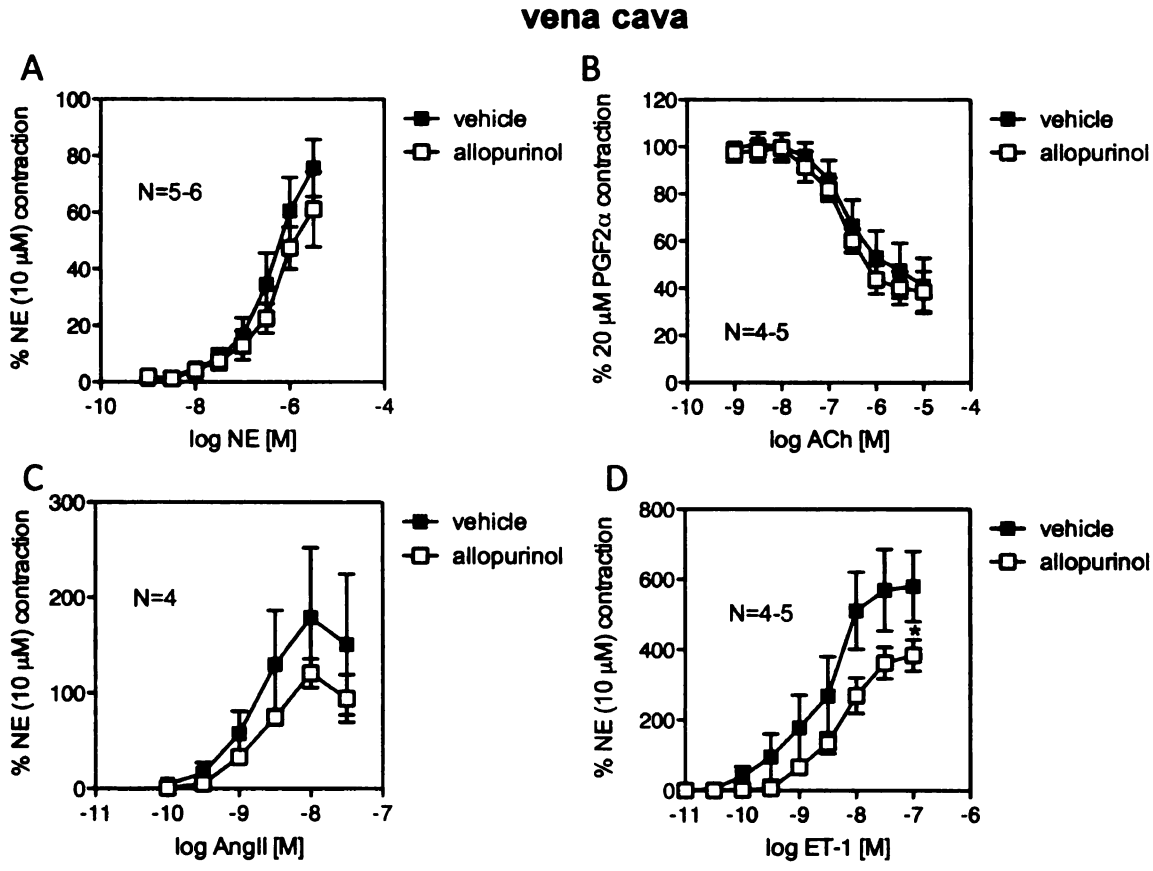

Figure 30. Cumulative concentration-response curves to norepinephrine **(A)**, acetylcholine **(B)**, angiotensin II **(C)** and endothelin-1 **(D)** of endothelium-intact rat vena cava in the presence of allopurinol (100 µM) (open symbols) or vehicle (closed symbols), represented as percentage of contraction to 10 µM norepinephrine (NE) or 20 µM $PGF_{2\alpha}$. Points represent mean ± SEM for the respective N. * represents a statistically significant ($p<0.05$) difference.

statistically significant (fig 30C). However, allopurinol significantly reduced the maximal contraction to ET-1 (10^{-7} M) in the VC (fig 30D). As previously reported, AngII and ET-1 were more efficacious and more potent in VC compared to aortic rings, when reported as a percentage of the initial contraction to 10 μM NE (VC) or PE (aorta).

B. Impact of uric acid

XO may also influence contractile function through its other product, uric acid. Rodents express uricase, a urate-degrading enzyme. The expression of uricase, identified as the 64 KDa band corresponding to a uricase dimer, was higher in VC compared to aorta in normal rats (fig 31).

Uric acid may have multiple effects on vascular contractile function (see Introduction). Because XO expression, as well as its uric acid producing activity, was higher in the rat VC compared to aorta, we hypothesized that any direct contractile effects of uric acid would be higher in the VC compared to the aorta. To investigate the acute effects of uric acid on vascular contractile function, we performed isolated tissue bath experiments using uric acid in combination with oxonic acid, an inhibitor of uricase. Uric acid (10^{-9}-10^{-4} M), alone or in combination with oxonic acid (10 μM), did not induce contraction of endothelial-intact rat aorta or VC rings (fig 32A). Uric acid (100 μM) in combination with oxonic acid (10 μM) did not significantly change acetylcholine (ACh)-induced

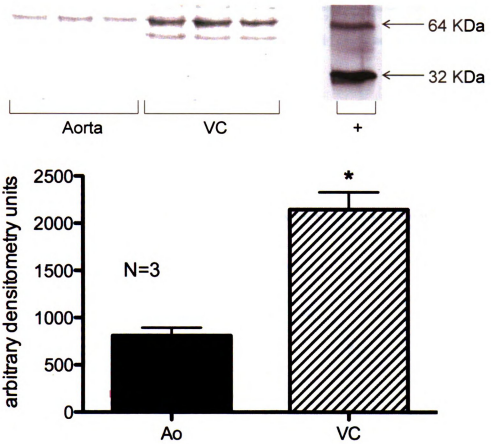

Figure 31. (top) Uricase protein expression in normal rat aorta and vena cava. Positive control (+) for uricase expression is a rat liver lysate. (bottom) Band densitometry quantification of 64 KDa band depicted above. Represented as mean ± SEM for the respective N. * represents a statistically significant difference ($p<0.05$).

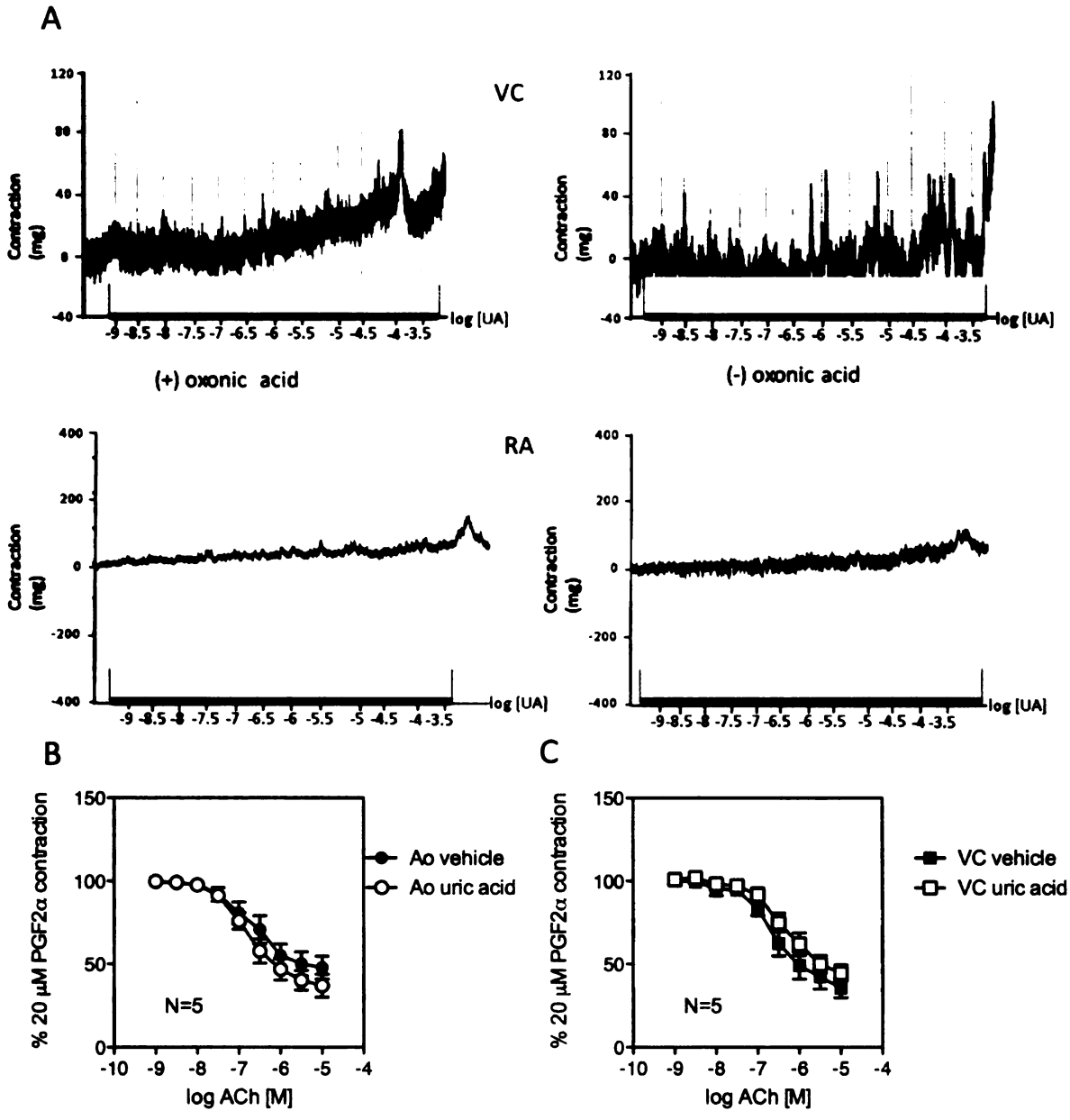

Figure 32. A. Tracings of cumulative concentration response curves to uric acid (10^{-9} M to $3*10^{-4}$ M) in the presence (left) or absence (right) of oxonic acid (10 µM) in endothelium-intact normal rat vena cava (top) and aorta (bottom) rings. **B, C.** Cumulative concentration response curves to acetylcholine (ACh, 10^{-9}-10^{-5} M) of endothelium-intact aorta **(B)** and vena cava **(C)** in the presence of vehicle (closed symbols) or uric acid (100 µM) plus oxonic acid (10 µM) (open symbols). Points represent means ± SEM of % of contraction induced by 20 µM $PGF_{2\alpha}$.

relaxation curves of endothelial-intact rat aorta or VC rings contracted with 20 μM $PGF_{2\alpha}$ (fig 32B-C).

III. Impact of flavoenzymes on endothelin-1 induced contraction of aorta and vena cava

Because we observed allopurinol inhibiting maximal contractions induced by ET-1 in the vena cava, as well as higher expression of XO and DUOX enzymes (both flavoenzymes) in the vena cava compared to aorta, we investigated whether a general flavoenzyme inhibitor would alter ET-1-induced contraction of these tissues in isolated tissue bath experiments. Concentration response curves to ET-1 were performed on endothelium-intact aorta and VC rings in the presence of diphenyleniodonium (DPI) or vehicle (fig 33). ET-1-induced contraction was not altered in the aorta (fig 33A), however it was significantly decreased in the VC upon exposure to DPI (fig 33B), suggesting flavoenzymes contribute to ET-1 mediated contraction of VC, but not aorta.

IV. Arterial and venous endothelial function in normal rats and during DOCA-salt hypertension

Arterial endothelial function is characteristically impaired in human and animal models of hypertension. There are multiple mechanisms behind the hypertensive endothelial dysfunction, but the increased ROS production commonly observed

in hypertension is a generally accepted pathogenetic factor. The most obvious argument supporting this idea is the fact that superoxide, the initiator of the ROS cascade, directly reacts with NO, the endothelial-derived relaxing factor, thus decreasing its bioavailability. The decreased NO levels and the impaired NO-mediated relaxation are hallmarks of endothelial dysfunction. Because we observed higher ROS production in veins compared to arteries (see aim1), we hypothesized that venous endothelial function would be affected by hypertension to at least a similar, if not a higher degree as compared to arteries.

We tested the endothelial function of aorta and VC from normal and DOCA-salt hypertensive rats in isolated tissue bath experiments by performing ACh-induced relaxation curves on rings of tissues stably contracted with $PGF_{2\alpha}$ (20 μM). In normal conditions, VC relaxed in a similar fashion to ACh as the aorta (fig 34A). To confirm the dependence of ACh-induced relaxation on NO production, we performed the same experiment in the presence of LNNA, a NOS inhibitor (fig 34B). We observed complete abolishment of ACh-induced relaxation in the presence of LNNA, suggesting that both aorta and VC ACh-mediated responses are dependent on NOS function. In tissues from DOCA-salt hypertensive rats, while we confirmed the characteristic hypertensive arterial endothelial dysfunction, i.e. a significant decrease in the ACh-induced relaxation in aorta rings, we did not observe any loss in the endothelial function of VC with hypertension (fig 35A). The ACh-mediated responses in tissues from DOCA-salt rats appeared to maintain their dependence on NOS function, as evidenced by their abolishment in the presence of LNNA (fig 35B).

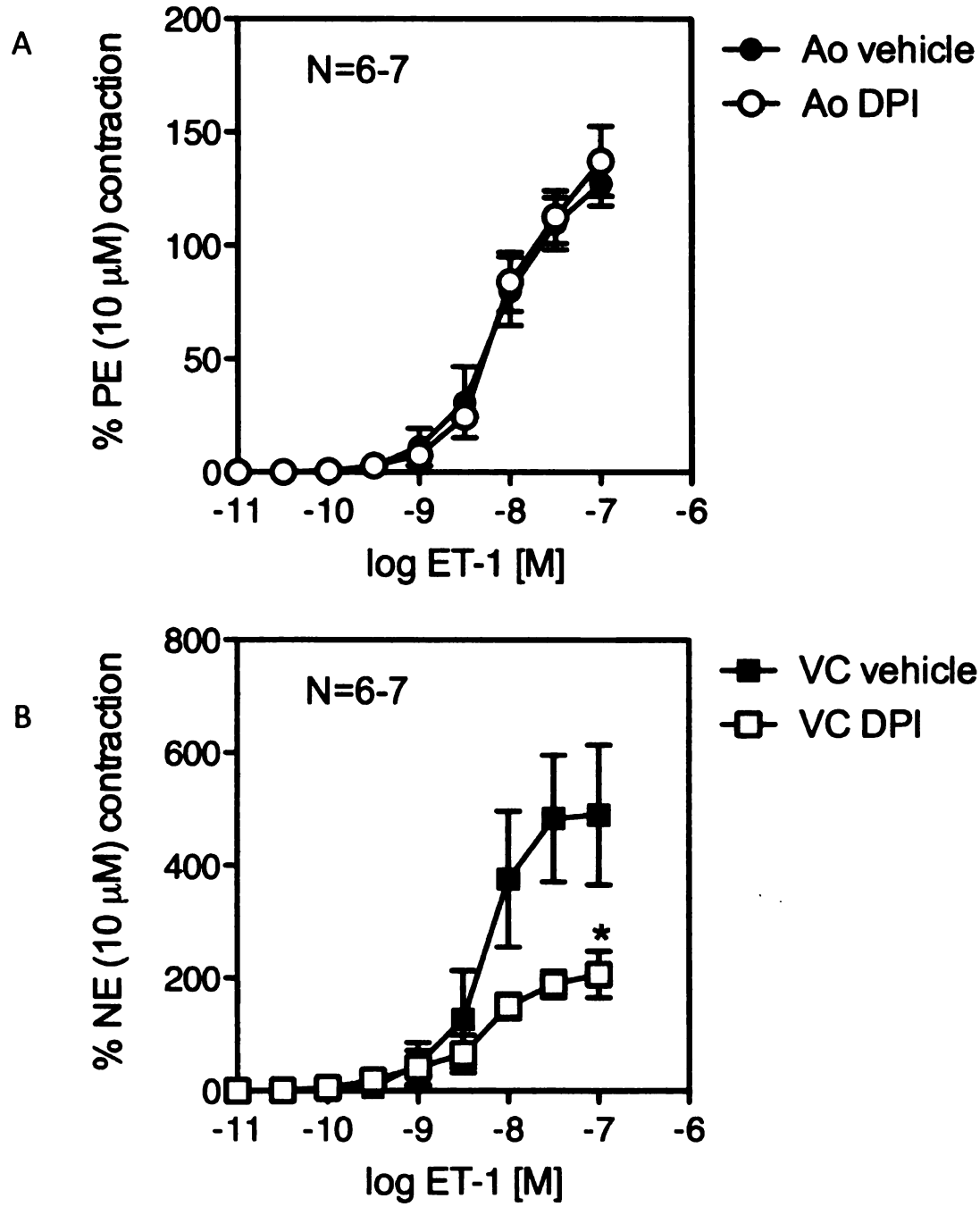

Figure 33. Cumulative concentration response curves to endothelin-1 (ET-1, 10^{-11}-10^{-7} M) of endothelium-intact rat aorta **(A)** and vena cava **(B)** in the presence of vehicle (closed symbols) or diphenyleniodonium (DPI, 10 µM) (open symbols). Points represent means ± SEM percentage of initial contraction induced by 10 µM phenylephrine (PE) or norepinephrine (NE) for aorta and vena cava, respectively.

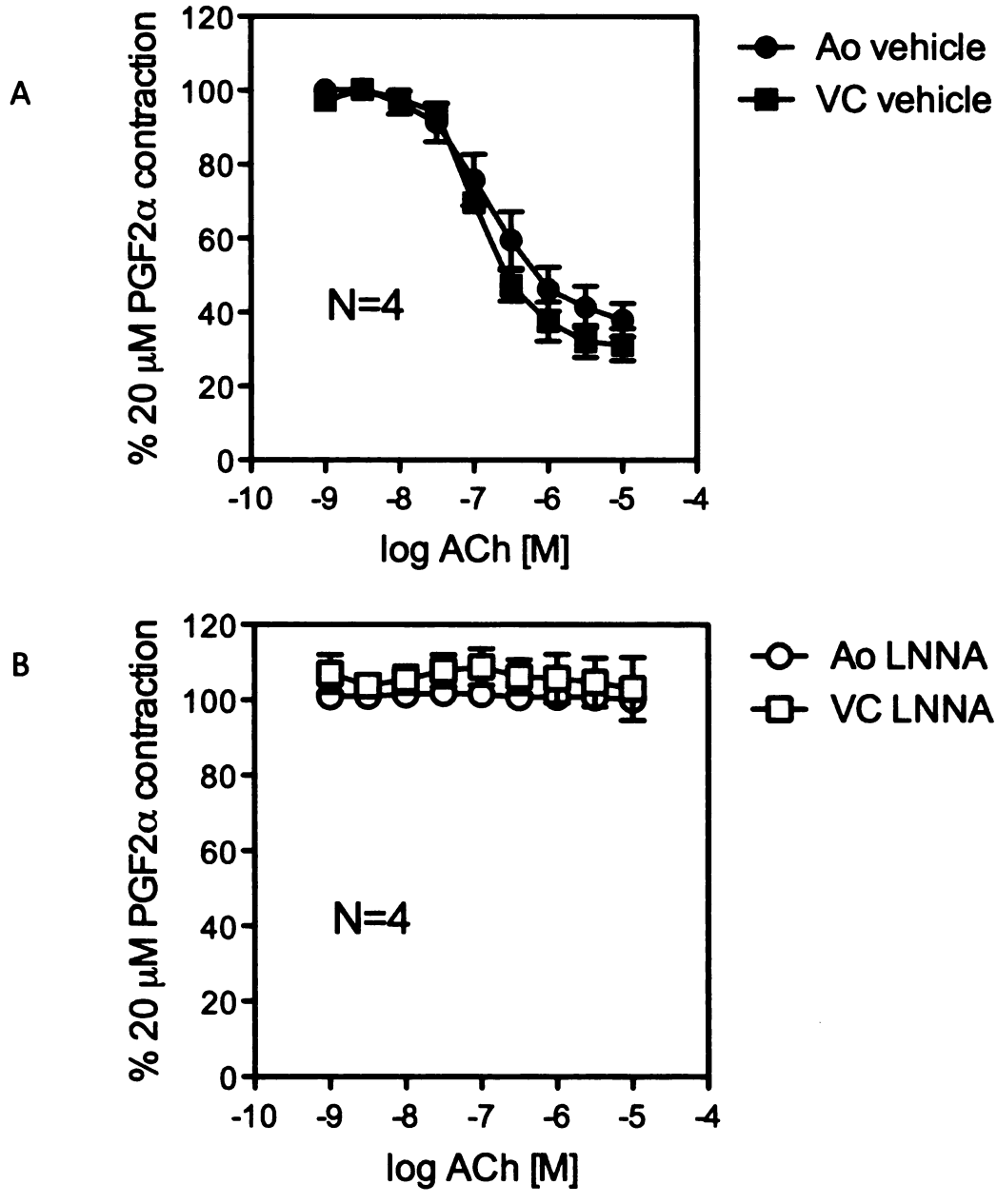

Figure 34. Cumulative concentration response curves to acetylcholine (ACh, 10^{-9}-10^{-5} M) of rat aorta (RA) and vena cava (RVC) rings from normal rats in the presence of vehicle (**A**, closed symbols) or LNNA (100 µM) (**B**, open symbols). Points represent means ± SEM percentage of contraction induced by 20 µM $PGF_{2\alpha}$.

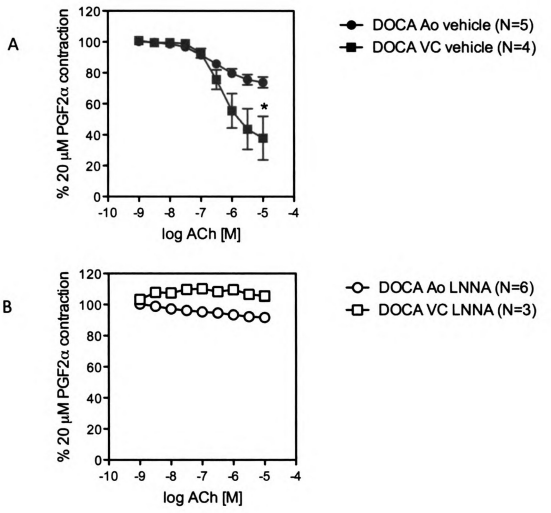

Figure 35. Cumulative concentration response curves to acetylcholine (ACh, 10^{-9}-10^{-5} M) of rat aorta (RA) and vena cava (RVC) rings from DOCA-salt hypertensive rats in the presence of vehicle (**A**, closed symbols) or LNNA (100 µM) (**B**, open symbols). Points represent means ± SEM percentage of contraction induced by 20 µM $PGF_{2\alpha}$.

V. Impact of XO on arterial endothelial function in DOCA-salt hypertension

Because we did not observe endothelial dysfunction in the VC during DOCA-salt hypertension, we pursued the following experiments only in aorta tissues from sham normotensive and DOCA-salt hypertensive rats.

A. Impact of XO

To evaluate the potential impact of XO on the aortic endothelial dysfunction, we tested the effect of allopurinol on ACh-induced relaxation of sham and DOCA aorta. Endothelial function, assessed as relaxation to ACh (10^{-9}-10^{-5} M) from 20 μM $PGF_{2\alpha}$-induced contraction, was again expectedly impaired in aorta from DOCA-salt hypertensive rats compared to normotensive sham controls (fig 36, vehicle), as evidenced by a decreased relaxation response to ACh. Inhibition of XO enzyme activity with allopurinol (100 μM) did not significantly change ACh-induced relaxation curves of sham and DOCA rat aorta rings contracted with 20 μM $PGF_{2\alpha}$ (fig 36, allopurinol), suggesting that acute inhibition of both uric acid and ROS production by XO does not improve nor worsen DOCA-salt aorta endothelial dysfunction.

B. Impact of uric acid

We performed the same experiment as above to explore the direct effects of uric acid on the endothelial dysfunction in DOCA aorta. Addition of uric acid (100 μM)

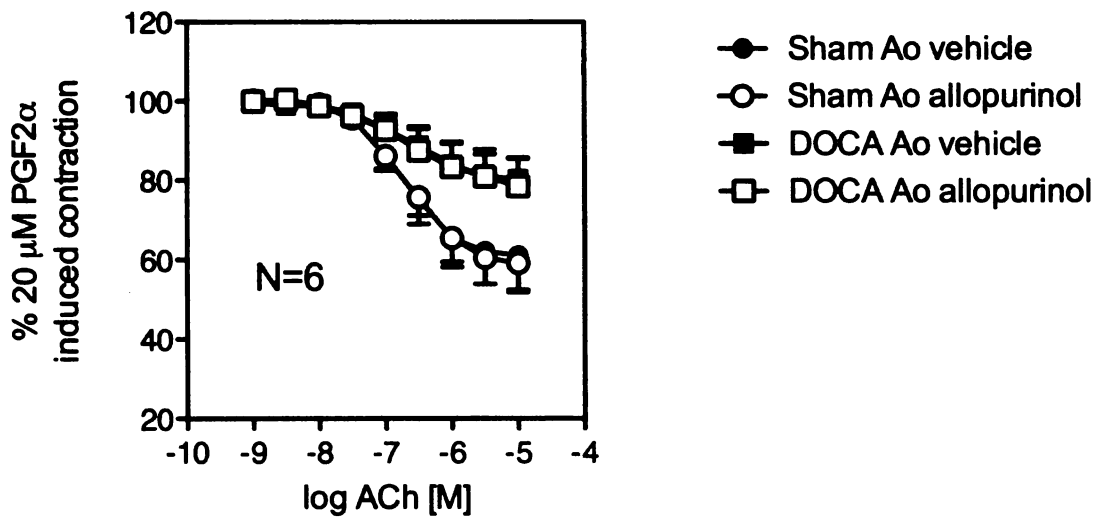

Figure 36. Cumulative concentration response curves to acetylcholine (ACh, 10^{-9}-10^{-5} M) of aorta (Ao) rings from sham normotensive (circles) and DOCA-salt hypertensive rats (squares) in the presence of vehicle (closed symbols) or allopurinol (100 µM) (open symbols). Points represent means ± SEM percentage of contraction induced by 20 µM $PGF_{2\alpha}$.

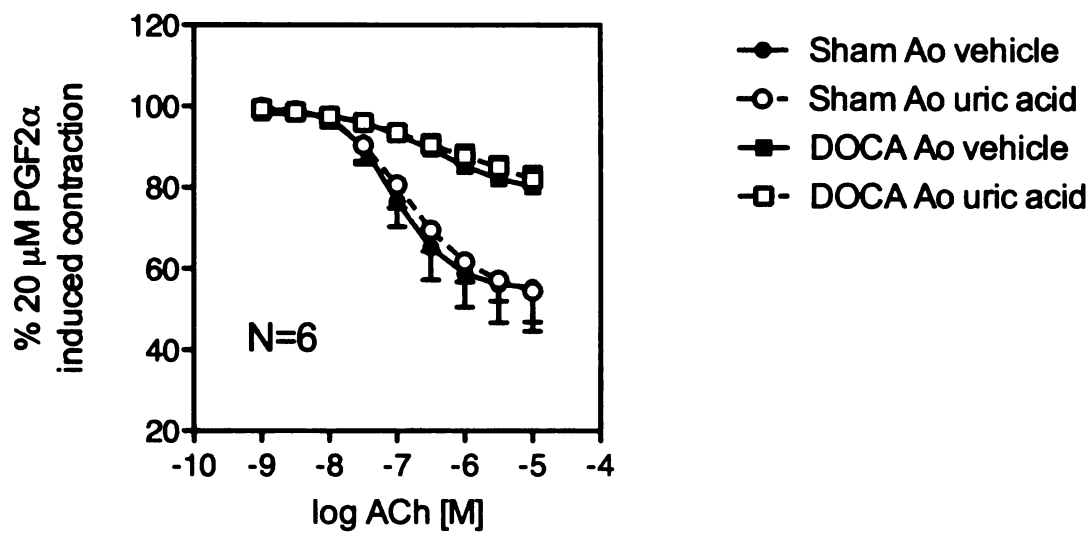

Figure 37. Cumulative concentration response curves to acetylcholine (ACh, 10^{-9}-10^{-5} M) of aorta (Ao) rings from sham normotensive (circles) and DOCA-salt hypertensive rats (squares) in the presence of vehicle (closed symbols) or uric acid (100 µM) plus oxonic acid (10 µM) (open symbols). Points represent means ± SEM percentage of contraction induced by 20 µM $PGF_{2\alpha}$.

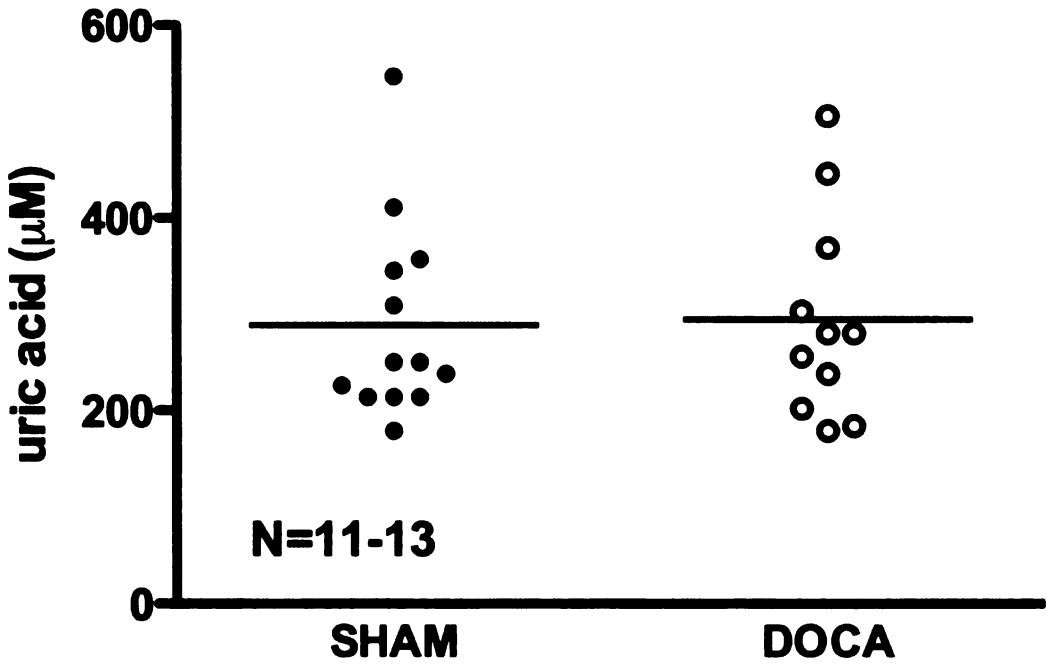

Figure 38. Uric acid levels in arterial blood of individual sham normotensive (closed symbols) and DOCA-salt hypertensive (open symbols) rats. Line represents average uric acid for the respective N.

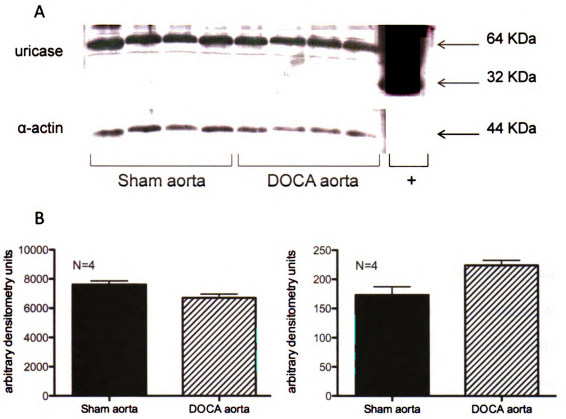

Figure 39. A. Uricase (upper panel) and control α-actin (lower panel) protein expression in aorta from sham normotensive and DOCA-salt hypertensive rats. Positive control (+) for uricase expression is a rat liver lysate. **B.** Band densitometry quantification of the 64 KDa band represented in the upper panel (left) and represented as a percent of the densitometry quantification of α-actin band represented in the lower panel (right).

in combination with oxonic acid (10 μM) did not significantly change the ACh-induced relaxation curves of sham and DOCA rat aorta (fig 37), suggesting that acute exposure to exogenous uric acid does not improve nor worsen DOCA-salt aorta endothelial dysfunction.

We also explored the possibility of a chronic decrease in antioxidant uric acid levels in the DOCA-salt hypertension model that would contribute to arterial endothelial dysfunction. Uricemia was measured in sham normotensive and DOCA-salt hypertensive rats. No significant changes were observed between the two groups (figure 38). Moreover, no significant correlation was found between the uric acid level and blood pressure of individual rats (not shown).

Since XO expression and activity do not change in aorta during DOCA-salt hypertension, suggesting that local aortic uric acid production is not changed, we decided to also investigate the aortic protein expression of uricase, the urate-degrading enzyme (fig 39). Quantification of the 64 KDa band densitometry itself or expressed as percentage of the smooth muscle α-actin band densitometry revealed no significant change between the sham and the DOCA aorta.

Section summary: The functional impact of ROS on contraction was higher in veins compared to arteries. In basal conditions, XO appeared to play little role in arterial contractile function, however it contributed to venous ET-1-mediated contraction. In normal conditions, the endothelial function of arteries and veins was similar. During DOCA-salt hypertension, arteries, but not veins, were

affected by endothelial dysfunction. XO did not appear to contribute to the arterial hypertensive dysfunction by either ROS or urate production.

Specific aim 3: Determine whether venous function and blood pressure can be influenced by changing ROS levels *in vivo*

Rationale: Our results showed that ROS levels were higher in venous tissue compared to arterial tissue. XO may contribute differentially to those levels, having a higher expression and activity as well as a greater influence on venous contraction to agonists such as ET-1. During DOCA-salt hypertension, venous, but not arterial XO activity was increased. Inhibition of ROS production was shown to have preventative or ameliorating effects in various animal models of hypertension. If the above are true, then inhibiting ROS, or particularly XO activity in vivo would have a differential effect in arteries and veins, preferentially lowering ROS levels in venous tissue over arterial tissue and diminishing the contractile effects of ET-1 (and perhaps other agonists) in veins. This would potentially lower venomotor tone, and therefore mean circulatory filling rpessure (MCFP). If MCFP is lowered by XO inhibition and if venomotor tone is a key parameter during the development of hypertension, then in vivo inhibition of XO should either reduce BP in the case of established hypertension or protect the animals from increases in BP in the initial stages of experimental hypertension.

I. XO inhibition in the established DOCA-salt hypertension

To inhibit XO activity *in vivo*, we used allopurinol, administered orally, at 50 mg/kg/day (in the drinking water). The dose/administration route chosen are the most commonly used in rodent XO research studies. We have also previously

attempted parenteral administration of allopurinol: subcutaneously (through osmotic minipumps) and intravenously (data not shown). Due to the poor water solubility of purine analogues and the adverse reactions seen with organic or strong basic solvents, we chose the oral route. Additionally, this route mimics the human administration of allopurinol. The chosen dose is a mid-range rodent allopurinol dose that has been proven to inhibit XO activity (see discussion).

To determine whether allopurinol would reduce BP of hypertensive animals, we performed a study (fig 40) administering allopurinol (50 mg/kg/day, orally) or vehicle to DOCA-salt hypertensive rats. The drug and its vehicle were administered for 7 days starting at 3 weeks after the DOCA-salt treatment was initiated.

Blood pressure was monitored through radiotelemetry. Urine was collected at three time points: before the initiation of DOCA-salt, after 2 weeks of DOCA-salt treatment and at the end of the allopurinol administration. Serum and tissues (aorta, vena cava, carotid artery, jugular vein, liver, kidney and heart) were collected at the end of the study. Urine, serum and tissue samples were used for HPLC measurements of uric acid and allantoin (products downstream of xanthine oxidase), hypoxanthine and xanthine (substrates upstream of xanthine oxidase) and allopurinol and oxypurinol (the drug and its active metabolite).

The results of the HPLC analysis of urine samples are displayed in figure 41. No significant changes from baseline were observed in the urinary levels of uric acid and allantoin after 2 weeks of DOCA treatment or at the end of allopurinol

administration in either group; and there were no significant changes of uric acid and allantoin between the allopurinol treated and the vehicle group at any time point (fig 41, top). Urinary levels of hypoxanthine and xanthine in the two treatment groups were similar at baseline and during DOCA-salt hypertension. However, these levels increased substantially in the allopurinol-treated group at the end of the treatment (fig 41, middle). Allopurinol and oxypurinol were detected in the urine of allopurinol-treated rats at the end of the treatment (fig 41, bottom).

The results of the HPLC analysis of serum samples collected at the end of the experiment are displayed in figure 42. A clear trend for reduction of both uric acid and allantoin was observed in the allopurinol-treated group, although at N=4 this was only statistically significant in the case of allantoin (fig 42, top). Similarly to urine samples, serum levels of hypoxanthine and xanthine were dramatically increased in the allopurinol-treated group (fig 42, middle). Allopurinol and its metabolite, oxypurinol, were detected only in serum samples of allopurinol-treated rats (fig 42, bottom).

Tissue samples were analyzed for XO metabolites through HPLC in a similar fashion (fig 43). Besides unusually high levels of allantoin in the carotid artery, allantoin was generally not detectable in tissue samples (fig 43A). Uric acid was significantly decreased in all the four blood vessels (aorta, vena cava, carotid artery, jugular vein) in the allopurinol-treated group (fig 43B). Hypoxanthine appeared increased in all samples in the allopurinol-treated group, statistical significance being reached in the case of the aorta, vena cava, jugular vein,

kidney and the heart (fig 43C). No significant change was observed in tissue xanthine levels (fig 43D).

Overall, the results of HPLC analysis indicated effective inhibition of XO metabolism with subsequent rise in XO substrate levels and decrease in XO products in tissues of interest.

The mean arterial pressure (MAP) observed over the course of this experiment is displayed in figure 44. The missing data points on this figure correspond to the removal of rats from the close proximity of receivers and their placing in metabolic cages necessary for urine collection (second timepoint, day 18). Expectedly, BP rose significantly following DOCA-salt treatment in all animals, reaching an average of 156 mmHg in the allopurinol group and 169 mmHg in the vehicle after 3 weeks, at this timepoint MAP being not statistically significant between the two treatment groups. Over the course of the 7-day allopurinol treatment that followed, MAP continued to rise in the allopurinol-treated group, following the same pattern observed in the vehicle group, with no statistically significant changes. Similarly, no changes were observed in the other hemodynamic parameters obtained through radiotelemetry (data not shown). These data suggest that allopurinol did not alter the course of hypertension in the established DOCA-salt model.

II. XO inhibition in the development of DOCA-salt hypertension

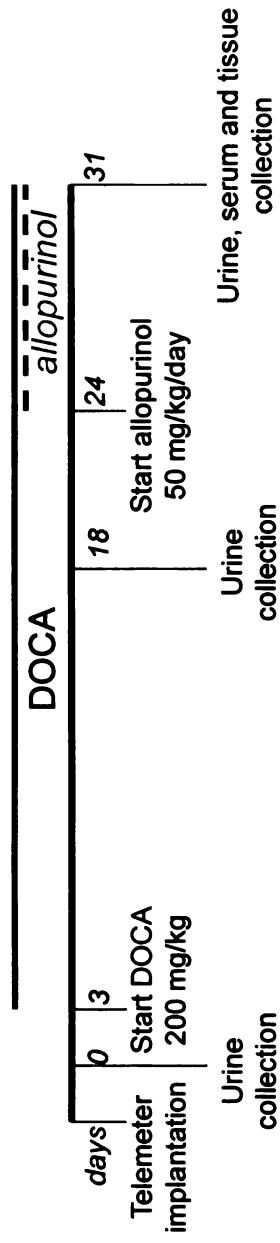

Figure 40. Study design for allopurinol effects on established DOCA-salt hypertension.

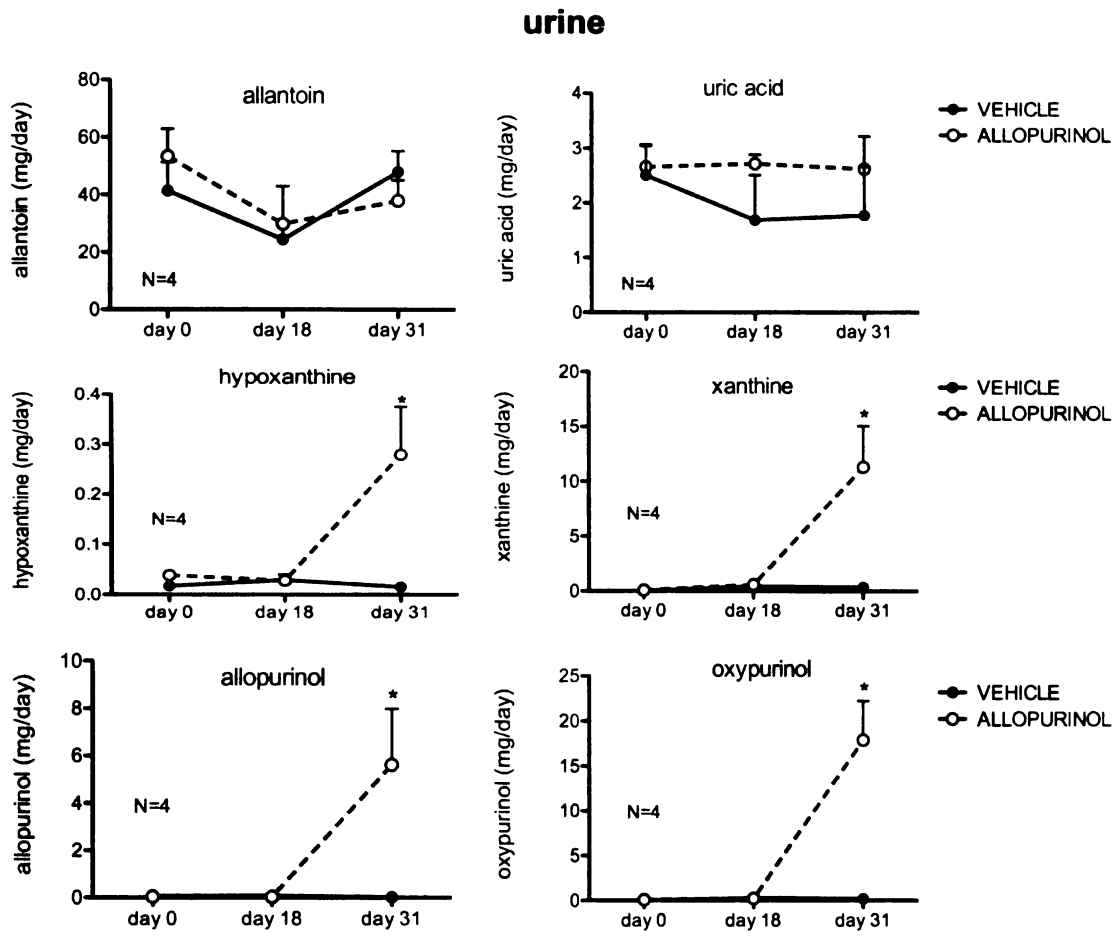

Figure 41. Urinary XO metabolites in vehicle (closed symbols) and allopurinol (open symbols)-treated rats, determined by HPLC: allantoin and uric acid (top, XO products); hypoxanthine and xanthine (middle, XO substrates); allopurinol and oxypurinol (bottom, XO inhibitors), represented as mean ± SEM for N=4. * represents a statistically significant difference ($p<0.05$) between treatment groups.

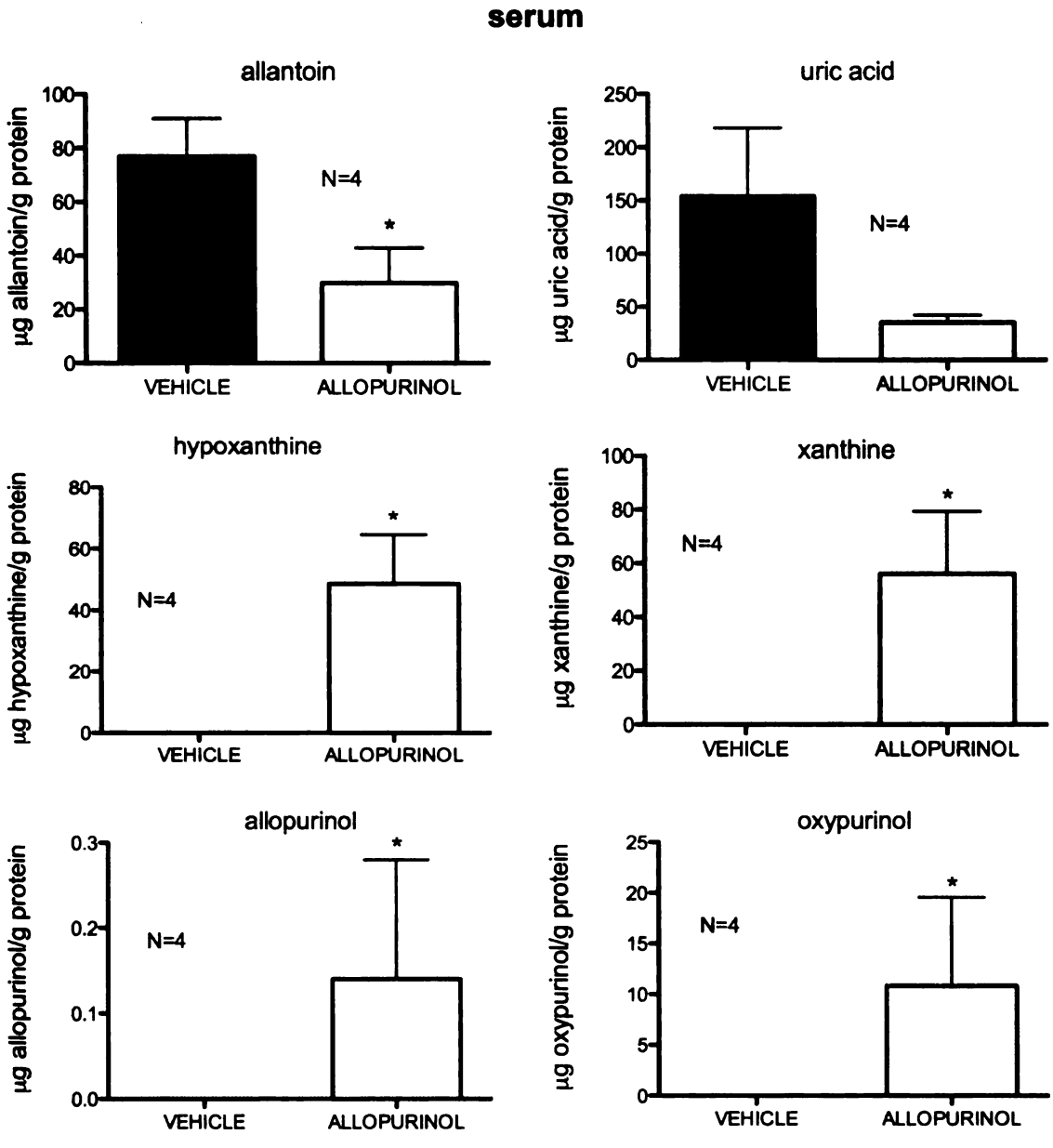

Figure 42. Serum XO metabolites in vehicle (closed symbols) and allopurinol (open symbols)-treated rats, determined by HPLC: allantoin and uric acid (top, XO products); hypoxanthine and xanthine (middle, XO substrates); allopurinol and oxypurinol (bottom, XO inhibitors), represented as mean ± SEM for N=4. * represents a statistically significant difference ($p<0.05$) between treatment groups.

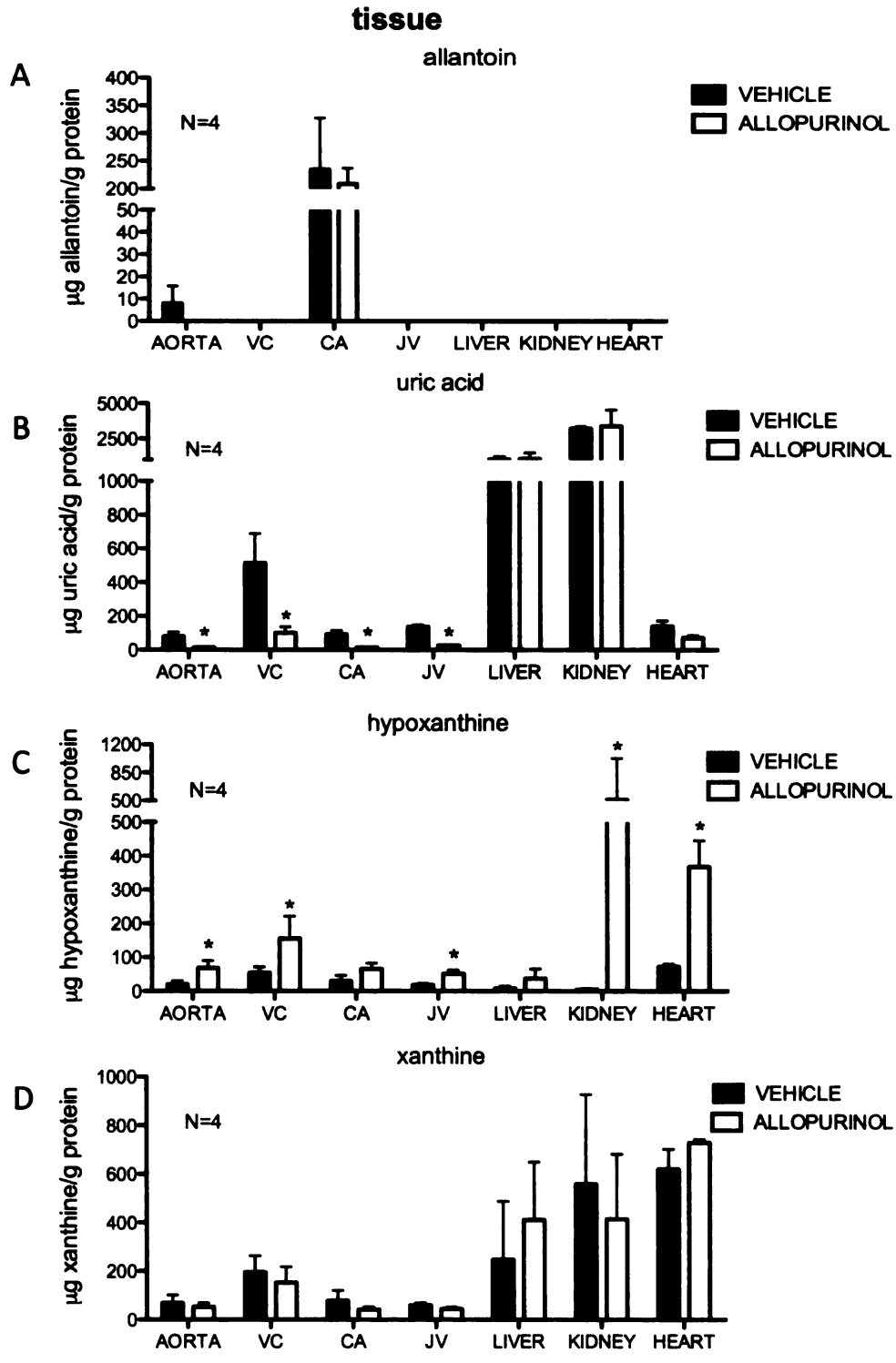

Figure 43. Tissue XO metabolites in vehicle (closed symbols) and allopurinol (open symbols)-treated rats, determined by HPLC: allantoin **(A)**, uric acid **(B)**, hypoxanthine **(C)** and xanthine **(D)** represented as mean ± SEM for N=4. * represents a statistically significant difference ($p<0.05$) between treatment groups.

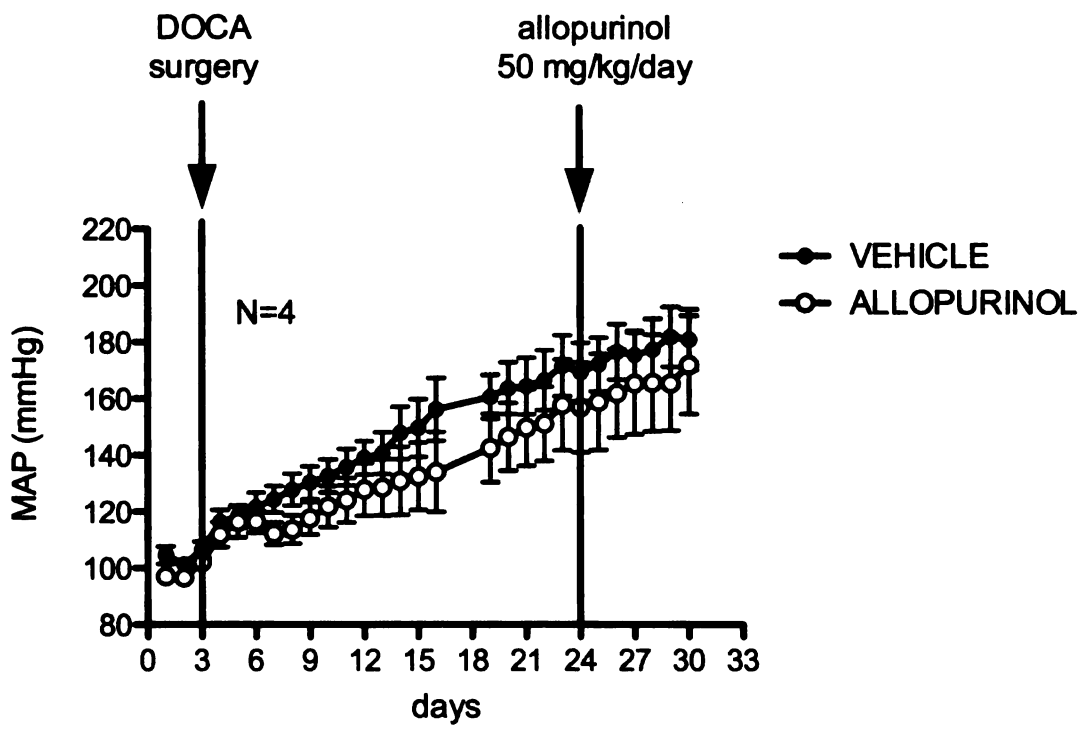

Figure 44. Blood pressure of vehicle (closed symbols) and allopurinol (open symbols)-treated rats, measured by radiotelemetry. Timing of interventions is represented by vertical lines. Data is represented as means ± SEM of 24h average mean arterial pressure (MAP) for N=4.

To determine whether allopurinol would attenuate the development of DOCA-salt hypertension, we performed a second study (fig 45) administering allopurinol (50 mg/kg/day, orally) or vehicle to rats 3 days before the start and throughout the course of DOCA-salt treatment (4 weeks).

Blood pressure was monitored through radiotelemetry. Urine was collected at two time points: before the initiation of allopurinol treatment and at the end of the 4 week DOCA-salt treatment. Serum and the same tissues (aorta, vena cava, carotid artery, jugular vein, liver, kidney and heart) were collected at the end of the study. Urine, serum and tissue samples were used for the same HPLC measurements of uric acid and allantoin (products downstream of xanthine oxidase), hypoxanthine and xanthine (substrates upstream of xanthine oxidase) and allopurinol and oxypurinol (the drug and its active metabolite). Additionally, the weight of heart and the right kidney was measured as a gross estimation of hypertensive end-organ damage. Histological examination of cross-sections of aorta was performed for qualitative assessment of hypertensive remodeling.

The results of the HPLC analysis of urine samples are displayed in figure 46. Urinary levels of uric acid and allantoin were decreased at the end of the study compared to baseline, however there was no difference between the vehicle and the allopurinol treatment (fig 46, top). Urinary levels of hypoxanthine and xanthine increased significantly in the allopurinol-treated group at the end of the treatment (fig 46, middle). Allopurinol and oxypurinol were detected in the urine of allopurinol-treated rats at the end of the treatment (fig 46, bottom).

The results of the HPLC analysis of serum samples collected at the end of the experiment are displayed in figure 47. A trend for reduction in uric acid levels was observed in the allopurinol-treated group, although this was not statistically significant. Surprisingly, allantoin was increased in the allopurinol-treated rats (fig 47, top). Similarly to urine samples, serum levels of hypoxanthine and xanthine were dramatically increased in the allopurinol-treated group (fig 47, middle). Allopurinol itself was not detected, however oxypurinol, its metabolite, was detected only in serum samples of allopurinol-treated rats (fig 47, bottom).

HPLC analysis of XO metabolites in tissue samples is displayed in figure 48. Allantoin was variably detectable in tissues (fig 48A). A statistically significant decrease in uric acid levels was observed in aorta, vena cava, jugular vein, liver and kidney, with a similar trend in all remaining tissues (fig 48B). A statistically significant increase in hypoxanthine was observed in the vena cava and liver (fig 48C). As opposed to the 7-day treatment described previously, xanthine tissue levels after the 4-week allopurinol treatment appeared overall decreased, this trend becoming statistically significant in the case of aorta, carotid artery, liver, kidney and heart (fig 48D).

Despite differences observed in serum and tissue levels of XO metabolites between the two experiments (7 day and 4 week allopurinol administration), the overall results of HPLC analysis in this experiment suggested inhibition of XO function by allopurinol treatment (see discussion).

The mean arterial pressure (MAP) observed over the course of this experiment is displayed in figure 49. DOCA-salt treatment effectively raised the BP of rats in both treatment groups. However, there was no significant difference in the MAP of allopurinol-treated compared to vehicle treated rats. These data suggest that allopurinol did not prevent and did not attenuate the development of DOCA-salt hypertension.

The other hemodynamic parameters obtained by radiotelemetry are displayed in figure 50. A trend for increased heart rate was observed in the allopurinol-treated group (fig 50B). Diastolic pressure was increased by allopurinol treatment (fig 50D), and there was a statistically significant decrease in pulse pressure ($P_{pulse}=P_{sys}-P_{dias}$) (fig 50E), with potentially important implications (see discussion). No difference was observed in activity (movement) between the two groups (fig 50F).

Despite the lack of effects of allopurinol on BP, XO inhibition may have protective effects on end-target organs of hypertensive complications. To investigate this possibility, we measured the heart (fig 51A) and kidney weight (fig 51B) at the end of the treatment (gross evaluation of left ventricular and renal hypertrophy). We observed no change in the heart weight and a surprising statistically significant increase in kidney weight in the allopurinol-treated group (see discussion). The histological characteristics of hematoxylin-eosin stained aorta sections did not appear qualitatively different between the two treatment groups (fig 52), suggesting that hypertensive aortic remodeling was not altered by allopurinol treatment.

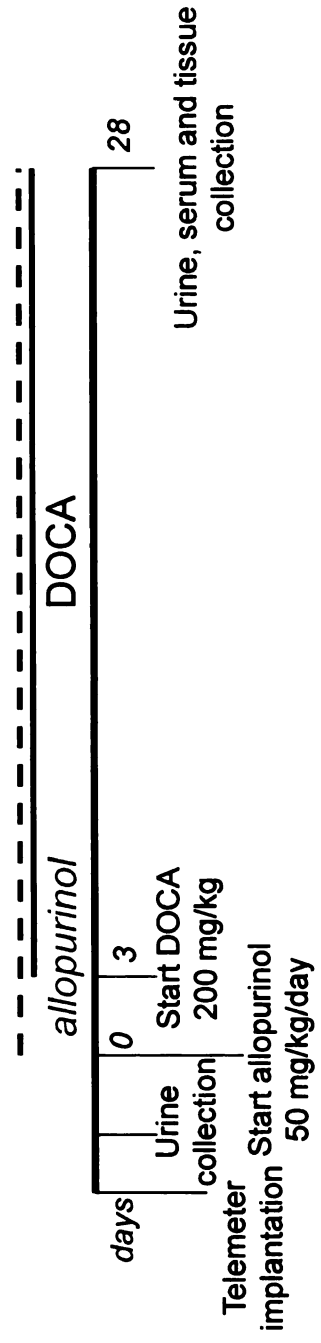

Figure 45. Study design for allopurinol effects on the development of DOCA-salt hypertension.

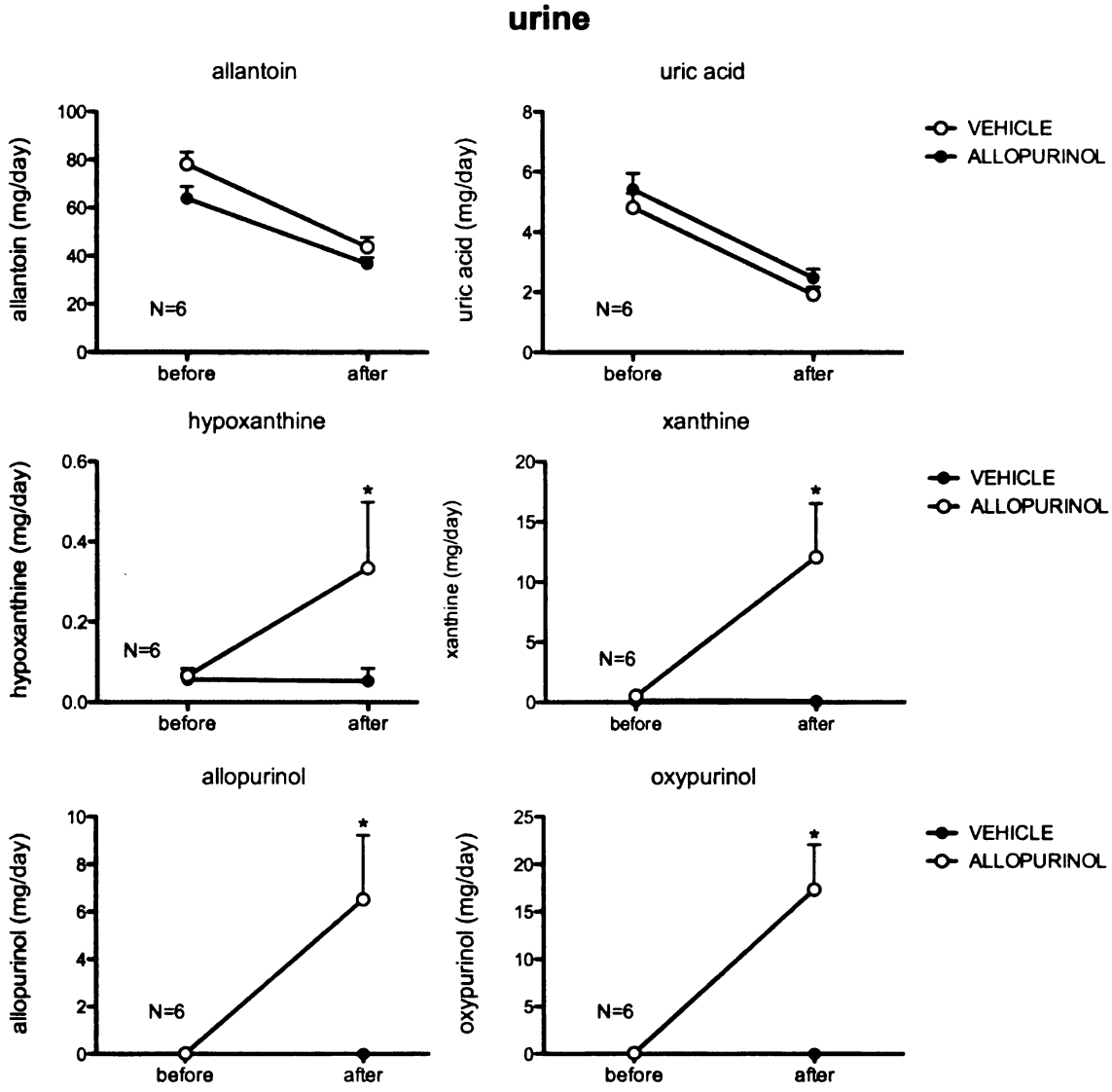

Figure 46. Urinary XO metabolites in vehicle (closed symbols) and allopurinol (open symbols)-treated rats, determined by HPLC: allantoin and uric acid (top, XO products); hypoxanthine and xanthine (middle, XO substrates); allopurinol and oxypurinol (bottom, XO inhibitors), represented as mean ± SEM for N=6. * represents a statistically significant difference ($p<0.05$) between treatment groups.

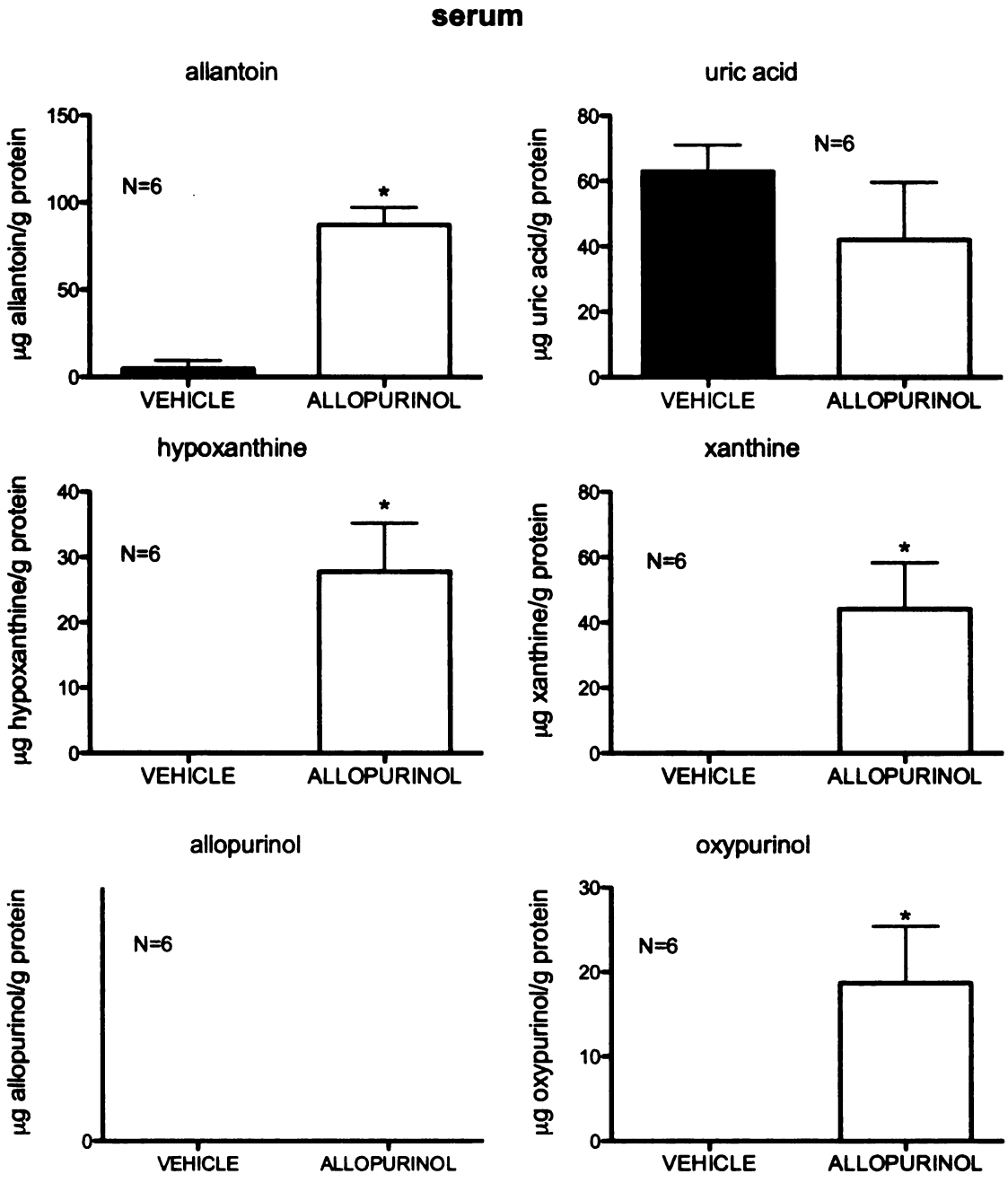

Figure 47. Serum XO metabolites in vehicle (closed symbols) and allopurinol (open symbols)-treated rats, determined by HPLC: allantoin and uric acid (top, XO products); hypoxanthine and xanthine (middle, XO substrates); allopurinol and oxypurinol (bottom, XO inhibitors), represented as mean ± SEM for N=6. * represents a statistically significant difference ($p<0.05$) between treatment groups.

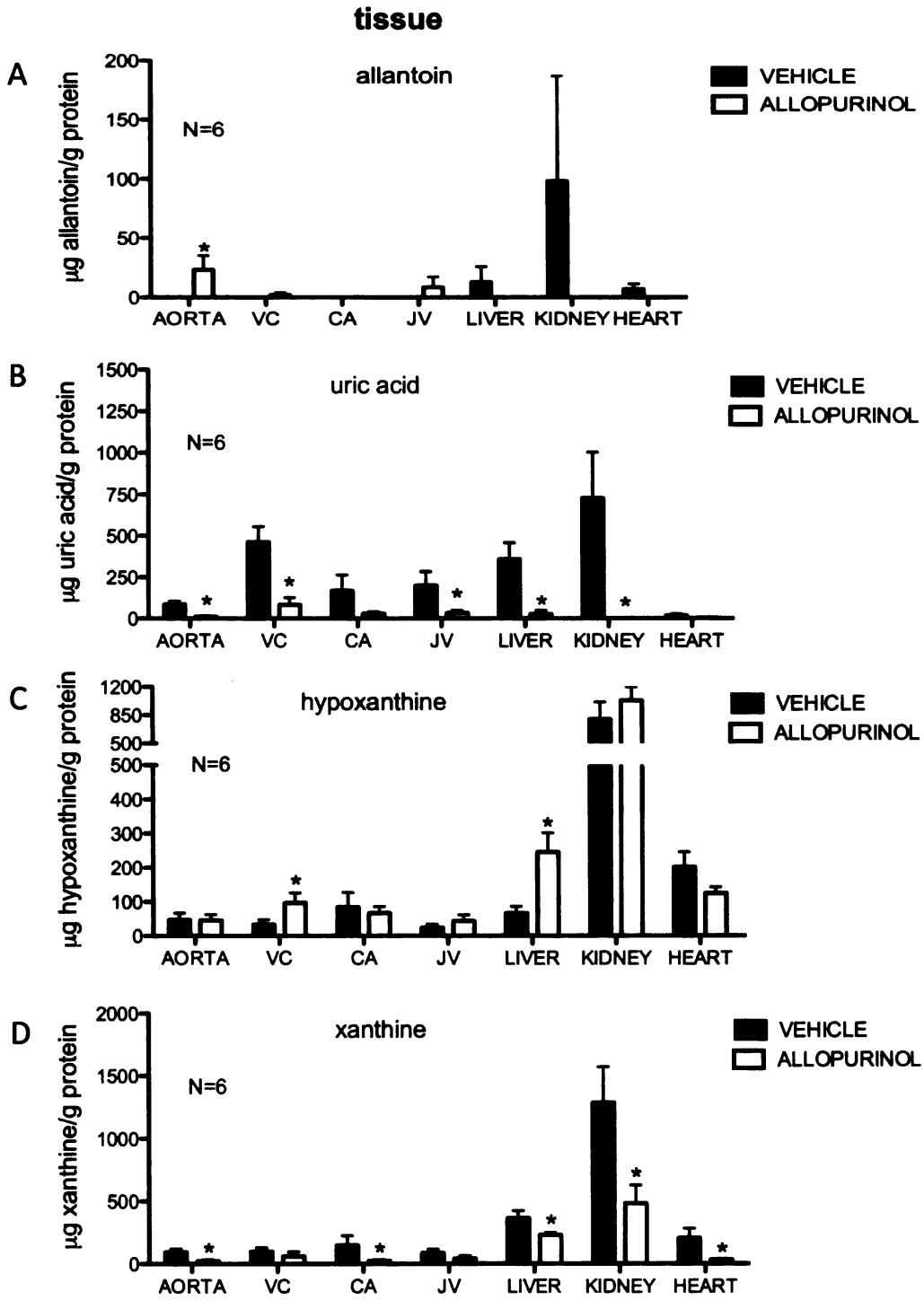

Figure 48. Tissue XO metabolites in vehicle (closed symbols) and allopurinol (open symbols)-treated rats, determined by HPLC: allantoin **(A)**, uric acid **(B)**, hypoxanthine **(C)** and xanthine **(D)** represented as mean ± SEM for N=6. * represents a statistically significant difference ($p<0.05$) between treatment groups.

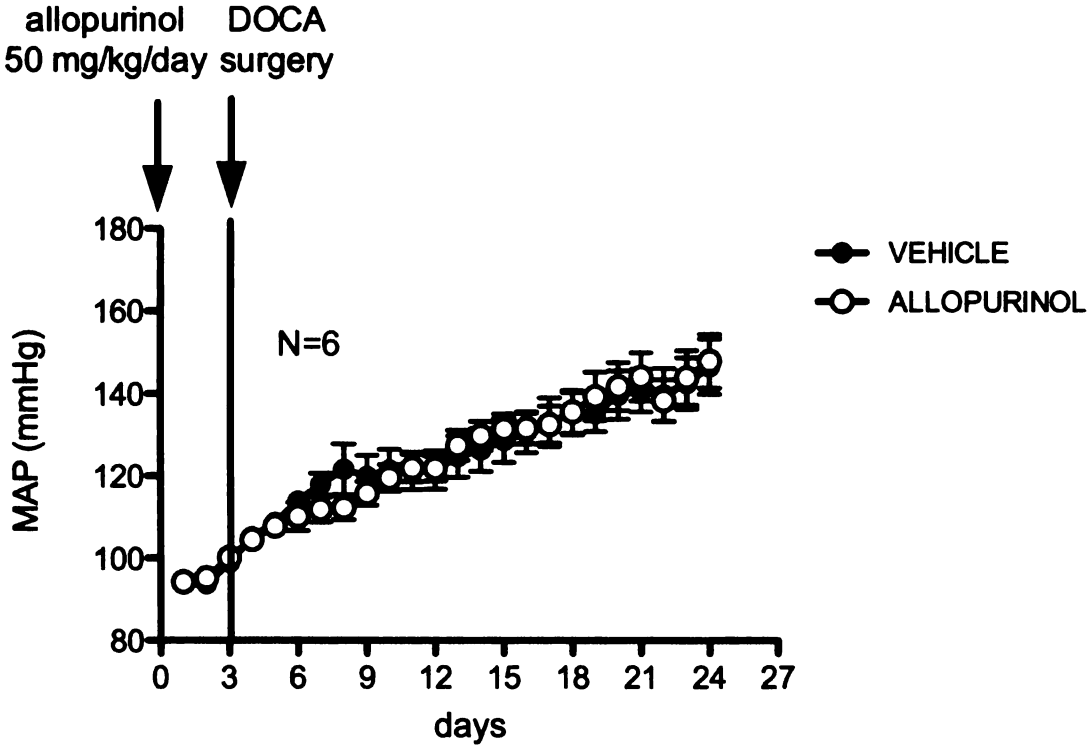

Figure 49. Blood pressure of vehicle (closed symbols) and allopurinol (open symbols)-treated rats, measured by radiotelemetry. Timing of interventions is represented by vertical lines. Data is represented as means ± SEM of 24h average mean arterial pressure (MAP) for N=6.

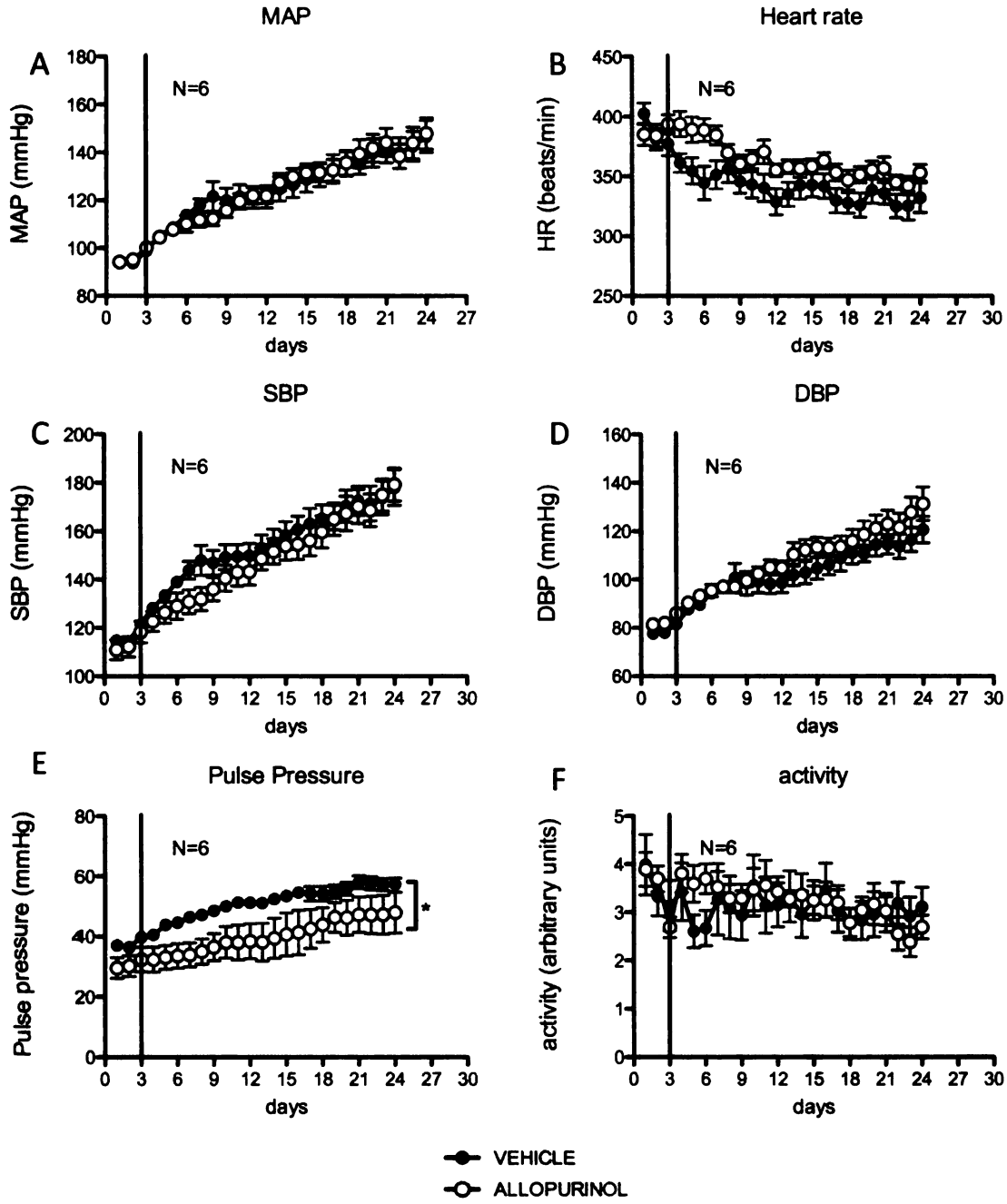

Figure 50. Hemodynamic parameters of vehicle (closed symbols) and allopurinol (open symbols)-treated rats: mean arterial pressure **(A)**, heart rate **(B)**, systolic blood pressure **(C)**, diastolic blood pressure **(D)**, pulse pressure **(E)** and activity **(F)**, represented as means ± SEM of 24h average values for N=6.

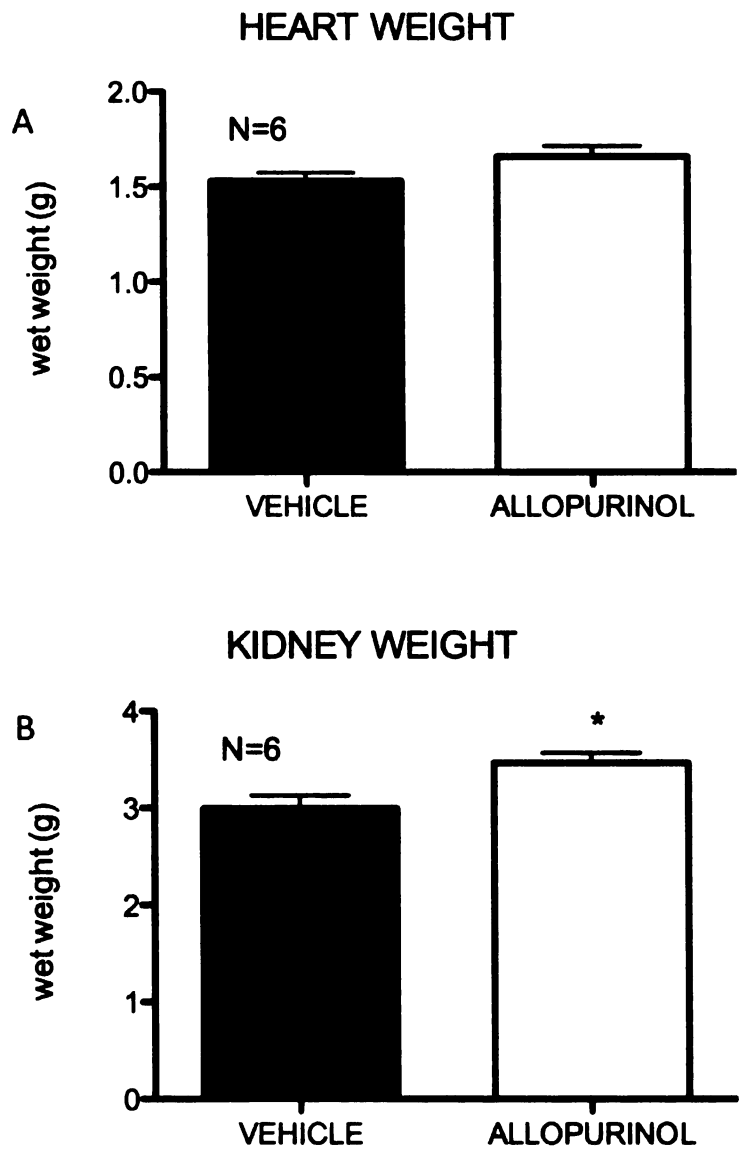

Figure 51. Heart **(A)** and right kidney **(B)** weight at the time of sacrifice of vehicle (closed bars) and allopurinol (open bars)-treated rats. Represented as mean ± SEM for N=6. * represents a statistically significant ($p<0.05$) difference between treatment groups.

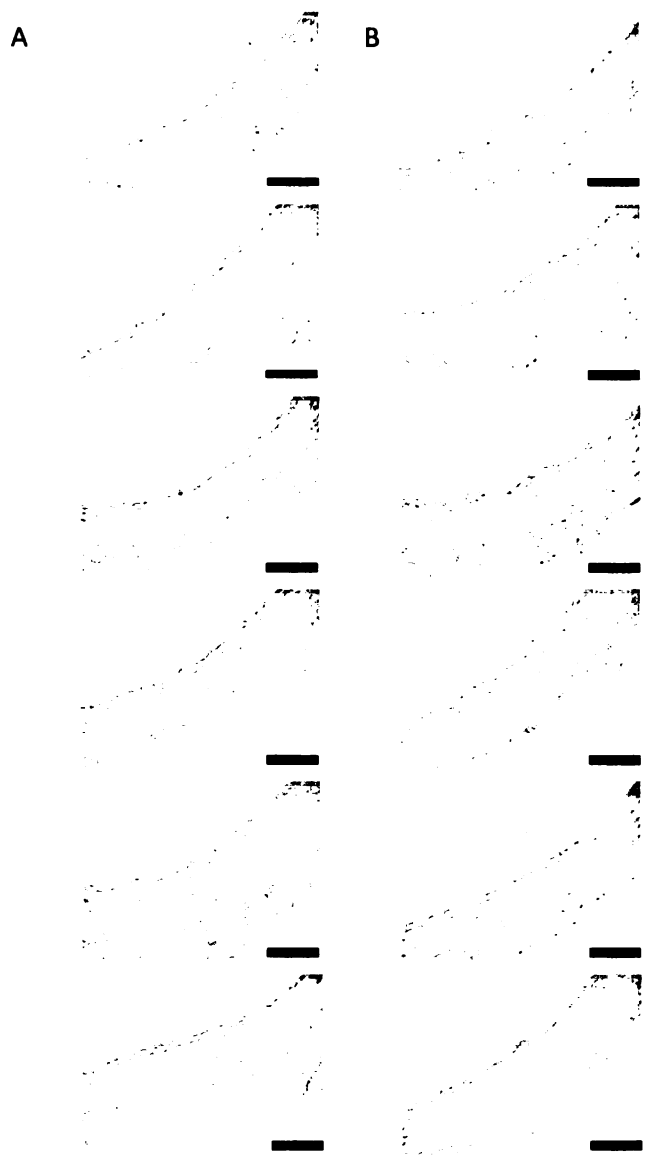

Figure 52. Hematoxylin-eosin cross-sections of aorta from vehicle **(A)** and allopurinol **(B)**-treated rats. Bars represent 100 µm.

III. Dose-dependent effects of allopurinol

For all *in vivo* experiments, we have used the same dose of allopurinol (50 mg/kg/day). This treatment, despite inhibiting XO activity, did not lead to significant changes in the BP of DOCA-salt treated rats. Because a published study (see discussion) reported decreased SBP in the DOCA-salt model with a higher dose of allopurinol (100 mg/kg/day), we investigated whether this dose would provide a better inhibition of XO.

We administered vehicle, 50 mg/kg/day allopurinol or 100 mg/kg/day allopurinol to normal rats for 7 consecutive days. At the end of this treatment, we collected urine and serum samples and performed HPLC analysis of XO metabolites.

Urinary allantoin and uric acid were not significantly changed between the three groups (fig 53 top). A statistically significant increase in urinary hypoxanthine and xanthine compared to vehicle was observed in both allopurinol-treated groups (fig 53 middle). Similarly, allopurinol and oxypurinol were significantly increased in the treated groups (fig 53 bottom). The effects on hypoxanthine, xanthine, allopurinol and oxypurinol appeared dose-dependent, however the difference in these metabolites was not statistically significant between the two allopurinol treated groups.

Serum levels of allantoin were surprisingly increased in the 100 mg/kg/day group compared to vehicle, while there was a trend for a dose-dependent decrease in uric acid levels in the allopurinol-treated groups compared to vehicle. This

decrease was statistically significant in the 100 mg/kg/day allopurinol group (fig 54 top). Hypoxanthine and xanthine levels increased in both allopurinol compared to vehicle treated groups (fig 54 middle). Oxypurinol increased in the treated groups, while allopurinol was close to the detection limit and not significantly changed between the three treatment groups (fig 54 bottom). The effects on hypoxanthine, xanthine, uric acid and oxypurinol appeared dose-dependent, however the difference in these metabolites was not statistically significant between the two allopurinol treated groups.

Section summary: We have inhibited XO activity in vivo, expecting as consequences a lowering of MCFP and therefore of BP in the DOCA-salt hypertensive model. We have monitored XO metabolites in the urine, serum and tissues of allopurinol-treated animals, overall observing increases in XO substrates and decreases in XO products. Despite what we considered effective XO inhibition, we have not observed any effect on BP of DOCA-salt hypertensive rats, regardless of the timing of this intervention.

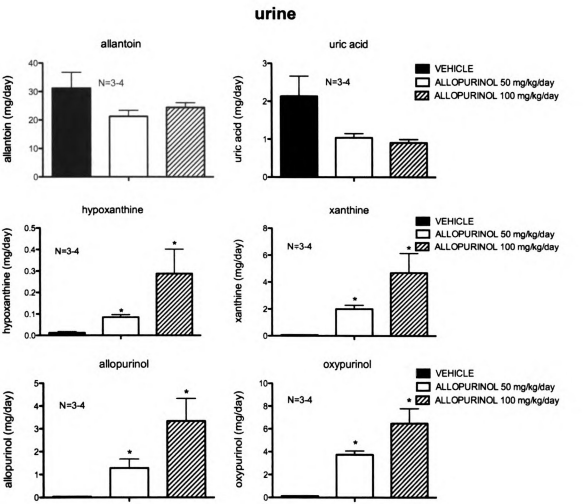

Figure 53. Urinary XO metabolites in vehicle (closed bars), 50 mg/kg/day allopurinol (open symbols), and 100 mg/kg/day allopurinol (hatched symbols)-treated rats, determined by HPLC: allantoin and uric acid (top, XO products); hypoxanthine and xanthine (middle, XO substrates); allopurinol and oxypurinol (bottom, XO inhibitors), represented as mean ± SEM for N=3-4. * represents a statistically significant difference ($p<0.05$) compared to vehicle.

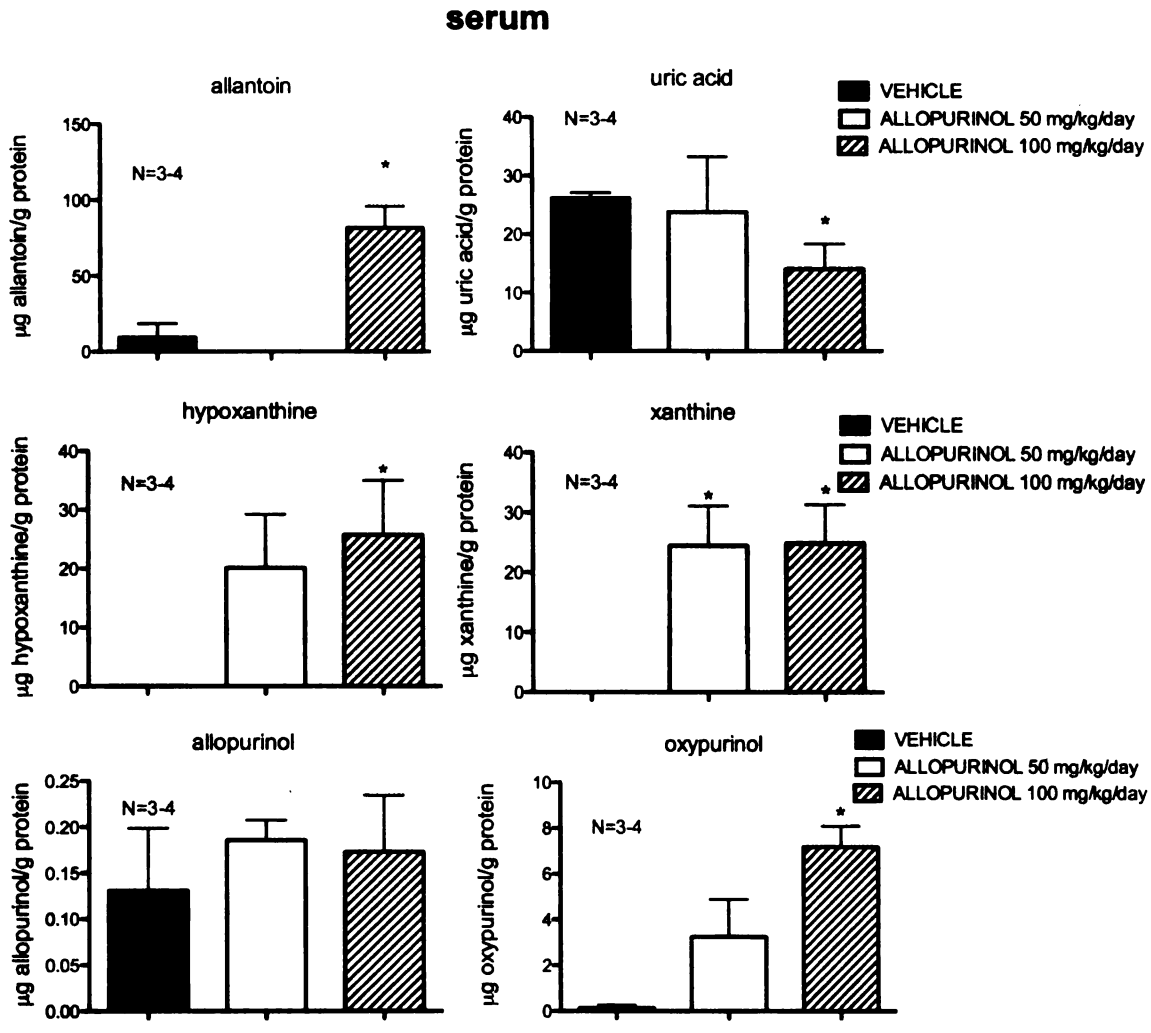

Figure 54. Serum XO metabolites in vehicle (closed bars), 50 mg/kg/day allopurinol (open symbols), and 100 mg/kg/day allopurinol (hatched symbols)-treated rats, determined by HPLC: allantoin and uric acid (top, XO products); hypoxanthine and xanthine (middle, XO substrates); allopurinol and oxypurinol (bottom, XO inhibitors), represented as mean ± SEM for N=3-4. * represents a statistically significant difference ($p<0.05$) compared to vehicle.

DISCUSSION

Aside from likely contributing to many aspects of normal vascular biology, reactive oxygen species are thought to play an important role in cardiovascular disease, and in particular, in hypertension. Veins and the contribution of venomotor tone to blood pressure control represent an understudied research area. In this study, we investigated the metabolism of ROS in veins as compared to arteries, their contribution to vascular contraction function, and finally their potential involvement in hypertension pathogenesis. A particular focus was placed on the role of xanthine oxidase. The male Sprague-Dawley rat DOCA-salt model of hypertension was used in these experiments, for reasons detailed in the introduction section.

I. ROS metabolism in veins vs arteries

A. Basal levels of ROS

We started our comparison of venous and arterial ROS metabolism by measuring the levels of two of the most important ROS: superoxide and H_2O_2. Several distinctions can be made between these two species. The half-life of superoxide is much shorter (ms) than that of H_2O_2 (minutes-hours). Superoxide local subcellular concentrations are highly dependent on the local concentration of superoxide dismutase (SOD), the enzyme that will readily metabolize it to

H_2O_2. On the other hand, superoxide is charged and therefore cannot freely cross the cell membrane, while the longer-lived H_2O_2 is membrane-permeable, extracellular concentrations measured at equilibrium being thus similar to intracellular ones. Both superoxide and H_2O_2 may critically influence vascular functions, and especially the contractile function that was at the core of this research.

We observed that in normal conditions, basal levels of both superoxide and H_2O_2 are higher in VC compared to aorta (fig 11-12). We have also observed higher superoxide levels in the superior mesenteric vein compared to the superior mesenteric artery, and higher H_2O_2 levels in the jugular vein compared to the carotid artery. Our results appear therefore to reflect a general artery-vein difference, rather than a vascular bed-specific characteristic. This difference could result from a higher rate of ROS production, a lower rate of ROS degradation, or both, in veins versus arteries.

We have measured superoxide in the presence of SOD inhibition, so that only differences in production, but not destruction of superoxide would be taken into account. Additionally, the use of SOD inhibition for superoxide detection also increases the magnitude of the superoxide signal, thus increasing the sensitivity of this method. The majority of H_2O_2 being produced in basal conditions appeared as superoxide-derived, as it was almost abolished by SOD inhibition through DDC. A limitation regarding our use of DDC is the fact that this copper chelator compound would only inhibit the two Cu-containing SOD isoforms, CuZn SOD and EC-SOD, but not Mn SOD, the mitochondrial isoform (55). However,

we observed no arterio-venous differences in Mn SOD, at least in terms of its protein expression (fig 24). Few comparisons of basal ROS levels were reported in the literature (see introduction section V). Thus, our study provides the only direct comparison of paired rat blood vessels ROS production in basal conditions.

An additional interesting arterio-venous comparison would be on ROS levels in the presence of contractile agonists that typically also stimulate ROS production (such as AngII or ET-1). In preliminary studies, we were not able to observe increases in whole tissue H_2O_2 in the presence of agonists. Further studies comparing agonist-stimulated ROS levels in arteries and veins may have to take into account the potential limitations of our H_2O_2 measurements, that use whole tissues and omit the addition of specific substrates.

B. ROS degradation

ROS production by living cells is normally counterbalanced by the activity of several antioxidant defense mechanisms such as SODs, catalase or glutathione peroxidases. In order to compare the status of these mechanisms between aorta and VC, we exposed vessels to exogenous H_2O_2 and assessed how much of that H_2O_2 is metabolized in the presence of tissue. We chose H_2O_2 and not superoxide for this purpose because H_2O_2 is more stable, capable of freely passing cellular membranes, easier to generate at definite concentrations and also more reliable to measure. We used H_2O_2 at a high enough concentration to

produce sufficient fluorescence such that its decrease in the presence of tissue would be measurable with our method. However this concentration (20 μM) may not reflect a physiological situation (~2.5 μM in normal plasma (4)), but rather mimic a state of oxidative stress or a localized increase in H_2O_2 concentrations such as the ones observed during the neutrophil oxidative burst. We have observed a higher consumption of H_2O_2 by the VC compared to the aorta, indicating a higher activity of antioxidant defense mechanisms, and possibly reflecting the increased ROS destruction in normal VC balancing the increased ROS production. However, in our results, the VC to aorta ratio of ROS generation (~15 times greater) does not numerically match the ratio of ROS destruction (~4 times greater), raising the question whether this is indeed a perfect balance or the VC is in fact exposed to oxidant stress. This method of measuring antioxidant capacity by exogenous H_2O_2 exposure does not discriminate among specific antioxidant mechanisms, although catalase is likely to be more important than glutathione peroxidase at high H_2O_2 concentrations due to its higher Km (181). This would be consistent with the higher catalase expression that we observed in VC compared to aorta (fig 19).

C. ROS metabolizing enzymes

ROS metabolism is a highly complex biological pathway with many important enzymatic and non-enzymatic players involved. We have attempted to investigate the profile of ROS producers that may contribute to the differences

observed between arterial and venous ROS levels. We used three different approaches, with only partially overlapping results.

1. Protein expression

The protein expression analysis performed here (fig 16-19) is by no means complete. Due to unavailable tools, we could not confidently assess the expression of different Nox isoforms and various subunits of NADPH oxidase, a major ROS producer repeatedly proven as important in vascular biology. In human vessels, protein as well as mRNA expression of NADPH oxidase subunits was reported as significantly different between the saphenous vein and internal mammary artery. Additionally, a literature report suggested enzymatic activity of NADPH oxidase to be contributing to total superoxide levels in a higher degree in the vein than in the artery, (51). Also absent from our results are an entire range of other ROS metabolizing systems that may also contribute to the differences observed in ROS levels such as: other mitochondrial ROS production sites (complex III), uncoupling proteins, other isoforms of NO synthase (nNOS, iNOS), lipoxygenase, cyclooxygenase, myeloperoxidase, heme oxygenase, the extracellular isoform of SOD, glutathione peroxidases. A comparison of SOD expression in human saphenous vein and internal mammary artery reported similar expression of the cytosolic (CuZn SOD) and mitochondrial (MnSOD) isoforms (50). To our knowledge however, there are no other studies comparing the arterial and venous expression of eNOS, an important enzyme in vascular biology, that when uncoupled becomes capable of producing superoxide. We did not find differences in the expression of eNOS between aorta and VC, correlated

with the similar endothelium-dependent relaxation found in these tissues in normal conditions (fig 34). However, from the differences we did observe in protein expression between aorta and VC, only XO and DUOX1, as superoxide producers, would help explain the higher superoxide levels found in basal conditions in veins. Furthermore CuZn SOD, a cytosolic enzyme that converts superoxide to H_2O_2, and catalase, responsible for further degrading H_2O_2, were both more heavily expressed in the vein, potentially correlated with the higher superoxide/ H_2O_2 levels.

Any protein expression analysis does not entirely reflect protein activity in living tissues. Therefore, to fully explore arterial versus venous ROS metabolizing systems, more studies would be necessary.

2. mRNA expression

The PCR array used for this experiment queried only a small number of probes quantifying mRNA expression of enzymes tested in the western blot analyses discussed above. Of them, DUOX1 had a higher mRNA expression, correlating with the increased protein expression. No difference was observed however in the mRNA expression of catalase and any SOD isoform, while XO was not present on this array. The lack of correlation between protein and mRNA levels using broad expression profiling methods was previously described (47, 49) and may be attributed to posttranscriptional events, posttranslational modifications, variations in mRNA half-life and in protein stability, as well as technical errors. Both DUOX isoforms higher venous mRNA expression was confirmed by RT-

PCR analysis. Of potential interest was also the higher expression of Nox4 in aorta compared to VC. This result however, even if correlated with a higher protein expression and activity of Nox4 in arteries, would not help explain the higher ROS levels observed in veins and was not explored further.

3. Pharmacological inhibition of basal H_2O_2 levels

We observed higher *in vitro* basal H_2O_2 levels in veins than in arteries, when measured in whole tissues. A logical means of identifying the source of this increase would then be to inhibit potential sources in the same settings and assign contributions of various sources to these basal ROS levels. Literature reports on whole tissue ROS production are scarce compared to those on cell cultures or cell fractions and to our knowledge, this particular type of assay was not previously attempted for tissue production of H_2O_2. Rather, most investigations tend to assess the activity of one or other of ROS producers in the presence of specific substrates (such as NADPH for NADPH oxidase activity). In these experiments, we used tissues originating in the same animal to quantify inhibition as a percentage of the respective basal level. We did not use specific substrates for any of the enzymes assessed. Moreover, we did not use specific inhibition of catalase to amplify the H_2O_2 signal in these experiments, hypothesizing that a potentially higher venous catalase activity may be impacted differentially by catalase inhibition, thus biasing the results towards more efficient reductions in H_2O_2 levels in arteries. The basal H_2O_2 levels in the two arteries used (aorta and carotid artery) were often not measurable, thus making inhibition observations in arteries impossible and lowering the experimental statistical

significance. We chose drug concentrations to use based on multiple published results demonstrating efficient *in vitro* enzyme inhibition. Apocynin decreased the basal H_2O_2 levels in most tissues, suggesting that NADPH oxidase was a significant source of basal vascular ROS, as noted by previous reports. However, recent studies have questioned the specificity of apocynin action, which was instead shown to have antioxidant effects by non-specifically scavenging ROS (56). The same potential scavenging effect was reported for indomethacin (36), a non-specific COX inhibitor, which in our hands had no effect on basal H_2O_2 levels. Ketorolac, another non-specific COX inhibitor, decreased venous H_2O_2 levels, thus rendering the COX inhibition experiments overall inconclusive. Based on our XO expression analyses, we were expecting to observe a significant decrease in basal venous ROS levels with allopurinol. This however did not occur for VC, but only for JV. The higher venous compared to arterial XO activity was however later shown in separate experiments, performed in the presence of the XO substrate, xanthine (fig 26). Surprisingly, venous H_2O_2 levels were significantly decreased by rotenone, a mitochondrial complex I inhibitor. A trend for decreased venous H_2O_2 levels was observed with DPI, a flavoprotein (NADPH oxidases including DUOX, xanthine oxidase and eNOS) inhibitor. Inhibition of NOS with LNNA did not significantly alter basal H_2O_2 levels of any tissue, suggesting that in normal conditions, superoxide production from uncoupled eNOS is not a major phenomenon. Overall, because of the absence of enzyme substrates and the lack of more specific inhibitors, we believe that the conclusions to be drawn from these experiments should be limited. More in depth

analyses of *in vitro* H_2O_2 production are needed and may include future interesting studies incorporating agonist-stimulation of H_2O_2 production in the presence of the ROS enzyme substrates and inhibitors.

D. Oxidative stress in arteries *vs* veins

We have observed increased basal ROS levels in veins compared to arteries, despite increased venous *vs* arterial antioxidant capacity. These data suggest that production of ROS in veins is much higher than that in arteries. Also, these results raise the question of the function or effects of the ROS that, regardless of their molecular source, are being produced, but are not being degraded in these blood vessels. When production exceeds degradation of ROS, leading to accumulation of deleterious levels of ROS, the state of oxidative stress ensues. However, measurable levels of ROS and markers of oxidative stress are also present in normal conditions. We hypothesized that these markers may be accordingly higher in veins compared to arteries. We used 4-HNE, a marker of lipid peroxidation, in VC versus aorta. We have observed a more intense general 4-HNE staining in the VC compared to the aorta. 4-HNE can also form covalent bounds to proteins (113). However when attempting to quantify the 4-HNE protein adducts through western blotting, these appeared to have a less intense banding pattern in veins versus arteries. The use of other oxidation markers (see introduction) may therefore be needed to allow stating a clear conclusion

regarding lipid peroxidation or general oxidative stress in normal veins vs arteries.

E. ROS metabolism in DOCA-salt hypertension

Increases in ROS generation and markers of oxidative stress were reported in virtually all forms of hypertension, human and animal models. Similar to the situation in normal rats, little information is available on differences between the arterial and the venous ROS metabolism during hypertension. We have observed that the increased production of ROS by veins *vs* arteries is maintained in DOCA-salt hypertension. However, we were not able to confirm the increased basal H_2O_2 levels within the same type of tissue with hypertension in the absence of substrates (e.g. sham compared to DOCA aorta). However, this does not exclude the possibility that given specific substrates for various ROS enzymes, ROS production would not be increased with hypertension. We would also expect the response in tissue ROS production to the presence of contractile agonists (such as AngII or ET-1) to be amplified in tissues from hypertensive animals. We have not observed a significant change in the protein expression pattern of ROS producers and destroyers between sham normotensive and DOCA-salt hypertensive rats in aorta or VC samples, suggesting that potential changes observed between arteries and veins during hypertension would not be supported by changes in protein expression of these ROS enzymes, and may be

attributed to changes in protein activity, as well as to changes in other mediators of vascular function affected by hypertension.

F. Xanthine oxidase

A significant focus was placed on XO throughout this study due to the *in vitro* results of XO expression and activity in venous vs arterial tissues (figs 16, 25-27). Most of these results have been published (147).

Circulating XO binds to glucosaminoglycans on the vascular endothelium, still retaining specific activity (62). The results presented in figure 25 represent a novel finding in that they demonstrate for the first time that blood vessels produce the XO mRNA locally, and that binding of circulatory XO to endothelial cells is not the only mechanism responsible for the detection of XO activity in these tissues. We observed a higher protein and mRNA expression, as well as a higher activity of XO in VC than in aorta from normal rats. It should be noted here that our mRNA and protein expression studies do not distinguish between xanthine dehydrogenase (XDH) and XO, the two isoforms of xanthine oxidoreductase (XOR). These isoforms are generated by posttranslational modifications (11), therefore they have the same mRNA source; because of the small difference in protein structure between XDH and XO, antibodies will also recognize both isoforms. However, our XO activity assays specifically (fig 26) assess the enzyme activity that uses oxygen (XO), as they are performed in the absence of NAD^+, the substrate for XDH. The differences in XO expression between the vein

and the artery could be mediated by a number of factors and processes regulating XO expression such as cytokines or oxygen tension (9). An interesting report in bovine aortic endothelial cells, which appears to be consistent with our findings, has implicated a feed-forward mechanism by which increases in H_2O_2 stimulate the conversion of XDH to XO, potentially leading to even higher H_2O_2 levels generated by XO (99).

No effect on XO expression or activity was observed with hypertension between sham and DOCA aorta samples (fig 27). One study reported an increase in xanthine-stimulated superoxide production in the DOCA aorta, implying an increased XO activity (163). We did not obtain results leading to the same conclusion, although we used two separate specific measures of XO activity in the aorta. However, DOCA VC had a higher XO activity (urate-producing) than normal VC, despite the lack of protein expression change. DOCA jugular vein had also a higher XO activity (H_2O_2-producing) than sham jugular vein. These results would support the idea that during hypertension, although overall (XDH+XO) expression levels are similar, there is an increase in the XO to XDH ratio, perhaps caused by an increased XDH-XO conversion, supporting increases in XO activity that are not paralleled by increases in expression.

It is important to also note the lack of numerical correlation between the two activity assays. The stoichiometric relationship between the two XO products depends largely on the presence of other substrates, and is largely inclined towards urate. Moreover, these two tests were performed in different types of

samples: we used tissue homogenates for the urate-based assay, and whole tissues for the H_2O_2-based assay.

II. Impact of ROS on venous and arterial contractile function

A. Normal conditions

1. ROS-mediated contraction

We have observed that both the aorta and the VC from normal rats respond to exogenous superoxide with contraction, and that this contraction is higher in VC than in aorta, as a percentage of adrenergic responses. The combination of xanthine with XO has long been used as a laboratory tool to produce superoxide. Some researchers have suggested that superoxide can enter living cells through Cl^- channels (63). However, the accepted view in the ROS field is that because it carries a negative charge, superoxide does not cross membranes. Therefore we can assume that contraction induced by extracellular xanthine/XO is mediated either by extracellular superoxide or by H_2O_2 as the product of superoxide degradation, a longer-lived molecule that can freely diffuse across membranes. The contraction we observed with xanthine/XO is indeed parallel to the H_2O_2 contraction we previously observed in the same tissues (150, 151). However, to effectively claim this, experiments with xanthine/XO should be performed in the presence of catalase. The mechanisms for the direct contractile effects of ROS are complex, involving among others an interference with endothelium-released NO (2, 13). In our experiments, removal of endothelium did not alter aortic

contraction to exogenous superoxide (data not shown). The fact that the contraction induced by xanthine/XO was higher in VC would suggest that any alteration of ROS metabolism is likely to have a more important impact on venous rather than arterial contraction.

2. XO impact on normal vascular contractile function

Smooth muscle contraction signaling pathways may be modulated by ROS in many ways. Some contracting agents such as angiotensin II (AngII) are widely known as being capable of inducing superoxide release (48). General ROS scavengers, catalase or specific ROS enzyme inhibitors have variably decreased the arterial contractile response induced by agonists such as NE, AngII or ET-1 (92, 137, 156). ET-1, a potent venoconstrictor, also stimulates superoxide production. Similarly to the Ang II-induced superoxide production, the mechanism mostly responsible for this increase in superoxide release seems to be NADPH oxidase activation (86). We asked specifically whether XO-produced ROS could contribute to the normal contraction induced by NE, AngII or ET-1 and normal relaxation induced by ACh. Inhibition of XO activity with allopurinol did not alter any of the aortic responses to these agonists (fig 29). However, the maximal ET-1-mediated contraction of the VC was significantly decreased in the presence of allopurinol. These data suggest that XO contributes to ET-1-mediated venoconstriction in a way that it does not in the aorta. Although we did not see effects on AngII-induced contraction in our study, long-term exposure to Ang II can also induce XO activation in cultured endothelial cells (83).

XO may theoretically influence endothelial function in at least one other way besides ROS production, specifically through the production of uric acid. Uric acid may impact endothelial function at least by the following mechanisms: a. by directly interacting with NO (46) and therefore decreasing its bioavailability; b. by interacting with superoxide (7) and therefore decreasing the amount of superoxide available to quench NO, thus increasing NO bioavailability; c. by interacting with peroxynitrite, the reaction product of superoxide and NO, to form a product shown to have vasorelaxant properties (133) or to decrease peroxynitrite availability. Peroxynitrite, in its turn, was shown to decrease guanylate cyclase activity and oxidize BH_4, an important cofactor for eNOS activity (127). Paradoxically, peroxynitrite also presents vasorelaxant properties (172). Additionally, uric acid may have antioxidant or other effects intracellularly in vascular smooth muscle cells, where it is taken up by a specific transporter (115).

However, when we inhibited urate production with allopurinol, we did not observe any changes in the ACh-induced relaxation of either aorta or VC from normal rats. Moreover, uric acid itself did not induce any direct contractile effects on rat aorta or VC and it did not modify ACh-induced relaxation in any of these tissues. We used uric acid at concentrations previously proven to have antioxidant properties *in vitro*, and within the range of normal uricemia (7). Additionally, we used oxonic acid at a concentration proven to inhibit uricase activity (42), therefore preventing degradation of uric acid. We have not tested whether uric acid would directly induce relaxation of $PGF_{2\alpha}$–contracted rat aorta, but the lack

of direct vasodilatory effects of uric acid alone in rat aorta was previously reported (133).

We also assessed protein expression of uricase in aorta and VC as the 64 KDa band observed in our samples. This molecular weight was previously observed and attributed to a uricase dimer (162). We observed an increase in the VC uricase expression, compared to aorta (fig 31). This finding correlates with our other results showing a higher urate-producing activity in VC compared to aorta.

Since contraction to ET-1 was diminished in the presence of allopurinol, and expression of DUOX1 was increased in the VC, we tested the effects of a general flavoenzyme inhibitor, DPI, which should block both XO and DUOX1 activities. Unfortunately, no specific pharmacological inhibitor for DUOX1 is available presently. As expected, we observed a significant decrease of the ET-1-mediated contraction of VC, but not aorta. These data suggest that the contribution of flavoenzymes such as XO and DUOX1 to ET-1-mediated contraction is higher in VC than in aorta. These results do not however exclude the contribution of any other Nox isoform or any other flavoprotein to ET-1-induced contraction of these blood vessels.

3. Normal arterial and venous endothelial function

Published studies have demonstrated lower venous vs arterial NO production in some vascular beds (130). Moreover, there is a widely known interaction between superoxide and NO with subsequent decreases in NO bioavailability (8), and in our experiments we observed higher venous than arterial superoxide

levels. In this context, we hypothesized that there would be decreased relaxation to ACh in normal venous vs arterial tissue. However this was not the case, as both aorta and VC relaxed similarly to ACh, and both fully depended on NOS function for this effect (fig 34).

B. DOCA-salt hypertension

1. Arterial and venous endothelial function in hypertension

Arterial endothelial function is characteristically impaired in human and animal models of hypertension (144). The DOCA-salt hypertensive rat is no exception, DOCA aorta exhibiting endothelial dysfunction, as evidenced by an impaired relaxation to ACh. DOCA VC, however, maintained its normal ACh-mediated responses. Both aorta and VC were still fully dependent on NOS function for the ACh-mediated relaxation (fig 35). The mechanisms behind the loss of arterial endothelial function in hypertension extend beyond the obvious detrimental effect of pressure increases. The fact that VC was not similarly affected to aorta in hypertension may be attributed to VC not being exposed to the same regime of increased pressure that the aorta is. However a role may also be played by differences in the anti-inflammatory or other properties of VC that enable it to handle the changes in deleterious circulating mediators that may be associated with hypertension.

2. XO impact on arterial endothelial function in hypertension

Many reports show improvements in endothelial function *in vitro* and *in vivo* by inhibition of XO activity, sometimes independently of other effects (14) but mostly in the context of lowering blood pressure or improving end-organ damage (110, 141). It is however impossible to distinguish between direct effects of allopurinol on endothelial function and the effects of simultaneous lowering of blood pressure. Additionally, in these studies, the effects of allopurinol on lowering uric acid cannot be discerned from effects on lowering ROS/oxidative stress. A convincing attempt was made in this direction in a clinical study which established that ameliorating endothelial dysfunction in chronic heart failure with allopurinol was accomplished by a uric acid-independent mechanism, since lowering uric acid to similar levels with the uricosuric agent probenecid did not have any effect on endothelial function (45). The authors therefore concluded that endothelial function was improved by allopurinol because of a reduction in XO-mediated ROS production. We observed no effect of allopurinol on the DOCA-salt rat aorta endothelial dysfunction (fig 36).

Moreover, no effect on DOCA aorta ACh-induced relaxation was observed with direct administration of uric acid, suggesting the lack of acute antioxidant effects of uric acid (fig 37). Uric acid, administered acutely (over 1h) at a dose that raised uricemia from normal to the hyperuricemic range, ameliorated the endothelial dysfunction of smokers and patients with diabetes type I, without an impact on the normal endothelial function of control subjects, although the serum antioxidant capacity was equally increased in all groups after the administration of uric acid (166). This would imply that the beneficial antioxidant effects of uric

acid may only become apparent when there is a pathophysiological excess of oxidants and consequently endothelial dysfunction. We excluded uricase degradation of uric acid in the rat tissue by co-administering oxonic acid, the uricase inhibitor. However, besides the presence of uricase in rat tissues, other species differences cannot be ruled out, such as differences in the presence and/or function of specific urate transporters in rodents compared to humans. Additionally, the endothelial dysfunction observed in type I diabetes (the condition in which urate had beneficial effects) may be different from the endothelial dysfunction associated with hypertension (the condition we studied), in which pressure-associated shear stress and endothelial injury may be less ROS-dependent. *In vivo* treatments with various nonspecific antioxidants have been shown experimentally to improve hypertensive endothelial dysfunction (157), however it is difficult to dissociate the direct effects of antioxidants on endothelium from the effects of the accompanying reduction in blood pressure upon antioxidant treatment.

One of our hypotheses regarding uric acid was that during DOCA-salt hypertension uricemia is decreased and the chronic lack of adequate levels of uric acid contributes to the endothelial dysfunction of hypertension. Uric acid levels in blood however were similar in hypertensive compared to normotensive rats (fig 38) and we could not establish any correlation between individual values of uricemia and blood pressure. This is a known association in humans (77), hypertensives having increased risk of gout and hyperuricemia increasing the risk for hypertension. As previously explained, rodents have significantly lower

uricemia levels than humans, as a result of the presence of functional uricase, the enzyme that degrades urate into allantoin, and that is not expressed in humans as a result of a mutation (178). Similarly to the expression of XO, uricase expression was also not changed in aorta from hypertensive compared to normotensive rats (fig 39).

Therefore, contrary to our hypothesis for these experiments, uric acid and inhibition of its main producer, XO, did not change the endothelial function of aorta from either normotensive or hypertensive rats. Our results do not, however, exclude the long-term involvement of uric acid in human vascular function through either its antioxidant, mitogenic or still uncovered properties. In the context of the beneficial *vs.* deleterious uric acid effects controversy, one has to be left wondering whether the evolutionary loss of uricase in higher primates and humans may be explained by hyperuricemia conferring a physiological advantage.

Yet, even if proven effective on endothelial function or as a general antioxidant, the desirability of any hyperuricemic treatment has to be questioned, given the controversial evidence and the clear pathophysiological associations of hyperuricemia in humans.

III. Results of *in vivo* XO inhibition in DOCA-salt hypertension

Given the *in vitro* differences seen in XO expression and activity between veins and arteries, the differences in the impact of XO on contractile function, as well

as the increase observed in venous XO activity during DOCA-salt hypertension, we expected that adequate inhibition of XO activity *in vivo* would have more important effects on the venous than the arterial system. Based on the idea that venomotor tone is a contributor to BP regulation, we hypothesized that if we influenced venomotor tone significantly by decreasing venous XO-mediated ROS levels and effects on veins, we would decrease BP during the established phase of DOCA-salt hypertension or attenuate the increase in BP in the initial phase of DOCA-salt hypertension.

We therefore administered allopurinol, the most common XO inhibitor, to DOCA-salt treated rats and compared the effects of this treatment with those of vehicle treatment.

We chose a mid-range dose of allopurinol, previously proven to be effective in inhibiting XO activity in rats *in vivo* (37) and the oral route of administration, for reasons explained above (see Results aim 3).

A. Validation of XO inhibition

Rather than only performing serum urate measurements or performing XO activity assays *ex vivo* on select tissues, such as the liver or our target tissues, the veins, we chose a more comprehensive approach and investigated the alterations in XO metabolites caused by XO inhibition in biological fluids (urine, serum) and several vascular (arteries and veins pairs and the heart) and other

organs (liver and kidney). This approach however precluded simultaneous measurements of ROS levels in veins following allopurinol treatment.

Allopurinol is administered to humans with hyperuricemia and gout with the intention of lowering serum urate levels below the solubility limit of urate (6 mg/dl or 360 μM). Until recently, allopurinol was the only XO inhibitor approved for use in humans. The allopurinol dose used in humans is low in comparison with the one used in typical rodent research (approx 1.25 – 3.75 to as high as 10 mg/kg/day in humans compared to 10-100 mg/kg/day for rodents), especially considering the aforementioned lack of uricase activity in humans and comparatively higher basal serum urate levels. This is partly due to adverse reactions observed at higher allopurinol doses (135). Successful treatment is evaluated based on whether a decrease is observed in serum urate levels on an individual basis. Statistically, this is variably achieved in ~20 up to 80% patients with a typical dose of allopurinol (300 mg/day), and there is a high percentage of non-compliance to treatment (171).

Allopurinol administration to rats is typically done without regard to cardiovascular parameters such as BP. Several published reports do not contain any type of validation for achieving XO inhibition with the chosen dose of allopurinol, while most show either a decrease in serum urate levels or in the XO activity of liver (37, 107, 163).

A few studies reported analysis of urine or serum XO metabolites by HPLC (19, 116, 159), however to our knowledge no such analysis was performed for tissues

from allopurinol-treated animals. We expected decreases in urate levels and potential accumulations in xanthine/hypoxanthine, paralleling the findings in human allopurinol administration.

1. Allopurinol administration in established DOCA-salt hypertension

When we administered allopurinol for 7 days at the end of the DOCA-salt treatment, we observed overall no significant changes of urate and allantoin in urine, a trend for their decrease in serum, as well as decreases in urate in tissue. This was accompanied by highly significant increases in hypoxanthine and xanthine, the XO substrates in urine, and serum and of hypoxanthine in tissues. We attribute the increases observed in hypoxanthine and xanthine to effective blockade of XO function, leading to accumulation of substrates. We validated the drug administration and effect on XO by also observing not only allopurinol, but also oxypurinol in both urine and serum of treated rats (fig 41-43). The longer half-life of oxypurinol is what likely explains the higher levels of oxypurinol compared to allopurinol detected in all our analyses.

2. Allopurinol administration in the developments of DOCA-salt hypertension

When administered from the beginning of DOCA-salt treatment, allopurinol had slightly different effects on XO metabolites as compared to the shorter (7 days) administration. We still did not observe significant decreases in urine and serum uric acid in allopurinol-treated rats, however urate levels decreased significantly in tissues. Similarly to results from the 7-day treatment, the levels of substrates

(hypoxanthine and xanthine) increased significantly in serum, urine and tissues. Contrary to the 7-day treatment results, when no significant changes were observed in tissue xanthine levels, we now observed a significant increase in xanthine levels in several tissues. A potential explanation for this phenomenon that would also take into account the opposite effects with hypoxanthine would be the feed-back on substrate levels in the context of long-term enzyme inhibition. Theoretically this may be achieved by modulation exerted on guanine deaminase, an enzyme that contributes to xanthine, but not hypoxanthine levels. Treatment validation was again obtained by observing levels of allopurinol and, more importantly, oxypurinol in urine and serum (fig 46-48).

3. Dose-dependency of allopurinol effects

Because we did not observe BP effects with 50 mg/kg/day, as opposed to another published study using DOCA-salt hypertensive rats (163) in which decreases in SBP were achieved with 100 mg/kg/day allopurinol, the question arose as to whether the lack of effects in our study was due to insufficient XO blockade and whether we could have inhibited XO activity more effectively with a higher dose of allopurinol. Before repeating BP studies in the DOCA-salt model with the higher allopurinol dose, we examined the comparative effects on XO metabolites of the two allopurinol doses: 50 and 100 mg/kg/day. Overall, these experiments demonstrated that the increases observed in hypoxanthine, xanthine, allopurinol and oxypurinol in urine and serum were dose-dependent. Numerically, these results did not overlap with those obtained in BP studies, probably due to the fact that BP studies were conducted in significantly older,

DOCA-salt treated rats. Serum urate decreased significantly with the higher allopurinol dose, however this was not significantly different from the lower dose. Moreover, the 100 mg/kg/day dose was previously reported as renal toxic in rats (142, 143), and this nephrotoxicity appeared enhanced by hypertension (158). Additionally, the DOCA-salt model used in the study with positive allopurinol results on BP (163) was different from ours, using a higher dose of DOCA (250 mg/kg as opposed to our 200 mg/kg). Moreover, measurements of BP in this study were made using the tail-cuff method, far less precise than the radiotelemetric one we employed. Therefore we concluded that repeating the BP studies with a higher dose of allopurinol was not needed, as likely little effects could be expected on BP with similar levels of XO inhibition. However, that does not exclude the benefits of potential experiments using a different, more specific pharmacological inhibitor or another method for XO inhibition.

B. Effects of allopurinol on BP in the DOCA-salt model of hypertension

We observed no effects on MAP with 50 mg/kg/day allopurinol, regardless of the timing of XO inhibition. A significant decrease in pulse pressure was however observed following allopurinol treatment. This hemodynamic parameter was independently associated with cardiovascular risk in humans (154). The decreased pulse pressure may therefore be a beneficial effect of allopurinol treatment, highlighting a potentially important role of XO aside from its direct impact on BP. Other secondary parameters observed with allopurinol

administration in the development of DOCA-salt hypertension were either not changed or the change was opposite to the one expected. More specifically, there was an increase in DBP, no change in heart weight and no qualitative changes in arterial remodeling (although quantitative comparisons of remodeling were not made). Additionally, we observed a surprising increase in kidney weight. We measured kidney weight as a gross measure of hypertensive nephropathy, however this may also have changed due to adverse renal effects of allopurinol (60, 142, 143).

The lack of effects on MAP with allopurinol treatment can have several explanations. We believe we excluded the explanation of an inefficient blockade of XO with the chosen dose of allopurinol by performing the additional studies comparing 50 with 100 mg/kg/day. However, due to additional specificity questions regarding the use of allopurinol (148), this explanation would be fully excluded only by inhibiting XO with different means: another pharmacological inhibitor, such as the newer, non-purine based febuxostat; or another method, such as *in vivo* siRNA inhibition of XO, although the latter may be hampered by a number of other factors that typically impact *in vivo* RNA_i experiments. Alternatively, even though XO inhibition may have successfully decreased the venous ROS levels *in vivo*, one or all of the hypotheses made based on *in vitro* findings may prove wrong *in vivo*: either the contribution of XO to overall ROS levels, or that of ROS to venomotor tone, or potentially that of the venomotor tone to BP control in the DOCA-salt hypertension model may have been overestimated.

IV. Conclusions

Unlike most studies on the role of ROS in vascular biology and/or hypertension pathogenesis, we took a venous-centric approach. We compared the metabolism of ROS as well as the functional implications of ROS to vascular contractility in veins *vs* arteries in normal conditions. We then tested the hypothesis that inhibition of XO-mediated ROS production would lead to a protective effect on BP in the DOCA-salt hypertensive rat model.

We observed an overall higher ROS environment in veins compared to arteries: higher basal levels of superoxide and H_2O_2 were accompanied by higher antioxidant capacity. Expression and/or activity of several ROS metabolizing enzymes was higher in veins vs arteries: XO, DUOX1, CuZn SOD and catalase. The functional impact of ROS was also higher in veins compared to arteries. Aside for the contribution of XO to venous, but not arterial ET-1-mediated contraction, XO and its metabolite, UA, did not appear to otherwise impact arterial or venous contractile function, and did not modify the arterial hypertensive endothelial dysfunction. XO inhibition with allopurinol *in vivo* did not lead to a decrease in BP in the established DOCA-salt hypertension and did not prevent or attenuate the increases in BP in the development of DOCA-salt hypertension.

Although the involvement of ROS in cardiovascular disease in general and in hypertension in particular has widely been accepted, the question of increases in

ROS as a cause or as an effect of pathological states still remains. Venous function in normal conditions, as well as the involvement of venomotor tone in hypertension pathogenesis are understudied subjects of research. Further studies are needed to elucidate the role of ROS in normal venous system biology as well as that of ROS metabolism on venomotor tone and BP control.

Limitations

A number of facts limit the conclusions that may be drawn from this research. In most of these experiments, we used the aorta-VC pair for comparison. As often the case in vascular research, different results on ROS metabolism may have been obtained in other vascular beds. Additionally, the use of blood vessels from the splanchnic circulation may especially be more relevant to blood pressure regulation. Second, we used a blood pressure model that, as most hypertension models, mimics a form of secondary hypertension, rather than the more often encountered essential one. Moreover, by using an induced hypertension model, the potential pathogenetic role of ROS may be obscured by the effects of the increased ROS that are a result, rather than one of the causes of the pathogenetic process. Third, when assigning a role in ROS metabolism or in vascular contraction to various enzymes, we relied on inhibition through pharmacological tools that generally may be less than perfect in their specificity and effectiveness. This limitation becomes particularly important in the case of allopurinol, on which we relied extensively for both our *in vitro* and *in vivo* studies.

Concerns associated with use of allopurinol and its metabolite oxypurinol include potential scavenging activities towards hydroxyl radical (21), as well as the previously mentioned off-target inhibitory effects on other enzymes, such as purine nucleoside phosphorylase and orotidine-5′-monophosphate decarboxylase, both also involved in nucleotide catabolism. Aside from being normotensive, the sham rats we used as surgery control for their DOCA hypertensive counterparts may be different from normal (untreated) Sprague-Dawley rats in other respects that we have not controlled for. Several other limitations are inherent to the methods for our experiments, the most obvious of which may be the ones related to ROS measurements. Due to a number of factors, one of which being the extremely short half-life of ROS, their measurements are so often inconsistent and fraught with such difficulty, that the consensus in the free radical field of study is that at least two different types of measurements are mandatory for formulating any conclusion on ROS levels. Another limitation that may set apart our results from those of other reports is the fact that in generating them we did not use pure cell cultures, but rather whole tissues and tissue homogenates. Although this approach brings the matter closer to the physiological setting, interpreting results thus obtained is more difficult, as they may reflect contributions by all the varied cell types as well as their interactions in a tissue.

Perspectives

Although we invalidated our hypothesis regarding the role of XO in the established or developing DOCA-salt hypertension, we have by no means excluded the important role of ROS in venous function or the not fully understood role of veins in hypertension pathogenesis. XO may be still involved in the modulation of vascular contractile function and thus indirectly in blood pressure regulation, and during hypertension it may still be responsible for specific damage of target organs. Other ROS metabolizing enzymes may also provide interesting alternatives, one of them being DUOX1, as evidenced by data from our first aim. By comparing veins and arteries we observed many molecular and functional differences. Findings such as these mandate further studies on uncovering the characteristics that enable each blood vessel type to perform optimally in its own environment, and that explain their response during pathological situations like hypertension.

REFERENCES

1. **Adams LD, Geary RL, McManus B, and Schwartz SM**. A comparison of aorta and vena cava medial message expression by cDNA array analysis identifies a set of 68 consistently differentially expressed genes, all in aortic media. *Circ Res* 87: 623-631, 2000.

2. **Ardanaz N, and Pagano PJ**. Hydrogen peroxide as a paracrine vascular mediator: regulation and signaling leading to dysfunction. *Exp Biol Med (Maywood)* 231: 237-251, 2006.

3. **Baldus S, Koster R, Chumley P, Heitzer T, Rudolph V, Ostad MA, Warnholtz A, Staude HJ, Thuneke F, Koss K, Berger J, Meinertz T, Freeman BA, and Munzel T**. Oxypurinol improves coronary and peripheral endothelial function in patients with coronary artery disease. *Free Radic Biol Med* 39: 1184-1190, 2005.

4. **Banerjee D, Madhusoodanan UK, Sharanabasappa M, Ghosh S, and Jacob J**. Measurement of plasma hydroperoxide concentration by FOX-1 assay in conjunction with triphenylphosphine. *Clin Chim Acta* 337: 147-152, 2003.

5. **Barja G**. Free radicals and aging. *Trends Neurosci* 27: 595-600, 2004.

6. **Barry-Lane PA, Patterson C, van der Merwe M, Hu Z, Holland SM, Yeh ET, and Runge MS**. p47phox is required for atherosclerotic lesion progression in ApoE(-/-) mice. *J Clin Invest* 108: 1513-1522, 2001.

7. **Becker BF**. Towards the physiological function of uric acid. *Free Radic Biol Med* 14: 615-631, 1993.

8. **Beckman JS, and Koppenol WH**. Nitric oxide, superoxide, and peroxynitrite: the good, the bad, and ugly. *Am J Physiol* 271: C1424-1437, 1996.

9. **Berry CE, and Hare JM**. Xanthine oxidoreductase and cardiovascular disease: molecular mechanisms and pathophysiological implications. *J Physiol* 555: 589-606, 2004.

10. **Beswick RA, Dorrance AM, Leite R, and Webb RC**. NADH/NADPH oxidase and enhanced superoxide production in the mineralocorticoid hypertensive rat. *Hypertension* 38: 1107-1111, 2001.

11. **Borges F, Fernandes E, and Roleira F**. Progress towards the discovery of xanthine oxidase inhibitors. *Curr Med Chem* 9: 195-217, 2002.

12. **Brand MD, Affourtit C, Esteves TC, Green K, Lambert AJ, Miwa S, Pakay JL, and Parker N**. Mitochondrial superoxide: production, biological

effects, and activation of uncoupling proteins. *Free Radic Biol Med* 37: 755-767, 2004.

13. **Buetler TM, Krauskopf A, and Ruegg UT**. Role of superoxide as a signaling molecule. *News Physiol Sci* 19: 120-123, 2004.

14. **Butler R, Morris AD, Belch JJ, Hill A, and Struthers AD**. Allopurinol normalizes endothelial dysfunction in type 2 diabetics with mild hypertension. *Hypertension* 35: 746-751, 2000.

15. **Cai H, and Harrison DG**. Endothelial dysfunction in cardiovascular diseases: the role of oxidant stress. *Circ Res* 87: 840-844, 2000.

16. **Callera GE, Tostes RC, Yogi A, Montezano AC, and Touyz RM**. Endothelin-1-induced oxidative stress in DOCA-salt hypertension involves NADPH-oxidase-independent mechanisms. *Clin Sci (Lond)* 110: 243-253, 2006.

17. **Chu Y, Iida S, Lund DD, Weiss RM, DiBona GF, Watanabe Y, Faraci FM, and Heistad DD**. Gene transfer of extracellular superoxide dismutase reduces arterial pressure in spontaneously hypertensive rats: role of heparin-binding domain. *Circ Res* 92: 461-468, 2003.

18. **Clempus RE, and Griendling KK**. Reactive oxygen species signaling in vascular smooth muscle cells. *Cardiovasc Res* 71: 216-225, 2006.

19. **Cooper N, Khosravan R, Erdmann C, Fiene J, and Lee JW**. Quantification of uric acid, xanthine and hypoxanthine in human serum by HPLC for pharmacodynamic studies. *J Chromatogr B Analyt Technol Biomed Life Sci* 837: 1-10, 2006.

20. **Corry DB, Eslami P, Yamamoto K, Nyby MD, Makino H, and Tuck ML**. Uric acid stimulates vascular smooth muscle cell proliferation and oxidative stress via the vascular renin-angiotensin system. *J Hypertens* 26: 269-275, 2008.

21. **Das DK, Engelman RM, Clement R, Otani H, Prasad MR, and Rao PS**. Role of xanthine oxidase inhibitor as free radical scavenger: a novel mechanism of action of allopurinol and oxypurinol in myocardial salvage. *Biochem Biophys Res Commun* 148: 314-319, 1987.

22. **Decoursey TE, and Ligeti E**. Regulation and termination of NADPH oxidase activity. *Cell Mol Life Sci* 62: 2173-2193, 2005.

23. **dela Paz NG, and D'Amore PA**. Arterial versus venous endothelial cells. *Cell Tissue Res* 335: 5-16, 2009.

24. **Deng DX, Spin JM, Tsalenko A, Vailaya A, Ben-Dor A, Yakhini Z, Tsao P, Bruhn L, and Quertermous T**. Molecular signatures determining coronary

artery and saphenous vein smooth muscle cell phenotypes: distinct responses to stimuli. *Arterioscler Thromb Vasc Biol* 26: 1058-1065, 2006.

25. **Deng DX, Tsalenko A, Vailaya A, Ben-Dor A, Kundu R, Estay I, Tabibiazar R, Kincaid R, Yakhini Z, Bruhn L, and Quertermous T**. Differences in vascular bed disease susceptibility reflect differences in gene expression response to atherogenic stimuli. *Circ Res* 98: 200-208, 2006.

26. **Duckles SP, Krause DN, Stirone C, and Procaccio V**. Estrogen and mitochondria: a new paradigm for vascular protection? *Mol Interv* 6: 26-35, 2006.

27. **Duerrschmidt N, Wippich N, Goettsch W, Broemme HJ, and Morawietz H**. Endothelin-1 induces NAD(P)H oxidase in human endothelial cells. *Biochem Biophys Res Commun* 269: 713-717, 2000.

28. **Dupont GP, Hueckstead TP, Marshall BC, Ryan US, Michael JR, and Hoidal JR**. Regulation of xanthine dehydrogenase and xanthine oxidase activity and gene expression in cultured rat pulmonary endothelial cells. *J Clin Invest* 89: 197-202, 1992.

29. **El-Benna J, Dang PM, Gougerot-Pocidalo MA, and Elbim C**. Phagocyte NADPH oxidase: a multicomponent enzyme essential for host defenses. *Arch Immunol Ther Exp (Warsz)* 53: 199-206, 2005.

30. **Esteves TC, and Brand MD**. The reactions catalysed by the mitochondrial uncoupling proteins UCP2 and UCP3. *Biochim Biophys Acta* 1709: 35-44, 2005.

31. **Faraci FM, and Didion SP**. Vascular protection: superoxide dismutase isoforms in the vessel wall. *Arterioscler Thromb Vasc Biol* 24: 1367-1373, 2004.

32. **Feig DI, Kang DH, and Johnson RJ**. Uric acid and cardiovascular risk. *N Engl J Med* 359: 1811-1821, 2008.

33. **Feig DI, Soletsky B, and Johnson RJ**. Effect of allopurinol on blood pressure of adolescents with newly diagnosed essential hypertension: a randomized trial. *Jama* 300: 924-932, 2008.

34. **Feissner RF, Skalska J, Gaum WE, and Sheu SS**. Crosstalk signaling between mitochondrial Ca2+ and ROS. *Front Biosci* 14: 1197-1218, 2009.

35. **Fennell JP, Brosnan MJ, Frater AJ, Hamilton CA, Alexander MY, Nicklin SA, Heistad DD, Baker AH, and Dominiczak AF**. Adenovirus-mediated overexpression of extracellular superoxide dismutase improves endothelial dysfunction in a rat model of hypertension. *Gene Ther* 9: 110-117, 2002.

36. **Fernandes E, Costa D, Toste SA, Lima JL, and Reis S**. In vitro scavenging activity for reactive oxygen and nitrogen species by nonsteroidal anti-

inflammatory indole, pyrrole, and oxazole derivative drugs. *Free Radic Biol Med* 37: 1895-1905, 2004.

37. **Fields M, Lewis CG, and Lure MD**. Allopurinol, an inhibitor of xanthine oxidase, reduces uric acid levels and modifies the signs associated with copper deficiency in rats fed fructose. *Free Radic Biol Med* 20: 595-600, 1996.

38. **Fink GD**. Arthur C. Corcoran Memorial Lecture. Sympathetic activity, vascular capacitance, and long-term regulation of arterial pressure. *Hypertension* 53: 307-312, 2009.

39. **Fink GD, Johnson RJ, and Galligan JJ**. Mechanisms of increased venous smooth muscle tone in desoxycorticosterone acetate-salt hypertension. *Hypertension* 35: 464-469, 2000.

40. **Finkel T, and Holbrook NJ**. Oxidants, oxidative stress and the biology of ageing. *Nature* 408: 239-247, 2000.

41. **Forstermann U, and Munzel T**. Endothelial nitric oxide synthase in vascular disease: from marvel to menace. *Circulation* 113: 1708-1714, 2006.

42. **Fridovich I**. The Competitive Inhibition of Uricase by Oxonate and by Related Derivatives of S-Triazines. *J Biol Chem* 240: 2491-2494, 1965.

43. **Ganong WF**. *Review of medical physiology*. New York: McGraw-Hill Medical, 2005.

44. **Gao YJ, and Lee RM**. Hydrogen peroxide is an endothelium-dependent contracting factor in rat renal artery. *Br J Pharmacol* 146: 1061-1068, 2005.

45. **George J, Carr E, Davies J, Belch JJ, and Struthers A**. High-dose allopurinol improves endothelial function by profoundly reducing vascular oxidative stress and not by lowering uric acid. *Circulation* 114: 2508-2516, 2006.

46. **Gersch C, Palii SP, Kim KM, Angerhofer A, Johnson RJ, and Henderson GN**. Inactivation of nitric oxide by uric acid. *Nucleosides Nucleotides Nucleic Acids* 27: 967-978, 2008.

47. **Greenbaum D, Colangelo C, Williams K, and Gerstein M**. Comparing protein abundance and mRNA expression levels on a genomic scale. *Genome Biol* 4: 117, 2003.

48. **Griendling KK, Minieri CA, Ollerenshaw JD, and Alexander RW**. Angiotensin II stimulates NADH and NADPH oxidase activity in cultured vascular smooth muscle cells. *Circ Res* 74: 1141-1148, 1994.

49. **Guo Y, Xiao P, Lei S, Deng F, Xiao GG, Liu Y, Chen X, Li L, Wu S, Chen Y, Jiang H, Tan L, Xie J, Zhu X, Liang S, and Deng H**. How is mRNA

expression predictive for protein expression? A correlation study on human circulating monocytes. *Acta Biochim Biophys Sin (Shanghai)* 40: 426-436, 2008.

50. **Guzik TJ, Olszanecki R, Sadowski J, Kapelak B, Rudzinski P, Jopek A, Kawczynska A, Ryszawa N, Loster J, Jawien J, Czesnikiewicz-Guzik M, Channon KM, and Korbut R**. Superoxide dismutase activity and expression in human venous and arterial bypass graft vessels. *J Physiol Pharmacol* 56: 313-323, 2005.

51. **Guzik TJ, Sadowski J, Kapelak B, Jopek A, Rudzinski P, Pillai R, Korbut R, and Channon KM**. Systemic regulation of vascular NAD(P)H oxidase activity and nox isoform expression in human arteries and veins. *Arterioscler Thromb Vasc Biol* 24: 1614-1620, 2004.

52. **Guzik TJ, West NE, Pillai R, Taggart DP, and Channon KM**. Nitric oxide modulates superoxide release and peroxynitrite formation in human blood vessels. *Hypertension* 39: 1088-1094, 2002.

53. **Harrison R**. Physiological roles of xanthine oxidoreductase. *Drug Metab Rev* 36: 363-375, 2004.

54. **Haurani MJ, and Pagano PJ**. Adventitial fibroblast reactive oxygen species as autacrine and paracrine mediators of remodeling: bellwether for vascular disease? *Cardiovasc Res* 75: 679-689, 2007.

55. **Heikkila RE, Cabbat FS, and Cohen G**. In vivo inhibition of superoxide dismutase in mice by diethyldithiocarbamate. *J Biol Chem* 251: 2182-2185, 1976.

56. **Heumuller S, Wind S, Barbosa-Sicard E, Schmidt HH, Busse R, Schroder K, and Brandes RP**. Apocynin is not an inhibitor of vascular NADPH oxidases but an antioxidant. *Hypertension* 51: 211-217, 2008.

57. **Hisaki R, Fujita H, Saito F, and Kushiro T**. Tempol attenuates the development of hypertensive renal injury in Dahl salt-sensitive rats. *Am J Hypertens* 18: 707-713, 2005.

58. **Ho YS, Magnenat JL, Gargano M, and Cao J**. The nature of antioxidant defense mechanisms: a lesson from transgenic studies. *Environ Health Perspect* 106 Suppl 5: 1219-1228, 1998.

59. **Hohler B, Holzapfel B, and Kummer W**. NADPH oxidase subunits and superoxide production in porcine pulmonary artery endothelial cells. *Histochem Cell Biol* 114: 29-37, 2000.

60. **Horiuchi H, Ota M, Nishimura S, Kaneko H, Kasahara Y, Ohta T, and Komoriya K**. Allopurinol induces renal toxicity by impairing pyrimidine metabolism in mice. *Life Sci* 66: 2051-2070, 2000.

61. **Hottenstein OD, and Kreulen DL**. Comparison of the frequency dependence of venous and arterial responses to sympathetic nerve stimulation in guinea-pigs. *J Physiol* 384: 153-167, 1987.

62. **Houston M, Estevez A, Chumley P, Aslan M, Marklund S, Parks DA, and Freeman BA**. Binding of xanthine oxidase to vascular endothelium. Kinetic characterization and oxidative impairment of nitric oxide-dependent signaling. *J Biol Chem* 274: 4985-4994, 1999.

63. **Ikebuchi Y, Masumoto N, Tasaka K, Koike K, Kasahara K, Miyake A, and Tanizawa O**. Superoxide anion increases intracellular pH, intracellular free calcium, and arachidonate release in human amnion cells. *J Biol Chem* 266: 13233-13237, 1991.

64. **Inkster ME, Cotter MA, and Cameron NE**. Treatment with the xanthine oxidase inhibitor, allopurinol, improves nerve and vascular function in diabetic rats. *Eur J Pharmacol* 561: 63-71, 2007.

65. **Johnson F, and Giulivi C**. Superoxide dismutases and their impact upon human health. *Mol Aspects Med* 26: 340-352, 2005.

66. **Johnson RJ, Kang DH, Feig D, Kivlighn S, Kanellis J, Watanabe S, Tuttle KR, Rodriguez-Iturbe B, Herrera-Acosta J, and Mazzali M**. Is there a pathogenetic role for uric acid in hypertension and cardiovascular and renal disease? *Hypertension* 41: 1183-1190, 2003.

67. **Jung O, Marklund SL, Xia N, Busse R, and Brandes RP**. Inactivation of extracellular superoxide dismutase contributes to the development of high-volume hypertension. *Arterioscler Thromb Vasc Biol* 27: 470-477, 2007.

68. **Jung O, Schreiber JG, Geiger H, Pedrazzini T, Busse R, and Brandes RP**. gp91phox-containing NADPH oxidase mediates endothelial dysfunction in renovascular hypertension. *Circulation* 109: 1795-1801, 2004.

69. **Kasal DA, Neves MF, Oigman W, and Mandarim-de-Lacerda CA**. Allopurinol attenuates L-NAME induced cardiomyopathy comparable to blockade of angiotensin receptor. *Histol Histopathol* 23: 1241-1248, 2008.

70. **Kemp BK, Smolich JJ, and Cocks TM**. Evidence for specific regional patterns of responses to different vasoconstrictors and vasodilators in sheep isolated pulmonary arteries and veins. *Br J Pharmacol* 121: 441-450, 1997.

71. **Khosla UM, Zharikov S, Finch JL, Nakagawa T, Roncal C, Mu W, Krotova K, Block ER, Prabhakar S, and Johnson RJ**. Hyperuricemia induces endothelial dysfunction. *Kidney Int* 67: 1739-1742, 2005.

72. **Kim SY, De Vera MA, and Choi HK**. Gout and mortality. *Clin Exp Rheumatol* 26: S115-119, 2008.

73. **Kimura S, Zhang GX, Nishiyama A, Shokoji T, Yao L, Fan YY, Rahman M, Suzuki T, Maeta H, and Abe Y**. Role of NAD(P)H oxidase- and mitochondria-derived reactive oxygen species in cardioprotection of ischemic reperfusion injury by angiotensin II. *Hypertension* 45: 860-866, 2005.

74. **Kisker C, Schindelin H, and Rees DC**. Molybdenum-cofactor-containing enzymes: structure and mechanism. *Annu Rev Biochem* 66: 233-267, 1997.

75. **Kleinbongard P, Schulz R, Rassaf T, Lauer T, Dejam A, Jax T, Kumara I, Gharini P, Kabanova S, Ozuyaman B, Schnurch HG, Godecke A, Weber AA, Robenek M, Robenek H, Bloch W, Rosen P, and Kelm M**. Red blood cells express a functional endothelial nitric oxide synthase. *Blood* 107: 2943-2951, 2006.

76. **Kris-Etherton PM, Lichtenstein AH, Howard BV, Steinberg D, and Witztum JL**. Antioxidant vitamin supplements and cardiovascular disease. *Circulation* 110: 637-641, 2004.

77. **Krishnan E, Kwoh CK, Schumacher HR, and Kuller L**. Hyperuricemia and incidence of hypertension among men without metabolic syndrome. *Hypertension* 49: 298-303, 2007.

78. **Laakso J, Mervaala E, Himberg JJ, Teravainen TL, Karppanen H, Vapaatalo H, and Lapatto R**. Increased kidney xanthine oxidoreductase activity in salt-induced experimental hypertension. *Hypertension* 32: 902-906, 1998.

79. **Laakso JT, Teravainen TL, Martelin E, Vaskonen T, and Lapatto R**. Renal xanthine oxidoreductase activity during development of hypertension in spontaneously hypertensive rats. *J Hypertens* 22: 1333-1340, 2004.

80. **Lacza Z, Pankotai E, and Busija DW**. Mitochondrial nitric oxide synthase: current concepts and controversies. *Front Biosci* 14: 4436-4443, 2009.

81. **Landmesser U, Cai H, Dikalov S, McCann L, Hwang J, Jo H, Holland SM, and Harrison DG**. Role of p47(phox) in vascular oxidative stress and hypertension caused by angiotensin II. *Hypertension* 40: 511-515, 2002.

82. **Landmesser U, Dikalov S, Price SR, McCann L, Fukai T, Holland SM, Mitch WE, and Harrison DG**. Oxidation of tetrahydrobiopterin leads to uncoupling of endothelial cell nitric oxide synthase in hypertension. *J Clin Invest* 111: 1201-1209, 2003.

83. **Landmesser U, Spiekermann S, Preuss C, Sorrentino S, Fischer D, Manes C, Mueller M, and Drexler H**. Angiotensin II induces endothelial xanthine oxidase activation: role for endothelial dysfunction in patients with coronary disease. *Arterioscler Thromb Vasc Biol* 27: 943-948, 2007.

84. **Lassegue B, and Clempus RE**. Vascular NAD(P)H oxidases: specific features, expression, and regulation. *Am J Physiol Regul Integr Comp Physiol* 285: R277-297, 2003.

85. **Lassegue B, Sorescu D, Szocs K, Yin Q, Akers M, Zhang Y, Grant SL, Lambeth JD, and Griendling KK**. Novel gp91(phox) homologues in vascular smooth muscle cells : nox1 mediates angiotensin II-induced superoxide formation and redox-sensitive signaling pathways. *Circ Res* 88: 888-894, 2001.

86. **Li L, Fink GD, Watts SW, Northcott CA, Galligan JJ, Pagano PJ, and Chen AF**. Endothelin-1 increases vascular superoxide via endothelin(A)-NADPH oxidase pathway in low-renin hypertension. *Circulation* 107: 1053-1058, 2003.

87. **Li L, Watts SW, Banes AK, Galligan JJ, Fink GD, and Chen AF**. NADPH oxidase-derived superoxide augments endothelin-1-induced venoconstriction in mineralocorticoid hypertension. *Hypertension* 42: 316-321, 2003.

88. **Linder N, Rapola J, and Raivio KO**. Cellular expression of xanthine oxidoreductase protein in normal human tissues. *Lab Invest* 79: 967-974, 1999.

89. **Lloyd-Jones D, Adams R, Carnethon M, De Simone G, Ferguson TB, Flegal K, Ford E, Furie K, Go A, Greenlund K, Haase N, Hailpern S, Ho M, Howard V, Kissela B, Kittner S, Lackland D, Lisabeth L, Marelli A, McDermott M, Meigs J, Mozaffarian D, Nichol G, O'Donnell C, Roger V, Rosamond W, Sacco R, Sorlie P, Stafford R, Steinberger J, Thom T, Wasserthiel-Smoller S, Wong N, Wylie-Rosett J, and Hong Y**. Heart disease and stroke statistics--2009 update: a report from the American Heart Association Statistics Committee and Stroke Statistics Subcommittee. *Circulation* 119: e21-181, 2009.

90. **London GM, Safar ME, Weiss YA, Laurent S, and London AM**. Renal and systemic hemodynamics in borderline hypertension. *Am J Hypertens* 1: 127S-130S, 1988.

91. **London GM, Safar ME, Weiss YA, and Simon CA**. Total effective compliance of the vascular bed in essential hypertension. *Am Heart J* 95: 325-330, 1978.

92. **Loomis ED, Sullivan JC, Osmond DA, Pollock DM, and Pollock JS**. Endothelin mediates superoxide production and vasoconstriction through activation of NADPH oxidase and uncoupled nitric-oxide synthase in the rat aorta. *J Pharmacol Exp Ther* 315: 1058-1064, 2005.

93. **Mackay J, Mensah GA, World Health Organization., and Centers for Disease Control and Prevention (U.S.)**. *The atlas of heart disease and stroke*. Geneva: World Health Organization, 2004, p. 112 p.

94. **Macmillan-Crow LA, and Cruthirds DL**. Invited review: manganese superoxide dismutase in disease. *Free Radic Res* 34: 325-336, 2001.

95. **Madamanchi NR, Vendrov A, and Runge MS**. Oxidative stress and vascular disease. *Arterioscler Thromb Vasc Biol* 25: 29-38, 2005.

96. **Martin DS, Rodrigo MC, and Appelt CW**. Venous tone in the developmental stages of spontaneous hypertension. *Hypertension* 31: 139-144, 1998.

97. **Mazzali M, Hughes J, Kim YG, Jefferson JA, Kang DH, Gordon KL, Lan HY, Kivlighn S, and Johnson RJ**. Elevated uric acid increases blood pressure in the rat by a novel crystal-independent mechanism. *Hypertension* 38: 1101-1106, 2001.

98. **McNally JS, Davis ME, Giddens DP, Saha A, Hwang J, Dikalov S, Jo H, and Harrison DG**. Role of xanthine oxidoreductase and NAD(P)H oxidase in endothelial superoxide production in response to oscillatory shear stress. *Am J Physiol Heart Circ Physiol* 285: H2290-2297, 2003.

99. **McNally JS, Saxena A, Cai H, Dikalov S, and Harrison DG**. Regulation of xanthine oxidoreductase protein expression by hydrogen peroxide and calcium. *Arterioscler Thromb Vasc Biol* 25: 1623-1628, 2005.

100. **Mollnau H, Wendt M, Szocs K, Lassegue B, Schulz E, Oelze M, Li H, Bodenschatz M, August M, Kleschyov AL, Tsilimingas N, Walter U, Forstermann U, Meinertz T, Griendling K, and Munzel T**. Effects of angiotensin II infusion on the expression and function of NAD(P)H oxidase and components of nitric oxide/cGMP signaling. *Circ Res* 90: E58-65, 2002.

101. **Motwani JG, and Topol EJ**. Aortocoronary saphenous vein graft disease: pathogenesis, predisposition, and prevention. *Circulation* 97: 916-931, 1998.

102. **Munzel T, Afanas'ev IB, Kleschyov AL, and Harrison DG**. Detection of superoxide in vascular tissue. *Arterioscler Thromb Vasc Biol* 22: 1761-1768, 2002.

103. **Nakazono K, Watanabe N, Matsuno K, Sasaki J, Sato T, and Inoue M**. Does superoxide underlie the pathogenesis of hypertension? *Proc Natl Acad Sci U S A* 88: 10045-10048, 1991.

104. **Newaz MA, Yousefipour Z, and Oyekan A**. Oxidative stress-associated vascular aging is xanthine oxidase-dependent but not NAD(P)H oxidase-dependent. *J Cardiovasc Pharmacol* 48: 88-94, 2006.

105. **Nishino T, Okamoto K, Eger BT, Pai EF, and Nishino T**. Mammalian xanthine oxidoreductase - mechanism of transition from xanthine dehydrogenase to xanthine oxidase. *Febs J* 275: 3278-3289, 2008.

106. **Nyhof RA, Laine GA, Meininger GA, and Granger HJ**. Splanchnic circulation in hypertension. *Fed Proc* 42: 1690-1693, 1983.

107. **Ong SL, Vickers JJ, Zhang Y, McKenzie KU, Walsh CE, and Whitworth JA**. Role of xanthine oxidase in dexamethasone-induced hypertension in rats. *Clin Exp Pharmacol Physiol* 34: 517-519, 2007.

108. **Onuma S, and Nakanishi K**. Superoxide dismustase mimetic tempol decreases blood pressure by increasing renal medullary blood flow in hyperinsulinemic-hypertensive rats. *Metabolism* 53: 1305-1308, 2004.

109. **Ookawara T, Eguchi H, Nishimura M, Kizaki T, Eiji T, Saitoh D, Ohno H, and Suzuki K**. Effects of oxidative stress on the nuclear translocation of extracellular superoxide dismutase. *Biochem Biophys Res Commun* 303: 914-919, 2003.

110. **Pacher P, Nivorozhkin A, and Szabo C**. Therapeutic effects of xanthine oxidase inhibitors: renaissance half a century after the discovery of allopurinol. *Pharmacol Rev* 58: 87-114, 2006.

111. **Pan YJ, and Young DB**. Experimental aldosterone hypertension in the dog. *Hypertension* 4: 279-287, 1982.

112. **Payeli SK, Latini R, Gebhard C, Patrignani A, Wagner U, Luscher TF, and Tanner FC**. Prothrombotic gene expression profile in vascular smooth muscle cells of human saphenous vein, but not internal mammary artery. *Arterioscler Thromb Vasc Biol* 28: 705-710, 2008.

113. **Poli G, Biasi F, and Leonarduzzi G**. 4-Hydroxynonenal-protein adducts: A reliable biomarker of lipid oxidation in liver diseases. *Mol Aspects Med* 29: 67-71, 2008.

114. **Potter SZ, and Valentine JS**. The perplexing role of copper-zinc superoxide dismutase in amyotrophic lateral sclerosis (Lou Gehrig's disease). *J Biol Inorg Chem* 8: 373-380, 2003.

115. **Price KL, Sautin YY, Long DA, Zhang L, Miyazaki H, Mu W, Endou H, and Johnson RJ**. Human vascular smooth muscle cells express a urate transporter. *J Am Soc Nephrol* 17: 1791-1795, 2006.

116. **Putterman GJ, Shaikh B, Hallmark MR, Sawyer CG, Hixson CV, and Perini F**. Simultaneous analysis of substrates, products, and inhibitors of xanthine oxidase by high-pressure liquid chromatography and gas chromatography. *Anal Biochem* 98: 18-26, 1979.

117. **Rao GN, Corson MA, and Berk BC**. Uric acid stimulates vascular smooth muscle cell proliferation by increasing platelet-derived growth factor A-chain expression. *J Biol Chem* 266: 8604-8608, 1991.

118. **Redon J, Oliva MR, Tormos C, Giner V, Chaves J, Iradi A, and Saez GT**. Antioxidant activities and oxidative stress byproducts in human hypertension. *Hypertension* 41: 1096-1101, 2003.

119. **Rey FE, Cifuentes ME, Kiarash A, Quinn MT, and Pagano PJ**. Novel competitive inhibitor of NAD(P)H oxidase assembly attenuates vascular O(2)(-) and systolic blood pressure in mice. *Circ Res* 89: 408-414, 2001.

120. **Ricksten SE, Yao T, and Thoren P**. Peripheral and central vascular compliances in conscious normotensive and spontaneously hypertensive rats. *Acta Physiol Scand* 112: 169-177, 1981.

121. **Rothe CF**. Reflex control of veins and vascular capacitance. *Physiol Rev* 63: 1281-1342, 1983.

122. **Rozen S, and Skaletsky H**. Primer3 on the WWW for general users and for biologist programmers. *Methods Mol Biol* 132: 365-386, 2000.

123. **Rueckschloss U, Galle J, Holtz J, Zerkowski HR, and Morawietz H**. Induction of NAD(P)H oxidase by oxidized low-density lipoprotein in human endothelial cells: antioxidative potential of hydroxymethylglutaryl coenzyme A reductase inhibitor therapy. *Circulation* 104: 1767-1772, 2001.

124. **Rueckschloss U, Quinn MT, Holtz J, and Morawietz H**. Dose-dependent regulation of NAD(P)H oxidase expression by angiotensin II in human endothelial cells: protective effect of angiotensin II type 1 receptor blockade in patients with coronary artery disease. *Arterioscler Thromb Vasc Biol* 22: 1845-1851, 2002.

125. **Saetrum Opgaard O, and Edvinsson L**. Effect of parasympathetic and sensory transmitters on human epicardial coronary arteries and veins. *Pharmacol Toxicol* 78: 273-279, 1996.

126. **Schmieder RE, Schobel HP, and Messerli FH**. Central blood volume: a determinant of early cardiac adaptation in arterial hypertension? *J Am Coll Cardiol* 26: 1692-1698, 1995.

127. **Schulz E, Jansen T, Wenzel P, Daiber A, and Munzel T**. Nitric oxide, tetrahydrobiopterin, oxidative stress, and endothelial dysfunction in hypertension. *Antioxid Redox Signal* 10: 1115-1126, 2008.

128. **Schulz R, Rassaf T, Massion PB, Kelm M, and Balligand JL**. Recent advances in the understanding of the role of nitric oxide in cardiovascular homeostasis. *Pharmacol Ther* 108: 225-256, 2005.

129. **Selemidis S, Sobey CG, Wingler K, Schmidt HH, and Drummond GR**. NADPH oxidases in the vasculature: molecular features, roles in disease and pharmacological inhibition. *Pharmacol Ther* 120: 254-291, 2008.

130. **Shapira OM, Xu A, Aldea GS, Vita JA, Shemin RJ, and Keaney JF, Jr.** Enhanced nitric oxide-mediated vascular relaxation in radial artery compared with internal mammary artery or saphenous vein. *Circulation* 100: II322-327, 1999.

131. **Shi W, Eidelman DH, and Michel RP**. Differential relaxant responses of pulmonary arteries and veins in lung explants of guinea pigs. *J Appl Physiol* 83: 1476-1481, 1997.

132. **Shi Y, Patel S, Davenpeck KL, Niculescu R, Rodriguez E, Magno MG, Ormont ML, Mannion JD, and Zalewski A**. Oxidative stress and lipid retention in vascular grafts: comparison between venous and arterial conduits. *Circulation* 103: 2408-2413, 2001.

133. **Skinner KA, White CR, Patel R, Tan S, Barnes S, Kirk M, Darley-Usmar V, and Parks DA**. Nitrosation of uric acid by peroxynitrite. Formation of a vasoactive nitric oxide donor. *J Biol Chem* 273: 24491-24497, 1998.

134. **Smith RA, Kelso GF, Blaikie FH, Porteous CM, Ledgerwood EC, Hughes G, James AM, Ross MF, Asin-Cayuela J, Cocheme HM, Filipovska A, and Murphy MP**. Using mitochondria-targeted molecules to study mitochondrial radical production and its consequences. *Biochem Soc Trans* 31: 1295-1299, 2003.

135. **So A**. Developments in the scientific and clinical understanding of gout. *Arthritis Res Ther* 10: 221, 2008.

136. **Spiekermann S, Landmesser U, Dikalov S, Bredt M, Gamez G, Tatge H, Reepschlager N, Hornig B, Drexler H, and Harrison DG**. Electron spin resonance characterization of vascular xanthine and NAD(P)H oxidase activity in patients with coronary artery disease: relation to endothelium-dependent vasodilation. *Circulation* 107: 1383-1389, 2003.

137. **Srivastava P, Hegde LG, Patnaik GK, and Dikshit M**. Role of endothelial-derived reactive oxygen species and nitric oxide in norepinephrine-induced rat aortic ring contractions. *Pharmacol Res* 38: 265-274, 1998.

138. **St-Pierre J, Buckingham JA, Roebuck SJ, and Brand MD**. Topology of superoxide production from different sites in the mitochondrial electron transport chain. *J Biol Chem* 277: 44784-44790, 2002.

139. **Stralin P, Karlsson K, Johansson BO, and Marklund SL**. The interstitium of the human arterial wall contains very large amounts of extracellular superoxide dismutase. *Arterioscler Thromb Vasc Biol* 15: 2032-2036, 1995.

140. **Sumimoto H, Miyano K, and Takeya R**. Molecular composition and regulation of the Nox family NAD(P)H oxidases. *Biochem Biophys Res Commun* 338: 677-686, 2005.

141. **Suzuki H, DeLano FA, Parks DA, Jamshidi N, Granger DN, Ishii H, Suematsu M, Zweifach BW, and Schmid-Schonbein GW**. Xanthine oxidase activity associated with arterial blood pressure in spontaneously hypertensive rats. *Proc Natl Acad Sci U S A* 95: 4754-4759, 1998.

142. **Suzuki Y, Sato Y, Sudo J, and Tanabe T**. Renal lipid peroxidation induced by allopurinol-administration in rats. *Dev Toxicol Environ Sci* 14: 65-72, 1986.

143. **Suzuki Y, Sudo J, and Tanabe T**. Allopurinol toxicity: its toxic organ-specificity between the liver and the kidney in the rat. *J Toxicol Sci* 9: 343-351, 1984.

144. **Swales JD**. *Textbook of hypertension*. Oxford ; Boston: Blackwell Scientific Publications, 1994, p. xvi, 1328 p., [1326] p. of plates.

145. **Szasz T, Eddy S, Paulauskis J, Burnett R, Ellekilde M, Iovanna JL, and Watts SW**. Differential Expression of Pancreatitis-Associated Protein and Thrombospondins in Arterial versus Venous Tissues. *J Vasc Res* 46: 551-560, 2009.

146. **Szasz T, Thakali K, Fink GD, and Watts SW**. A comparison of arteries and veins in oxidative stress: producers, destroyers, function, and disease. *Exp Biol Med (Maywood)* 232: 27-37, 2007.

147. **Szasz T, Thompson JM, and Watts SW**. A comparison of reactive oxygen species metabolism in the rat aorta and vena cava: focus on xanthine oxidase. *Am J Physiol Heart Circ Physiol* 295: H1341-H1350, 2008.

148. **Takano Y, Hase-Aoki K, Horiuchi H, Zhao L, Kasahara Y, Kondo S, and Becker MA**. Selectivity of febuxostat, a novel non-purine inhibitor of xanthine oxidase/xanthine dehydrogenase. *Life Sci* 76: 1835-1847, 2005.

149. **Tanito M, Nakamura H, Kwon YW, Teratani A, Masutani H, Shioji K, Kishimoto C, Ohira A, Horie R, and Yodoi J**. Enhanced oxidative stress and impaired thioredoxin expression in spontaneously hypertensive rats. *Antioxid Redox Signal* 6: 89-97, 2004.

150. **Thakali K, Davenport L, Fink GD, and Watts SW**. Pleiotropic effects of hydrogen peroxide in arteries and veins from normotensive and hypertensive rats. *Hypertension* 47: 482-487, 2006.

151. **Thakali K, Demel SL, Fink GD, and Watts SW**. Endothelin-1-induced contraction in veins is independent of hydrogen peroxide. *Am J Physiol Heart Circ Physiol* 289: H1115-1122, 2005.

152. **Thakali K, Fink GD, and Watts SW**. Arteries and veins desensitize differently to endothelin. *J Cardiovasc Pharmacol* 43: 387-393, 2004.

153. **Thakali K, Galligan JJ, Fink GD, Gariepy CE, and Watts SW.** Pharmacological endothelin receptor interaction does not occur in veins from ET(B) receptor deficient rats. *Vascul Pharmacol* 2008.

154. **Thomas F, Blacher J, Benetos A, Safar ME, and Pannier B.** Cardiovascular risk as defined in the 2003 European blood pressure classification: the assessment of an additional predictive value of pulse pressure on mortality. *J Hypertens* 26: 1072-1077, 2008.

155. **Titorenko VI, and Rachubinski RA.** The peroxisome: orchestrating important developmental decisions from inside the cell. *J Cell Biol* 164: 641-645, 2004.

156. **Torrecillas G, Boyano-Adanez MC, Medina J, Parra T, Griera M, Lopez-Ongil S, Arilla E, Rodriguez-Puyol M, and Rodriguez-Puyol D.** The role of hydrogen peroxide in the contractile response to angiotensin II. *Mol Pharmacol* 59: 104-112, 2001.

157. **Touyz RM, and Schiffrin EL.** Reactive oxygen species in vascular biology: implications in hypertension. *Histochem Cell Biol* 122: 339-352, 2004.

158. **Trachtman H, Valderrama E, and Futterweit S.** Nephrotoxicity of allopurinol is enhanced in experimental hypertension. *Hypertension* 17: 194-202, 1991.

159. **Turnheim K, Krivanek P, and Oberbauer R.** Pharmacokinetics and pharmacodynamics of allopurinol in elderly and young subjects. *Br J Clin Pharmacol* 48: 501-509, 1999.

160. **Uddin M, Yang H, Shi M, Polley-Mandal M, and Guo Z.** Elevation of oxidative stress in the aorta of genetically hypertensive mice. *Mech Ageing Dev* 124: 811-817, 2003.

161. **Ulker S, McMaster D, McKeown PP, and Bayraktutan U.** Impaired activities of antioxidant enzymes elicit endothelial dysfunction in spontaneous hypertensive rats despite enhanced vascular nitric oxide generation. *Cardiovasc Res* 59: 488-500, 2003.

162. **Varela-Echavarria A, Montes de Oca-Luna R, and Barrera-Saldana HA.** Uricase protein sequences: conserved during vertebrate evolution but absent in humans. *Faseb J* 2: 3092-3096, 1988.

163. **Viel EC, Benkirane K, Javeshghani D, Touyz RM, and Schiffrin EL.** Xanthine oxidase and mitochondria contribute to vascular superoxide anion generation in DOCA-salt hypertensive rats. *Am J Physiol Heart Circ Physiol* 295: H281-288, 2008.

164. **Vorbach C, Scriven A, and Capecchi MR**. The housekeeping gene xanthine oxidoreductase is necessary for milk fat droplet enveloping and secretion: gene sharing in the lactating mammary gland. *Genes Dev* 16: 3223-3235, 2002.

165. **Waring WS, McKnight JA, Webb DJ, and Maxwell SR**. Lowering serum urate does not improve endothelial function in patients with type 2 diabetes. *Diabetologia* 50: 2572-2579, 2007.

166. **Waring WS, McKnight JA, Webb DJ, and Maxwell SR**. Uric acid restores endothelial function in patients with type 1 diabetes and regular smokers. *Diabetes* 55: 3127-3132, 2006.

167. **Watts SW, Fink GD, Northcott CA, and Galligan JJ**. Endothelin-1-induced venous contraction is maintained in DOCA-salt hypertension; studies with receptor agonists. *Br J Pharmacol* 137: 69-79, 2002.

168. **Watts SW, Rondelli C, Thakali K, Li X, Uhal B, Pervaiz MH, Watson RE, and Fink GD**. Morphological and biochemical characterization of remodeling in aorta and vena cava of DOCA-salt hypertensive rats. *Am J Physiol Heart Circ Physiol* 292: H2438-2448, 2007.

169. **Watts SW, Thakali K, Smark C, Rondelli C, and Fink GD**. Big ET-1 processing into vasoactive peptides in arteries and veins. *Vascul Pharmacol* 47: 302-312, 2007.

170. **Williams HC, and Griendling KK**. NADPH oxidase inhibitors: new antihypertensive agents? *J Cardiovasc Pharmacol* 50: 9-16, 2007.

171. **Wortmann RL**. Recent advances in the management of gout and hyperuricemia. *Curr Opin Rheumatol* 17: 319-324, 2005.

172. **Wu M, Pritchard KA, Jr., Kaminski PM, Fayngersh RP, Hintze TH, and Wolin MS**. Involvement of nitric oxide and nitrosothiols in relaxation of pulmonary arteries to peroxynitrite. *Am J Physiol* 266: H2108-2113, 1994.

173. **Xu H, Fink GD, and Galligan JJ**. Tempol lowers blood pressure and sympathetic nerve activity but not vascular O2- in DOCA-salt rats. *Hypertension* 43: 329-334, 2004.

174. **Yamamoto J, Trippodo NC, MacPhee AA, and Frohlich ED**. Decreased total venous capacity in Goldblatt hypertensive rats. *Am J Physiol* 240: H487-492, 1981.

175. **Yamamoto Y, Ogino K, Igawa G, Matsuura T, Kaetsu Y, Sugihara S, Matsubara K, Miake J, Hamada T, Yoshida A, Igawa O, Yamamoto T, Shigemasa C, and Hisatome I**. Allopurinol reduces neointimal hyperplasia in the

carotid artery ligation model in spontaneously hypertensive rats. *Hypertens Res* 29: 915-921, 2006.

176. **Yang H, Shi M, VanRemmen H, Chen X, Vijg J, Richardson A, and Guo Z**. Reduction of pressor response to vasoconstrictor agents by overexpression of catalase in mice. *Am J Hypertens* 16: 1-5, 2003.

177. **Yang Z, Oemar BS, Carrel T, Kipfer B, Julmy F, and Luscher TF**. Different proliferative properties of smooth muscle cells of human arterial and venous bypass vessels: role of PDGF receptors, mitogen-activated protein kinase, and cyclin-dependent kinase inhibitors. *Circulation* 97: 181-187, 1998.

178. **Yeldandi AV, Yeldandi V, Kumar S, Murthy CV, Wang XD, Alvares K, Rao MS, and Reddy JK**. Molecular evolution of the urate oxidase-encoding gene in hominoid primates: nonsense mutations. *Gene* 109: 281-284, 1991.

179. **You LR, Lin FJ, Lee CT, DeMayo FJ, Tsai MJ, and Tsai SY**. Suppression of Notch signalling by the COUP-TFII transcription factor regulates vein identity. *Nature* 435: 98-104, 2005.

180. **Zalba G, Beaumont FJ, San Jose G, Fortuno A, Fortuno MA, Etayo JC, and Diez J**. Vascular NADH/NADPH oxidase is involved in enhanced superoxide production in spontaneously hypertensive rats. *Hypertension* 35: 1055-1061, 2000.

181. **Zhang DX, and Gutterman DD**. Mitochondrial reactive oxygen species-mediated signaling in endothelial cells. *Am J Physiol Heart Circ Physiol* 292: H2023-2031, 2007.

182. **Zhou XF, Cui J, DeStefano AL, Chazaro I, Farrer LA, Manolis AJ, Gavras H, and Baldwin CT**. Polymorphisms in the promoter region of catalase gene and essential hypertension. *Dis Markers* 21: 3-7, 2005.